

\$5

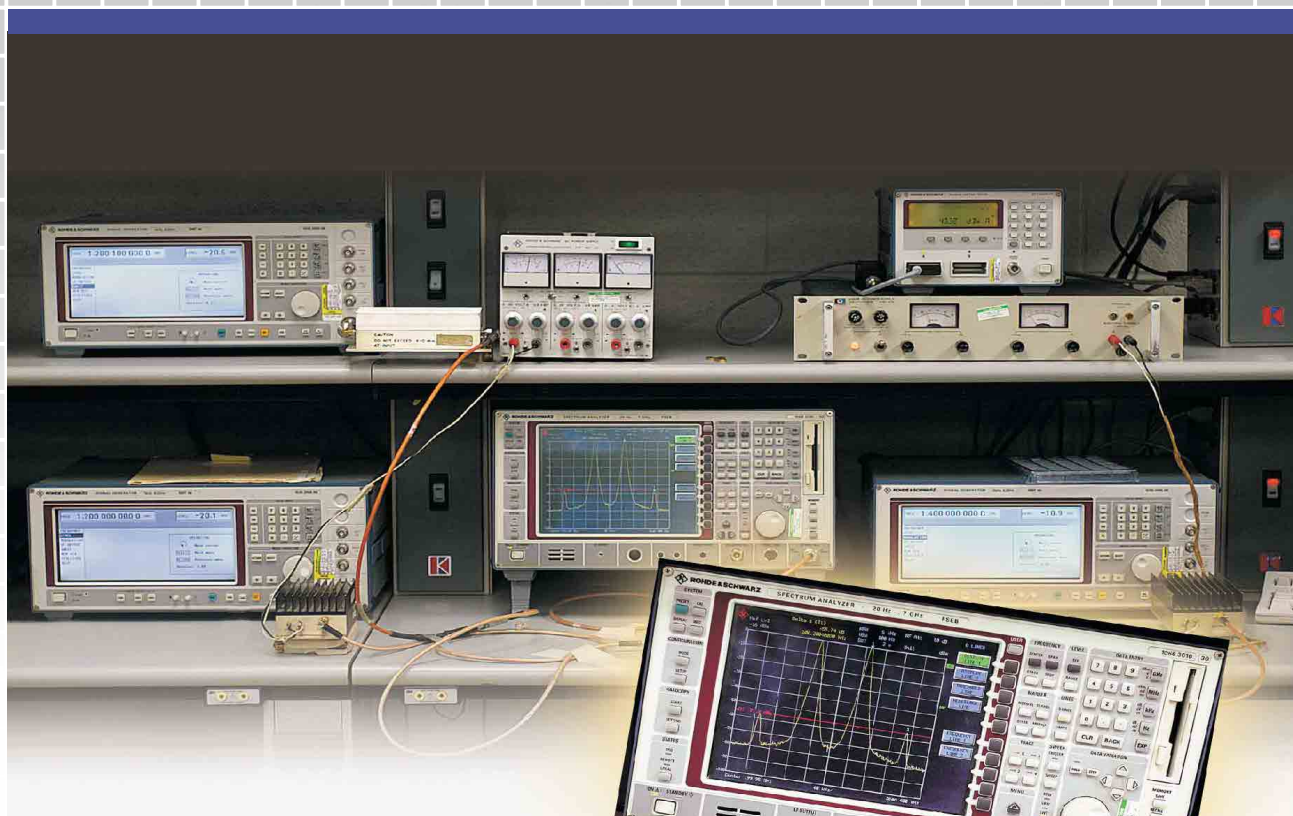


QEX

INCLUDING:
COMMUNICATIONS
QUARTERLY

Forum for Communications Experimenters

November/December 2002



Inside! Ulrich Rohde
begins a series on receiver
performance and measurements

ARRL *The national association for*
AMATEUR RADIO

225 Main Street
Newington, CT USA 06111-1494

Always revised!
The 2003 edition
includes:

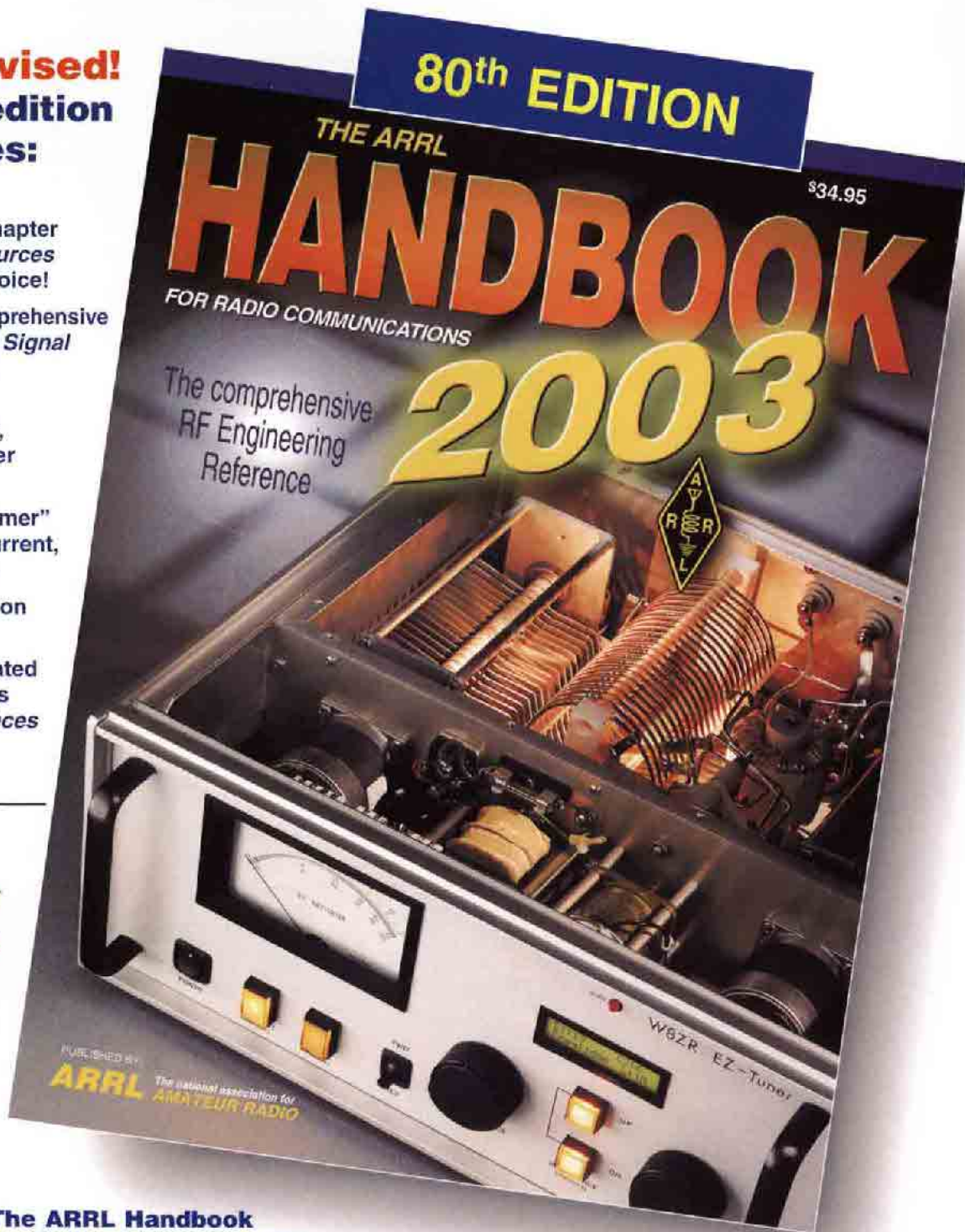
- ◆ An updated and comprehensive chapter on *Modulation Sources* including digital voice!
- ◆ A revised and comprehensive chapter on *Digital Signal Processing (DSP)* technology.
- ◆ A new high-power, automatic EZ-Tuner project by W8ZR.
- ◆ An "Ugly Transformer" project for high current, 120-V ac stations.
- ◆ A revised chapter on *Safety Practices*.
- ◆ A completely updated *Handbook Address List* in the *References* chapter.



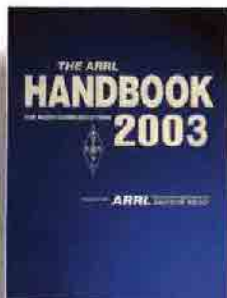
**GREAT
 GIFT
 IDEAS!**



ARRL The national association for
AMATEUR RADIO



**The ARRL Handbook
 for Radio Communications**



Softcover—
 ARRL Order No. 1921 \$34.95*
 *plus shipping \$7 US (UPS) /\$9 International

Hardcover—
 ARRL Order No. 1948 \$49.95*
 *plus shipping \$8 US (UPS) /\$10 International

**Available from ARRL publication
 dealers, everywhere!**

Sales tax is required for orders shipped
 to CA, CT, VA, and Canada.
 Prices subject to change without notice.

**The ARRL Handbook CD
 for Radio Communications**



**Version 7.0—for Windows
 and Macintosh****
View, Search and Print from
 the entire 2003 edition book!
 CD-ROM.
 ARRL Order No. 1956 \$39.95*

*plus shipping \$5 US (UPS)/\$7 International
 **Some supplementary software utilities
 included—for Windows and DCS only.



225 Main Street, Newington, CT 06111-1494 tel: 860-594-0355 fax: 860-594-0303

In the US call our toll-free number **1-888-277-5289** 8 AM-8 PM Eastern time Mon.-Fri.

www.arrl.org/shop

QEX 11/2002

QEX

INCLUDING: COMMUNICATIONS
QUARTERLY

QEX (ISSN: 0886-8093) is published bimonthly in January, March, May, July, September, and November by the American Radio Relay League, 225 Main Street, Newington CT 06111-1494. Yearly subscription rate to ARRL members is \$24; nonmembers \$36. Other rates are listed below. Periodicals postage paid at Hartford, CT and at additional mailing offices.

POSTMASTER: Send address changes to: QEX, 225 Main St, Newington, CT 06111-1494 Issue No 215

Mark J. Wilson, K1RO
Publisher

Doug Smith, KF6DX
Editor

Robert Schetgen, KU7G
Managing Editor

Lori Weinberg, KB1EIB
Assistant Editor

Peter Bertini, K1ZJH
Zack Lau, W1VT
Ray Mack, WD5IFS
Contributing Editors

Production Department

Steve Ford, WB8IMY
Publications Manager

Michelle Bloom, WB1ENT
Production Supervisor

Sue Fagan
Graphic Design Supervisor

David Pingree, N1NAS
Technical Illustrator

Joe Shea
Production Assistant

Advertising Information Contact:

Joe Bottiglieri, AA1GW, Account Manager
860-594-0329 direct
860-594-0200 ARRL
860-594-4285 fax

Circulation Department

Debra Jahnke, Circulation Manager
Kathy Capodicasa, Senior Fulfillment Supervisor
Cathy Stepina, QEX Circulation

Offices

225 Main St, Newington, CT 06111-1494 USA
Telephone: 860-594-0200
Telex: 650215-5052 MCI
Fax: 860-594-0259 (24 hour direct line)
e-mail: qex@arri.org

Subscription rate for 6 issues:

In the US: ARRL Member \$24,
nonmember \$36;

US by First Class Mail:
ARRL member \$37, nonmember \$49;

Elsewhere by Surface Mail (4-8 week delivery):
ARRL member \$31, nonmember \$43;

Canada by Airmail: ARRL member \$40,
nonmember \$52;

Elsewhere by Airmail: ARRL member \$59,
nonmember \$71.

Members are asked to include their membership control number or a label from their QST wrapper when applying.

In order to ensure prompt delivery, we ask that you periodically check the address information on your mailing label. If you find any inaccuracies, please contact the Circulation Department immediately. Thank you for your assistance.

Copyright ©2002 by the American Radio Relay League Inc. For permission to quote or reprint material from QEX or any ARRL publication, send a written request including the issue date (or book title), article, page numbers and a description of where you intend to use the reprinted material. Send the request to the office of the Publications Manager (permission@arri.org)



About the Cover

Receiver measurements defined: The article begins on [page 3](#).



Features

3 Theory of Intermodulation and Reciprocal Mixing: Practice, Definitions and Measurements in Devices and Systems, Part 1

By Ulrich L. Rohde, KA2WEU/DJ2LR/HB9AWE

16 A 700-W Switch-Mode Transmitter for 137 kHz

By Andy Talbot, G4JNT

27 A Software Defined Radio for the Masses, Part 3

By Gerald Youngblood, AC5OG

37 Linrad: New Possibilities for the Communications Experimenter, Part 1

By Leif Åsbrink, SM5BSZ

42 A Guy-Wire-Interaction Case Study

By Dick Weber, K5IU

49 Using the HP Z3801A GPS Frequency Standard

By Bill Jones, K8CU

Columns

54 Tech Notes

62 Letters to the Editor

56 RF By Zack Lau, W1VT

63 Next issue in QEX

60 2002 Index

Nov/Dec 2002 QEX Advertising Index

Active Electronics: 64

American Radio Relay League: [Cov II](#),
[61](#), [Cov III](#), [Cov IV](#)

Atomic Time, Inc.: 26

Buylegacy.com: 55

Down East Microwave Inc.: 59

Roy Lewallen, W7EL: 59

Nemal Electronics International, Inc.: 59

National RF: 55

Noble Publishing Corp: 55

Teri Software: 55

Tucson Amateur Packet Radio Corp: 64

Universal Radio: 26



The American Radio Relay League, Inc. is a noncommercial association of radio amateurs, organized for the promotion of interests in Amateur Radio communication and experimentation, for the establishment of networks to provide communications in the event of disasters or other emergencies, for the advancement of radio art and of the public welfare, for the representation of the radio amateur in legislative matters, and for the maintenance of fraternalism and a high standard of conduct.

ARRL is an incorporated association without capital stock chartered under the laws of the state of Connecticut, and is an exempt organization under Section 501(c)(3) of the Internal Revenue Code of 1986. Its affairs are governed by a Board of Directors, whose voting members are elected every two years by the general membership. The officers are elected or appointed by the Directors. The League is noncommercial, and no one who could gain financially from the shaping of its affairs is eligible for membership on its Board.

"Of, by, and for the radio amateur," ARRL numbers within its ranks the vast majority of active amateurs in the nation and has a proud history of achievement as the standard-bearer in amateur affairs.

A bona fide interest in Amateur Radio is the only essential qualification of membership; an Amateur Radio license is not a prerequisite, although full voting membership is granted only to licensed amateurs in the US.

Membership inquiries and general correspondence should be addressed to the administrative headquarters at 225 Main Street, Newington, CT 06111 USA.

Telephone: 860-594-0200
Telex: 650215-5052 MCI
MCIMAIL (electronic mail system) ID: 215-5052
FAX: 860-594-0259 (24-hour direct line)

Officers

President: JIM D. HAYNIE, W5JBP

3226 Newcastle Dr., Dallas, TX 75220-1640
Executive Vice President: DAVID SUMNER, K1ZZ

The purpose of QEX is to:

- 1) provide a medium for the exchange of ideas and information among Amateur Radio experimenters,
- 2) document advanced technical work in the Amateur Radio field, and
- 3) support efforts to advance the state of the Amateur Radio art.

All correspondence concerning QEX should be addressed to the American Radio Relay League, 225 Main Street, Newington, CT 06111 USA. Envelopes containing manuscripts and letters for publication in QEX should be marked Editor, QEX.

Both theoretical and practical technical articles are welcomed. Manuscripts should be submitted on IBM or Mac format 3.5-inch diskette in word-processor format, if possible. We can redraw any figures as long as their content is clear. Photos should be glossy, color or black-and-white prints of at least the size they are to appear in QEX. Further information for authors can be found on the Web at www.arrl.org/qex/ or by e-mail to qex@arrl.org.

Any opinions expressed in QEX are those of the authors, not necessarily those of the Editor or the League. While we strive to ensure all material is technically correct, authors are expected to defend their own assertions. Products mentioned are included for your information only; no endorsement is implied. Readers are cautioned to verify the availability of products before sending money to vendors.

Empirical Outlook

New Technology Presents New Challenges

Amateur Radio systems are now being fielded that provide Internet gateways, store-and-forward functions, remote control and other fascinating possibilities. Additionally, new high-speed HF digital modes sporting upward of 3 kbps are coming that allow simultaneous voice, data and even video. It will not be long before they're here. Several HF systems having those features are slated for release in 2003.

We like to think we're allowed unlimited experimentation with those possibilities, but the current US Rules don't encourage high-speed data modes on HF. Symbol rates are limited to 300 bauds.

At their July 2002 meeting, the ARRL Board voted to petition for allocation of Amateur Radio sub-bands based on occupied bandwidth rather than on mode. Success would open the door to high-speed, voice-bandwidth digital simultaneous voice and data on HF. Note that other countries already have that, and it's been done in other services for many years now. It's a proposal that seems to make sense and we endorse it. The Board also authorized President Haynie to form a working group to investigate and report on such HF high-speed data modes, HF-Internet gateways and HF automatic control with a final report due by January 2003.

Because of its implications for our service, this important initiative deserves wide discussion. Its pros and cons must be carefully evaluated and details worked out. The ability to send a compressed 20-kbyte file in less than a minute and to construct high-speed networks on HF is state-of-the-art performance that hams should have.

Networking greatly amplifies the power of personal computing. Increased connectivity enhances the capacity and reliability of communications networks. Remote and automatic control, message store-and-forward systems and frequency diversity are among many fertile fields of experimentation in Amateur Radio. We have a chance to further our capabilities in high-speed data, digital voice and software radio. This may be part of the Amateur Radio resurgence we anticipated exactly three years or 18 issues ago. High-speed, bandwidth-conservative data modes tend to use what is called orthogonal frequency-division

multiplexing, or OFDM. It has gotten a lot of attention since high-definition digital television (HDTV) came onto the scene. OFDM is a way to increase throughput by using many sub-carriers, each of which bears a fraction of the total data rate. OFDM tends to produce high peak-to-average ratios that limit average power and place severe linearity demands. Subcarriers spaced at constant frequency intervals produce IMD that falls within adjacent sub-channels. Phase noise from nearby subcarriers may limit signal-to-noise ratios because of reciprocal mixing.

Designers are using predistortion in DSP and other adaptive-compensation techniques to combat deleterious effects. They are the subjects of ongoing research. Tie-ins among digital voice, software radio and high-speed multimedia networking are evident. Write us or visit www.arrl.org/tis/info/sdr.html for updates.

In This Issue

We are delighted to welcome back Ulrich Rohde, KA2WEU. He investigates receiver dynamic range and IMD measurements in the first segment of his two-part series. We're confident it is of interest to those serious about comparing the large-signal performance of receivers. Andy Talbot, G4JNT, of digital-voice fame (see May/June 2000) shows us how he built his LF transmitter. Be among the first on the air when we get 136 kHz!

Gerald Youngblood, AC5OG, continues his popular series on software-defined radio (SDR). Gerald's fourth segment will come in the Mar/Apr 2003 issue. For you in the Linux world, Leif Åsbrink, SM5BSZ, begins a presentation of his Linrad system. When coupled with minimal hardware, this shareware can get you into the SDR game very quickly.

Dick Weber, K5IU, donates his case study on guy-wire/antenna interaction. Modeling and measurement reconciled—hoorah! Bill Jones, K8CU, describes the use of surplus Hewlett-Packard GPS receivers as frequency standards for weak-signal work. In Tech Notes, Tom Cefalo, W1EX, describes a way to fashion custom meter faces with computer technology. In RF, Zack Lau, W1VT, analyzes operation of $\lambda/4$ dipoles.—Doug Smith, KF6DX, kf6dx@arrl.org □□

Theory of Intermodulation and Reciprocal Mixing: Practice, Definitions and Measurements in Devices and Systems, Part 1

A man of renown in the communications field begins an explanation of receiver performance.

By Ulrich L. Rohde, KA2WEU/DJ2LR/HB9AWE

This two-part paper deals with both analog and digital receivers and gives a treatment of intermodulation distortion. Starting from a mathematical—but simple—derivation, it looks at gain compression, intermodulation distortion and dynamic range. Furthermore, a new dynamic measure is introduced that allows one to differentiate between different receive systems much better. Other important characteristics are triple-beat distortion and cross modulation. To describe the performance of broadband systems, noise-power ratio is also considered.

Large-signal effects which go beyond the linear range, such as AM-to-PM conversion, spectral re-growth and adjacent-channel power ratio are considered, as well as phase-response differential group delay and reciprocal mixing.

Synergy Microwave Corporation
201 McLean Blvd
Paterson, NJ 07504
ulrohde@aol.com

This tutorial is a good prerequisite in preparation for looking into high-performance components such as high-IP₃ mixers and modern receiver architectures.

Amplitude Linearity Issues and Figures of Merit¹

A network's amplitude nonlinearity can be characterized by the expansion:

$$y = k_1 f(x) + k_2 [f(x)]^2 + k_3 [f(x)]^3 + \text{higher - order terms} \quad (\text{Eq 1})$$

where y represents the output, the coefficients k_n represent complex quantities whose values can be determined by an analysis of the output waveforms, and $f(x)$ represents the input. Although all practical networks exhibit amplitude nonlinearity, we can (and often do) refer to many networks as “linear.” We say this of networks that are *sufficiently amplitude-linear for our purposes*—for example: weakly nonlinear networks in which small-signal opera-

¹Notes appear on [page 15](#).

tion is assumed even though the signal levels involved are sufficient to cause slight distortion. For many practical purposes, the first three terms of Eq 1 adequately describe such a network's nonlinearity:

$$y = k_1 f(x) + k_2 [f(x)]^2 + k_3 [f(x)]^3 \quad (\text{Eq 2})$$

In adopting this simplification, we assume also that the nonlinearity is frequency-independent; that is, that the network has sufficient bandwidth to allow all of the products predicted by Eq 2 to appear at its output terminals unperturbed.

When multiple signals are present in a network, even weak nonlinearity can result in profound consequences. To illustrate this, we'll let $f(x)$ consist of the sum of two sinusoidal signals:

$$f(x) = A_1 \cos \omega_1 t + A_2 \cos \omega_2 t \quad (\text{Eq 3})$$

We'll assume that ω_1 and ω_2 are close enough so that the coefficients k_i can be considered equal for both signals. We'll also assume, for simplicity, that all of the k_i are real. If Eq 2 describes the network's response to an input $f(x)$, the response will be as shown in Eq 4 below.

The k_1 term of Eq 4 represents the results of amplitude-linear behavior. No new frequency components have appeared; the two sine waves have merely been "rescaled" by k_1 .

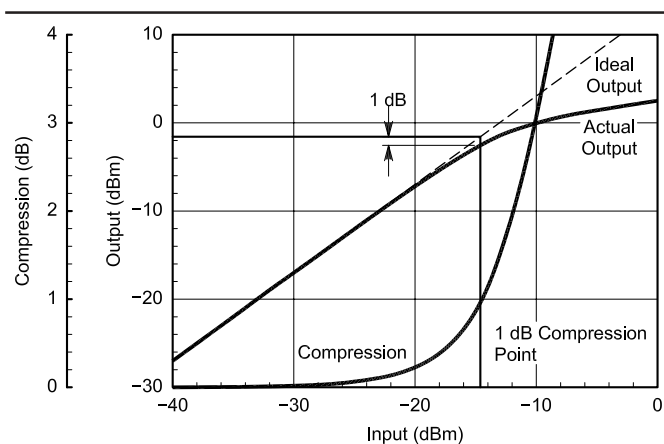


Fig 1—The power level at which a network's power output is down 1 dB relative to that of its ideally linear equivalent is a figure of merit known as the **1-dB compression point** ($P_{-1\text{dB}}$). The 1-dB compression point can be expressed relative to input power ($P_{-1\text{dB},\text{in}}$) or output power ($P_{-1\text{dB},\text{out}}$). For the amplifier simulated here, $P_{-1\text{dB},\text{in}} \approx -14.5$ dBm and $P_{-1\text{dB},\text{out}} \approx -1.3$ dBm.

The second- and third-order terms of Eq 4 represent the effects of harmonic distortion and intermodulation distortion. Second-order effects include second-harmonic distortion (the production of new signals at $2\omega_1$ and $2\omega_2$) and IMD (the production of new signals at $\omega_1 + \omega_2$ and $\omega_1 - \omega_2$). Third-order effects include gain compression, third-harmonic distortion (the production of new signals at $3\omega_1$ and $3\omega_2$), and IMD (the production of new signals at $2\omega_1 \pm \omega_2$ and $2\omega_2 \pm \omega_1$).

Gain Compression

Gain compression occurs when a network cannot increase its output amplitude in linear proportion to an amplitude increase at its input. Gain *saturation* occurs when a network's output amplitude stops increasing (in practice, it may actually decrease) with increases in input amplitude. We can deduce from Eq 4 that the amplitude of the $\cos \omega_1 t$ signal has become:

$$A_1' = k_1 A_1 + k_3 \left(\frac{3}{4} A_1^3 + \frac{3}{2} A_1 A_2^2 \right) \quad (\text{Eq 5})$$

Because k_3 will normally be negative, a large signal $A_2 \cos \omega_2 t$ can effectively mask a smaller signal $A_1 \cos \omega_1 t$ by reducing the network's gain. This third-order effect, known as *blocking* or *desensitization* when it occurs in a receiver, is a special case of gain compression. The presence of additional signals results in a greater reduction of gain; the gain reduction for each signal is a function of the relative levels of all signals present. A receiver's blocking behavior may be characterized by the level of off-channel signal necessary to reduce the strength of an in-band signal by a specified value, typically 1 dB. Alternatively, the decibel ratio of the off-channel signal's power to the receiver's noise-floor power may be cited as *blocking dynamic range*. Desensitization may be also characterized in terms of the

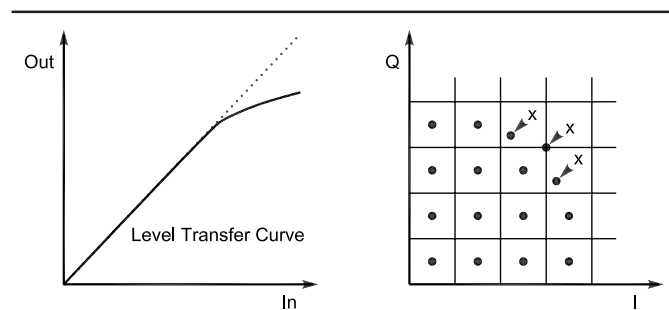


Fig 2—The influence of differential amplitude error (compression) on a QAM constellation.

$$\begin{aligned}
 y &= k_1 (A_1 \cos \omega_1 t + A_2 \cos \omega_2 t) + k_2 (A_1 \cos \omega_1 t + A_2 \cos \omega_2 t)^2 + k_3 (A_1 \cos \omega_1 t + A_2 \cos \omega_2 t)^3 \\
 &= k_1 (A_1 \cos \omega_1 t + A_2 \cos \omega_2 t) + k_2 \left[A_1^2 \frac{1 + \cos 2\omega_1 t}{2} + A_2^2 \frac{1 + \cos 2\omega_2 t}{2} + A_1 A_2 \frac{\cos(\omega_1 + \omega_2)t + \cos(\omega_1 - \omega_2)t}{2} \right] + \\
 &\quad \left\{ \left[A_1^3 \left(\frac{\cos \omega_1 t}{2} + \frac{\cos \omega_1 t}{4} + \frac{\cos 3\omega_1 t}{4} \right) + A_2^3 \left(\frac{3 \cos \omega_2 t}{4} + \frac{\cos 3\omega_2 t}{4} \right) \right] \right. \\
 &\quad \left. + A_1^2 A_2 \left[\frac{3}{2} \cos \omega_2 t + \frac{3}{4} \cos(2\omega_1 - \omega_2)t + \frac{3}{4} \cos(2\omega_1 + \omega_2)t \right] \right. \\
 &\quad \left. + A_2^2 A_1 \left[\frac{3}{2} \cos \omega_1 t + \frac{3}{4} \cos(2\omega_2 + \omega_1)t + \frac{3}{4} \cos(2\omega_2 - \omega_1)t \right] \right\} \quad (\text{Eq 4})
 \end{aligned}$$

off-channel-signal power necessary to degrade a system's SNR by a specified value.

Multiple signals need not be present for gain compression to occur. If only one signal were present, the ratio of gain with distortion to the network's idealized (linear) gain would be:

$$A'_1 = \frac{k_1 + k_3 \left(\frac{3}{4} A_1^2\right)}{k_1} \quad (\text{Eq 6})$$

This is referred to as the *single-tone gain-compression factor*. Fig 1 shows how the k_3 term causes a network's gain to deviate from the ideal. The point at which a network's power gain is down 1 dB from the ideal for a single signal is a figure of merit known as the *1-dB compression point* ($P_{-1\text{dB}}$). Many networks—including many receiving and low-level transmitting circuits, such as low-noise amplifiers, mixers and IF amplifiers—are usually operated under small-signal conditions, at levels sufficiently below $P_{-1\text{dB}}$ to maintain high linearity. As we'll see, however, some networks—including power amplifiers for wireless systems—may be operated under large-signal conditions near or in compression to achieve optimum efficiency at some specified level of linearity. Fig 2 shows what happens when a digital emission that uses amplitude to convey information is subjected to amplitude compression.

Intermodulation

The new signals produced through IMD can profoundly affect the performance of systems even when they are operated well below gain compression (Fig 3). IMD products of significant power can appear at frequencies remote from, in or near the system passband, resulting in demodulation errors in reception and interference to other communication in transmission. Where an IMD product appears

relative to the passband depends on the passband width and center frequency, the frequencies of the signals present at the system input and the order of the nonlinearity involved. These factors also determine the strength of an IMD product relative to the desired signal.

Second-order IMD (IM_2) results, for an input consisting of two signals ω_1 and ω_2 , in the production of new signals at $\omega_1 + \omega_2$ and $\omega_1 - \omega_2$. Third-order IMD (IM_3) results, for an input consisting of two signals ω_1 and ω_2 , in the production of new signals at $2\omega_1 \pm \omega_2$ and $2\omega_2 \pm \omega_1$.

Under small-signal conditions well below compression, the power of an IM_2 product varies by 2 dB, and the power of an IM_3 product varies by 3 dB, per decibel change in input power level. This allows us to derive a network figure of merit, the *intermodulation intercept point* (IP), for a given intermodulation order. We can do so by extrapolating a network's linear and intermodulation responses to their point of intersection (Fig 4). This is the point at which their powers would be equal if compression did not occur.

Because of the system noise and/or intermodulation distortion products, there is a minimum discernible signal (MDS) that limits the dynamic range at the lower end. Theoretically, Fig 4 should show a noise floor or IMD-spur floor for a given input signal that represents a lower limit below which signals cannot be detected. The intercept point for a given intermodulation order n can be expressed, and should always be characterized, relative to input power ($IP_{n,in}$) or output power ($IP_{n,out}$). The $IP_{n,in}$ and $IP_{n,out}$ values differ by the network's linear gain. For equal-level test tones, $IP_{n,in}$ can be determined by:

$$IP_{n,in} = \frac{nP_A - P_{IM_n}}{n-1} \quad (\text{Eq 7})$$

where n is the order, P_A is the input power (of one tone), P_{IM_n} is the power of the intermodulation product, and IP

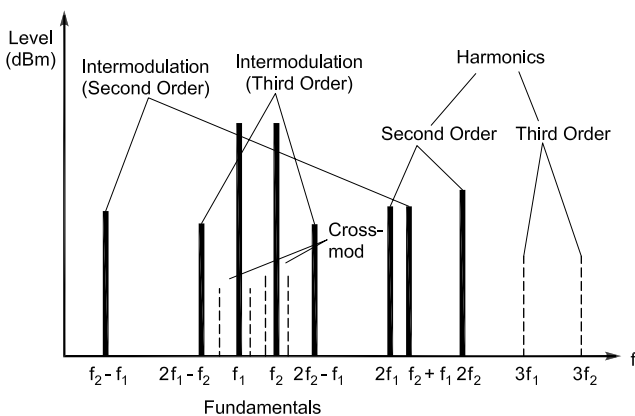
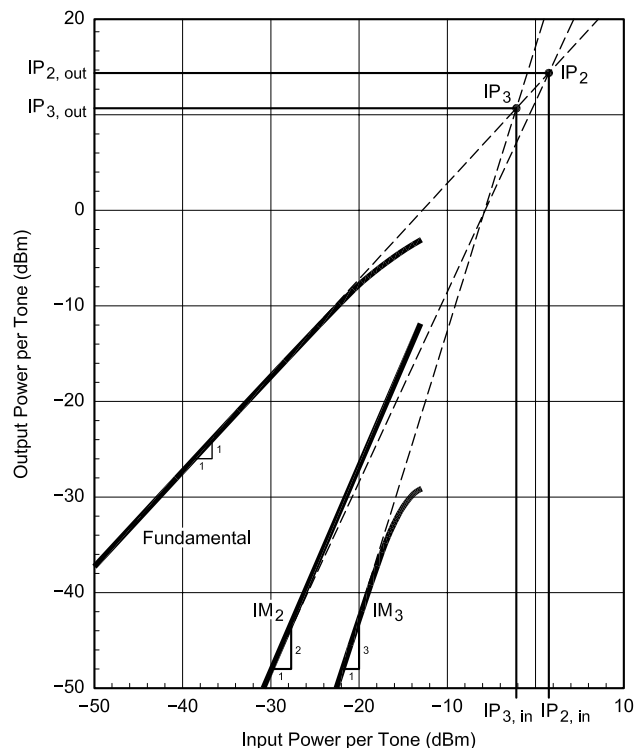


Fig 3—Relationships between fundamental and spurious signals, including harmonics and products of intermodulation.

Fig 4 (right)—The level at which the power of one of a network's intermodulation products equals that of the network's linear output is a figure of merit known as the *intermodulation intercept point* (IP). The intercept point for a given intermodulation order, n , can be expressed, and should always be characterized, relative to input power ($IP_{n,in}$) or output power ($IP_{n,out}$); the IP_{in} and IP_{out} values differ by the network's linear gain. For the amplifier simulated here, $IP_{2,in} \approx 1.5$ dBm, $IP_{2,out} \approx 14.5$ dBm, $IP_{3,in} \approx -2.3$ dBm and $IP_{3,out} \approx 10.7$ dBm. Each curve depicts the power in one tone of the response evaluated.



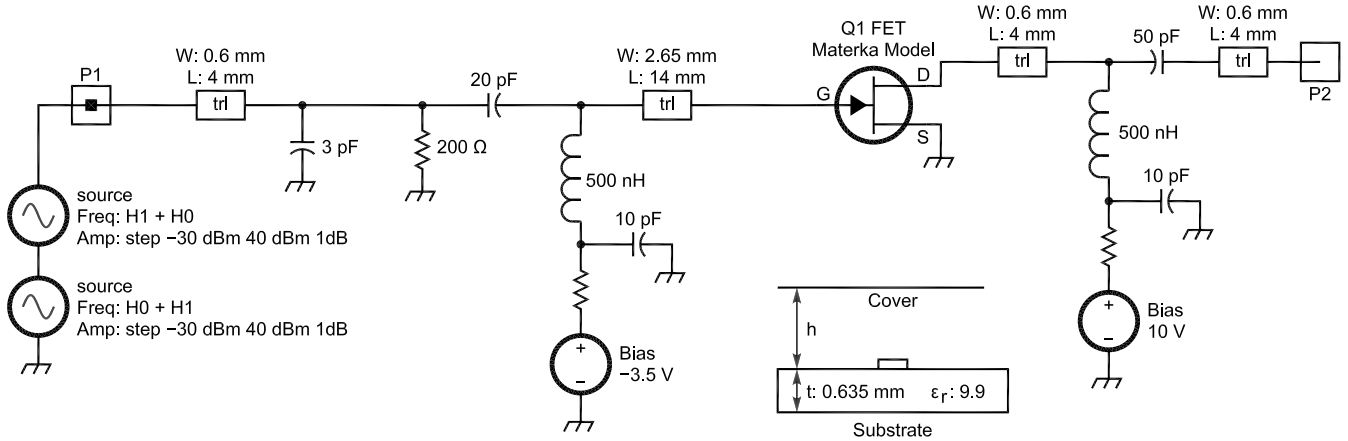


Fig 5—Circuit of a single-stage GaAs-FET amplifier operating at 120 mA used to demonstrate IP_2 and IP_3 for CAD analysis.

is the intercept point. The intercept point for cascaded networks can be determined from:

$$IP_{2,in} = \frac{1}{\left(\frac{1}{\sqrt{IP_1}} + \frac{G}{\sqrt{IP_2}}\right)^2} \quad (\text{Eq 8})$$

for IP_2 and from:

$$IP_{3,in} = \frac{1}{\frac{1}{IP_1} + \frac{G}{IP_2}} \quad (\text{Eq 9})$$

for IP_3 . In both equations, IP_1 is the input intercept of Stage 1 in watts, IP_2 is the input intercept of Stage 2 in watts and G is the gain of Stage 1 (as a numerical ratio, *not* in decibels). Both equations assume the worst-case condition, in which the distortion products of both stages add in-phase.

The ratio of the signal power to the intermodulation-product power, the *distortion ratio*, can be expressed as:

$$R_{dn} = (n-1) \left[IP_{n(in)} - P_{(in)} \right] \quad (\text{Eq 10})$$

where n is the order, R_{dn} is the distortion ratio, $IP_{n(in)}$ is the input intercept point and $P_{(in)}$ is the input power of one tone.²

Discussions of IMD have traditionally downplayed the importance of IM_2 . This is true because the incidental distributed filtering of the tuned circuitry, once common in radio communication systems, was usually enough to render out-of-passband IM_2 products caused by in-band signals and in-band IM_2 products caused by out-of-passband signals vanishingly weak compared to fundamental and IM_3 signals. In broadband systems that operate at bandwidths of an octave or more, however, in-passband signals may produce significantly strong in-passband IM_2 and second-harmonic products. In such applications, balanced circuit structures (such as push-pull amplifiers and balanced mixers) can be used to minimize IM_2 and other even-order nonlinear products.

As with IM_2 , the importance of specific IM_3 products depends on the spacing of the signals involved and the relative width of the system passband. If ω_1 and ω_2 are of approximately the same frequency, the additive products

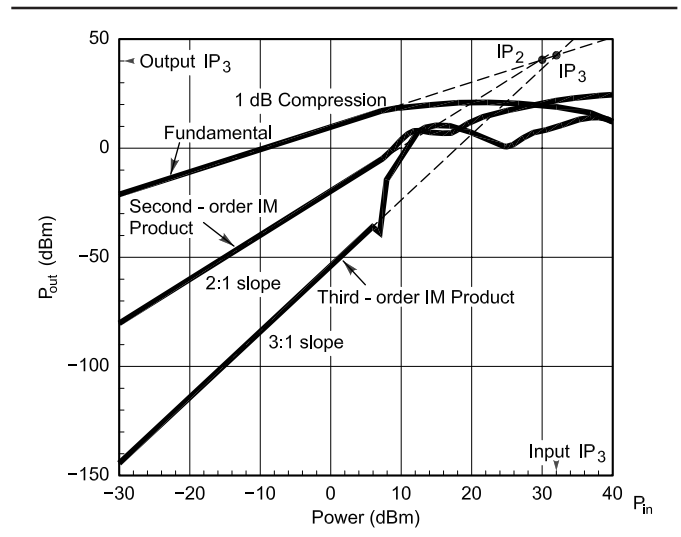


Fig 6—A simulation plot showing second and third-order IMD behavior for the one-stage amplifier shown in Fig 5.

$2\omega_1 + \omega_2$ and $2\omega_2 + \omega_1$ would be outside the passband of a narrow-bandwidth system. The subtractive products $2\omega_1 - \omega_2$ and $2\omega_2 - \omega_1$, however, will likely appear near or within the system passband. The IM_3 performance of any network subjected to multiple signals is therefore of critical importance. Consequently, an array of IM_3 -related, sometimes application-specific, figures of merit has evolved.

Example of a One-Stage FET Amplifier

The simulation of second- and third-order IMD products, based on the circuit shown in Fig 5, is shown in Fig 6. This gives a lot of insight into performance. The circuit in question is a simple single FET amplifier operating at about 120 mA dc. The top curve shows the fundamental and demonstrates 10-dB gain. At about 8 dBm of input, the 1-dB compression point occurs, and the fundamental amplitude actually gets smaller as the input power increases. The slope underneath is the fundamental referenced to the second-order IMD products. The crossover with the fundamental is called the second-order intercept point. A few decibels below the 1-dB compression point, the curve for the second-order IMD drastically deviates from the straight line; this is

due to clipping of harmonics. This curve has a 2:1 slope, meaning that with a 1 dB increase of the fundamental the products increase by 2 dB.

The final line starting at close to -150 dBm relates to the third-order IMD products. At about 7-dBm input, the IP_3 curve shows a dent. This is caused by the cancellation of the second-order harmonics, but then higher-level distortion is responsible for all kinds of deviation from linearity. Contrary to typical textbook plots, this curve shows a real, live amplifier performance.

Dynamic Range

As we have seen, thermal noise sets the lower limit of the power span over which a network can operate. Distortion—that is, degradation by distortion of the signal’s ability to convey information—sets the upper limit of a network’s power span. Because the power level at which distortion becomes intolerable varies with signal type and application, a generic definition has evolved: The upper limit of a network’s power span is the level at which the power of one intermodulation product of a specified order is equal in power to the network’s noise floor. The ratio of the noise-floor power to the upper-limit signal power is referred to as the network’s *dynamic range (DR)*. This is often more carefully characterized as *two-tone IMD dynamic range*, which, when evaluated with equal-power test tones, is a figure of merit commonly used to characterize receivers. The *MDS* relative to the input, as already defined, is $MDS_{in} = kTB + 3 \text{ dB} + NF$.

When $IP_{(n)in}$ and *MDS* are known, *IMD DR* can be determined from:

$$DR_n = \frac{(n-1)[IP_{n(in)} - MDS_{in}]}{n} \quad (\text{Eq 11})$$

where *DR* is the dynamic range in decibels, *n* is the order, $IP_{(in)}$ is the input intercept power in dBm and *MDS* is the minimum detectable signal power in dBm. The so-called *spurious-free dynamic range (SFDR or DR_{SF})* is calculated from:

$$DR_{SF} = \frac{2}{3}(IP_3 - 174 \text{ dBm} + NF + 3 \text{ dB}) \quad (\text{Eq 12})$$

This equation allows us to determine how to measure the spurious-free dynamic range. This is done by applying the two-tone signals (as in the case of IP_3) and increasing the two signals to the point where the signal-to-noise ratio deteriorates by 3 dB; or, if the measurement were done relative to *MDS*, where the noise floor rises by 3 dB. The “2/3” factor is derived from the fact that the levels of IM_3 outputs increase 3 dB for 1 dB of input increase. This definition of dynamic range now is referenced to a noise figure rather than a minimum level (in dBm) and is therefore independent of bandwidth. By choosing smaller bandwidths (1 kHz instead of 10 kHz), a dynamic-range measurement can be made to look better. Basing the specification on noise figure directly avoids this problem.

Dynamic Measure: A New Receiver Figure of Merit

Taken by themselves, the IP_n and *DR* figures of merit can be misleading in the sense that broadband, resistive attenuation directly improves them by the amount of attenuation added while directly degrading *NF* by the same amount. The *NF* and *MDS* figures of merit can mislead us

because they convey no sense of suitability to task. This can be significant when we interconnect networks and systems having different noise floors and IMD dynamic ranges—as we do, for example, when connecting a receiver to an antenna. Relative to noise figure and intercept point, a noise measure and a third-order-intercept (IP_3) measure have already been defined. Both these measures refer to a “minimum value.” In the case of noise, it addresses the minimum noise figure obtainable in a multistage arrangement. The IP_3 measure addresses the total resulting third-order products that result in a minimum value slightly less than that of the first stage, assuming that all stages are identical. As a means of better evaluating a receiver’s front-end performance, I propose a new figure of merit, *dynamic measure*, defined as:

$$DM = \left[(IP_{3,in} + Att) - (NF_r + Att + NF_{ant}) \right] \frac{NF_r}{NF_r + Att} \quad (\text{Eq 13})$$

where *DM* is the dynamic measure, a dimensionless number; $IP_{3,in}$ is the receiver’s third-order input intercept in dBμV (instead of dBm) without any added attenuation; NF_r is the receiver noise figure in decibels without any added attenuation; NF_{ant} is the antenna-system noise figure in decibels; and *Att* is the decibel value of any added attenuation, which is sometimes used to shift the upper and lower limits of a system’s dynamic range to higher absolute signal levels, increasing $IP_{3,in}$ at the expense of making the system more “deaf.” Our dynamic measure figure of merit considers this trade-off to allow more-straightforward comparisons of systems that have the same dynamic range but different sensitivities. Setting NF_{ant} equal to zero allows evaluation of receiver performance under laboratory conditions. Setting NF_{ant} equal to the measured or expected *NF* of the antenna system to which the receiver will be connected allows evaluation of receiver performance in a system sense. Rather than express IP_3 in dBm, we are going to express it in dBμV. This is necessary because for negative values of the difference between IP_3 and the added noise figure, the multiplier term will make the result larger when its numerical value is less than one.

The usefulness of the dynamic measure figure of merit is evident when we consider several examples. Example 1 evaluates a receiver that exhibits the characteristics $IP_{3,in} = 16 \text{ dBm}$ (123 dBμV), $NF_r = 8 \text{ dB}$ and $NF_{ant} = 10 \text{ dB}$. We calculate its laboratory DM by setting NF_{ant} equal to 0:

$$DM = [123 - (8 + 0)] \frac{8}{8 + 0} = [115]1 = 115 \quad (\text{Eq 14})$$

Setting NF_{ant} equal to 10 returns the receiver’s system DM:

$$DM = [123 - (8 + 10)] \frac{8}{8 + 0} = [105]1 = 105 \quad (\text{Eq 15})$$

Example 2 consists of the Example 1 receiver with a 10-dB pad switched in, resulting in the characteristics $IP_{3,in} = 26 \text{ dBm}$, $NF_r = 18 \text{ dB}$ and $NF_{ant} = 10 \text{ dB}$. Setting NF_{ant} equal to 0, we calculate its laboratory DM as:

$$DM = [133 - (8 + 10 + 0)] \frac{8}{8 + 10} = [115]0.4444 = 51.1 \quad (\text{Eq 16})$$

A comparison with Eq 14 shows that although

Table 1—Eight Dynamic Measure Cases Compared

Ex.	System	Base $IP_{3,in}$ (dBm)	Base $IP_{3,in}$ (dBμV)	Atten (dB)	Res. $IP_{3,in}$ (dBm)	Res. $IP_{3,in}$ (dBμV)	Base NF_R (dB)	Res. NF_R (dB)	NF_{ant} (dB)	DM_{lab}	DM_{system}
1	HF receiver	16.0	123.0	0.0	16.0	123.0	8.0	8.0	10.0	115.0	105.0
2	HF receiver with 10-dB pad	16.0	123.0	10.0	26.0	133.0	8.0	18.0	10.0	51.1	46.7
3	HF receiver with 2-dB pad	16.0	123.0	2.0	18.0	125.0	8.0	10.0	10.0	92.0	84.0
4	Rohde & Schwarz XK 2100 shortwave transceiver	40.0	147.0	0.0	40.0	147.0	10.0	10.0	10.0	137.0	127.0
5	XK 2100 with 10 dB of unnecessary attenuation	40.0	147.0	10.0	50.0	157.0	10.0	20.0	10.0	68.5	63.5
6	Satellite receiver	-2.2	104.8	0.0	-2.2	104.8	0.9	0.9	0.2	103.9	103.7
7	Wireless front end without duplexer/filter losses	-12.0	95.0	0.0	-12.0	95.0	2.6	2.6	2.0	92.4	90.4
8	Wireless front end with 3 dB duplexer/filter losses	-12.0	95.0	3.0	-9.0	98.0	2.6	5.6	2.0	42.9	42.0

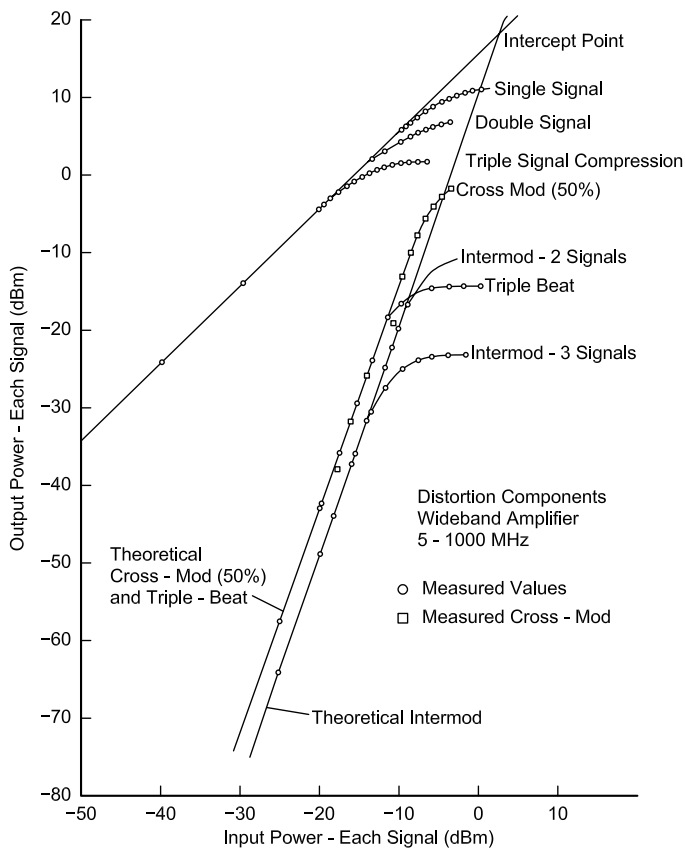


Fig 7—Measured distortion components in a wide-bandwidth (5 to 1000 MHz) amplifier.

inserting the 10-dB pad has shifted $IP_{3,in}$ from 16 dBm (123 dBμV) to 26 dBm (133 dBμV), it has also increased the resulting NF from 8 to 18 dB, reducing the DM from 115 to 51.1. Inserting the pad also degrades the receiver's system DM compared to Example 1, as we see by setting NF_{ant} equal to 10:

$$DM = [133 - (8 + 10 + 10)] \frac{8}{8 + 10} = [105] 0.4444 = 46.7 \quad (\text{Eq 17})$$

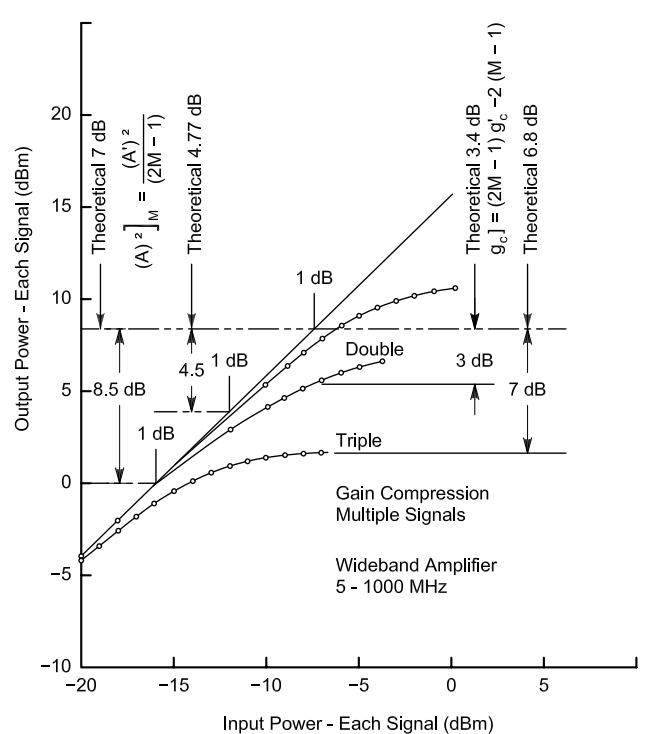


Fig 8—Measured multiple-signal gain compression of the 5- to 1000-MHz amplifier.

Example 3: On the other hand, had we inserted 2 dB of attenuation rather than 10 dB ($IP_{3,in} = 18$ dBm [125 dBμV], $NF_r = 10$ dB and $NF_{ant} = 10$ dB), the laboratory DM would have been:

$$DM = [125 - (8 + 2 + 0)] \frac{8}{8 + 2} = [115] 0.8 = 92 \quad (\text{Eq 18})$$

and the system DM would have been:

$$DM = [125 - (8 + 2 + 10)] \frac{8}{8 + 2} = [105] 0.8 = 84 \quad (\text{Eq 19})$$

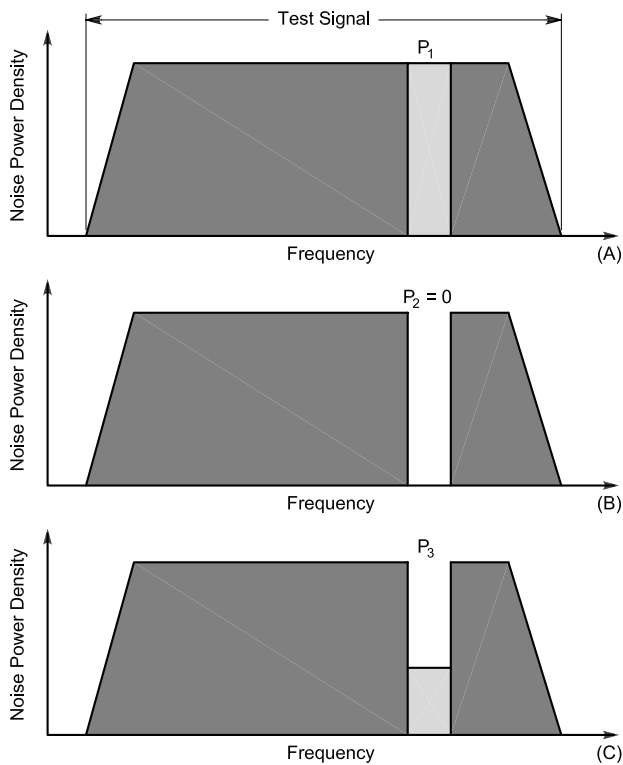


Fig 9—Determining a network's *noise-power ratio (NPR)* involves the application of a test signal consisting of thermal noise. The reference measurement-channel noise power, P_1 , is then measured (at A). Next, a stop-band filter is placed between the noise generator and network under test to keep the test signal out of the measurement channel (at B). Assuming sufficient filter attenuation, if the network were absolutely noiseless and linear, the ideal noise power in the measurement channel, P_2 , would then be zero. In practice, the network's own thermal noise and intermodulation between noise components outside the measurement channel result in an actual measurement-channel noise power (P_3) greater than zero. The noise-power ratio equals P_1/P_3 .

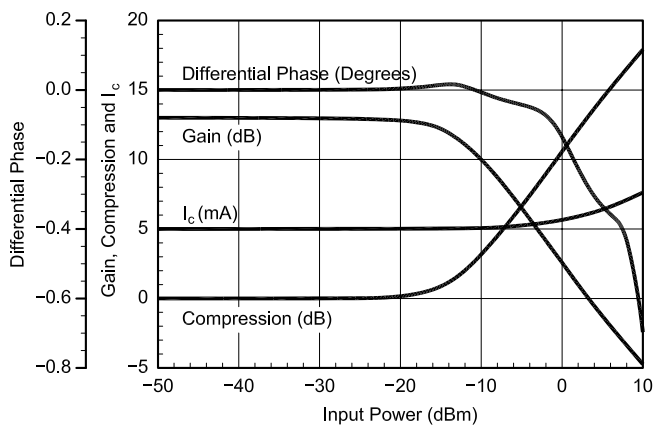


Fig 11—Driving a network into compression and saturation shifts the bias point(s) of its active device(s), changing their drive-dependent reactances and shifting the phase of the output signal relative to its value at input levels below compression. This graph shows the simulated performance of a single-BJT broadband amplifier driven by a single tone at 10 MHz.

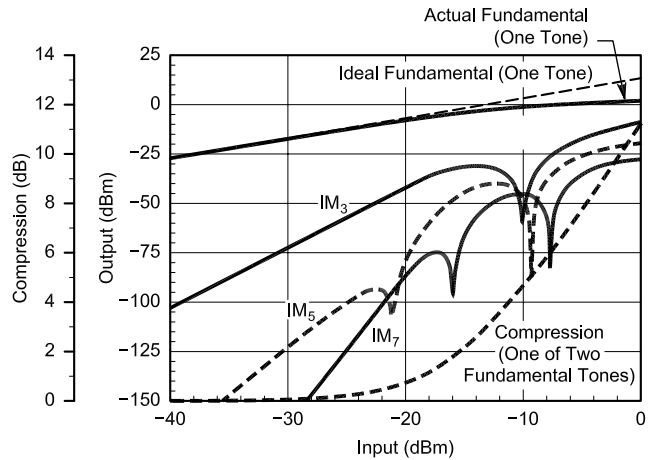


Fig 10—As a network is driven into compression, intermodulation products at odd orders higher than three become significant, and phase shifts in power-dependent device capacitances cause curves and dips in the intermodulation characteristics. The onset of these departures from intermodulation-response linearity occurs at generally lower input-power levels for higher intermodulation orders. Their severity and their positions on the intermodulation curves differ among the various products of a given order and varies with network topology and tone spacing. Figures of merit based on straight-line intermodulation responses fail to usefully predict nonlinear network behavior under these conditions. This graph shows the simulated performance of a single-BJT broadband amplifier driven by two equal-amplitude tones at 10 and 11 MHz.

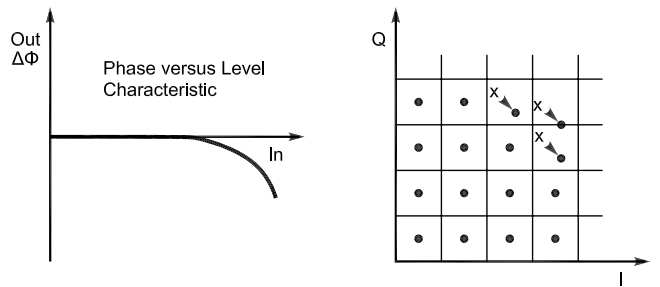


Fig 12—The influence of differential phase error (AM-to-PM conversion) on a QAM constellation.

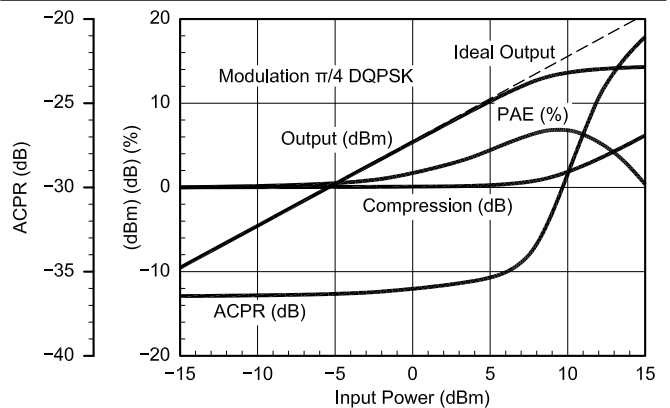


Fig 13—Keeping adjacent-channel interference under control can involve a critical trade-off between a wireless transmitter's power-added-efficiency (PAE) and ACPR, as shown in this graph showing the simulated behavior of a 1-GHz MESFET power amplifier. As the amplifier is driven into compression, a peak occurs in the PAE response—in this case, at P_{-1dB} —and ACPR rises sharply.

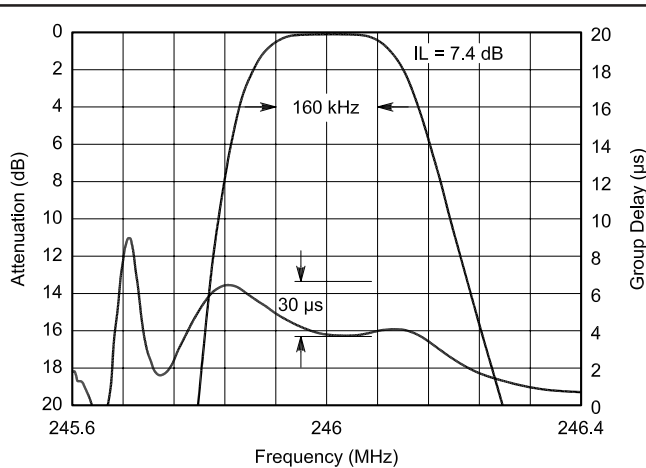


Fig 14—Close-in amplitude and group-delay responses for a 246-MHz SAW filter designed for GSM applications. This filter is well within its 3.0 μ s differential-group-delay specification across its passband (160 kHz at -3 dB); the peaks just outside the passband limits are characteristic of a network's transition-band phase response.

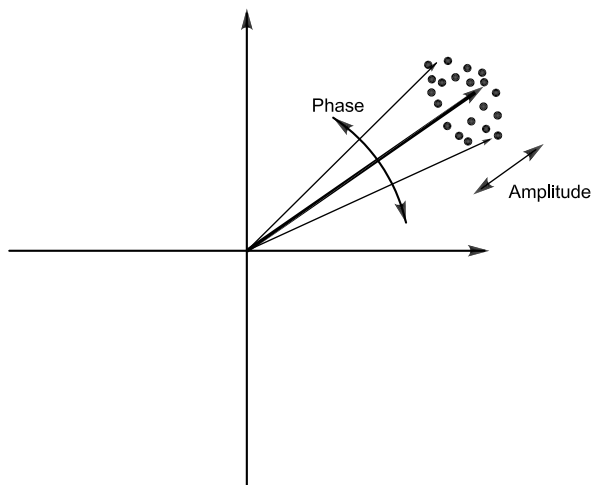


Fig 16—Oscillator noise can be split into amplitude and phase components.

Table 1 shows these and several additional examples for comparison.

The interested reader will notice the following: The Example 1 receiver (base NF 8 dB) was unnecessarily sensitive compared to the antenna NF of 10 dB, so adding a 2-dB pad increased the intercept point by 2 dB and matched the antenna noise floor. Yet, the equation rightfully indicates a loss of dynamic measure. The relationship between NF_{ant} and NF_r is not taken into consideration. In addition, we have decided to leave it to the reader to develop a formula that deals with the addition of a preamplifier rather than an attenuator. This will complicate the formula because the preamplifier gain and noise figure are not necessarily related.

Triple-Beat Distortion and Cross Modulation

P_{-1dB} is a single-tone figure of merit; blocking, intercept point and dynamic range evaluate two-tone behavior. For networks that must handle AM and composite (AM and angle

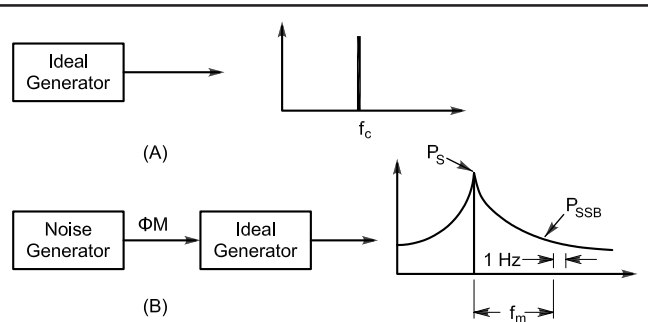
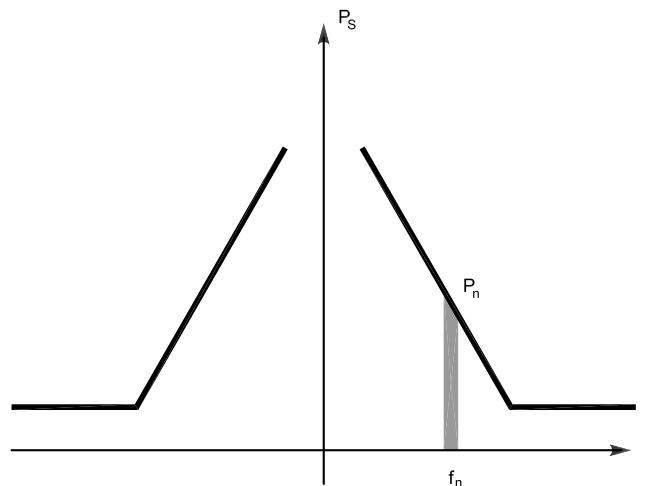


Fig 15—SSB phase noise. An ideal signal generator (A) would produce an absolutely pure carrier. A real signal generator (B), acts like an ideal generator driven by a noise generator, producing a noise-modulated carrier.



$$L(f) = 10 \log \frac{P_n}{P_S}$$

P_n = Sideband noise in 1 - Hz bandwidth at offset frequency f_n

P_S = Total signal power

Single - sideband phase noise is expressed in dBc measured in a bandwidth of 1 Hz [dBc(Hz)] at offset frequency f_n

Fig 17—Phase noise calculation.

modulation) signals very linearly, such as television transmitters and cable-TV distribution systems, a three-tone figure of merit called *triple-beat distortion* has gained acceptance. Signals at ω_1 and ω_2 (closely spaced) and ω_3 (positioned far away from ω_1 and ω_2) are applied to the network under test, at levels, frequencies and spacings that vary with the application. One triple-beat distortion figure of merit is the ratio, expressed in decibels, of the intermodulation product at $\omega_3 + (\omega_2 - \omega_1)$ to one of the network's linear outputs at a specified output level. Alternatively, the triple-beat figure of merit may express the network output level at which a specified triple-beat ratio occurs.

Triple-beat distortion is the mechanism underlying cross-

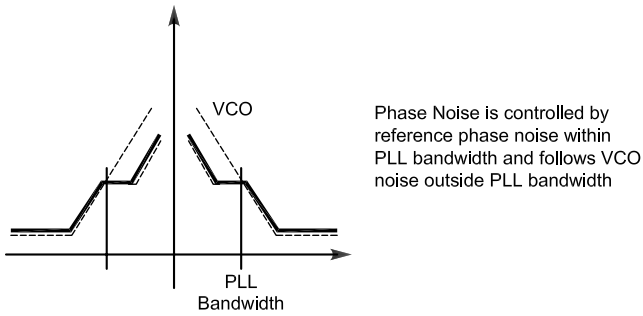


Fig 18—Phase noise of an oscillator controlled by a phase-locked loop.

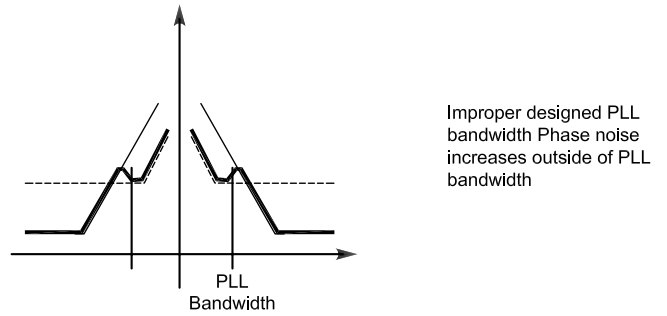


Fig 19—The effect of improper loop-filter design.

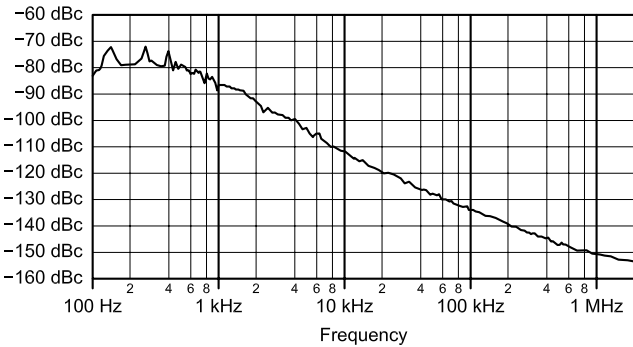


Fig 20—Measured phase noise of the Rohde & Schwarz SMY signal generator at 1 GHz. This signal generator has no provision for digital modulation and therefore shows the best possible phase noise in its class.

modulation—a form of intermodulation—in which one or more AM signals present in a network amplitude-modulate all signals present in the network. Angle-modulation-based wireless systems are largely immune to such effects. Figs 7 and 8 graph the results of gain compression, two-tone intermodulation, cross-modulation and triple-beat testing on a wideband (5 to 1000 MHz) amplifier.

Noise Power Ratio

Triple-beat testing is one way of improving on two-tone testing as a means of evaluating a network's intermodulation behavior in the presence of multiple signals. Another figure of merit—*noise power ratio (NPR)*—uses thermal noise as a test signal. The test measures the introduction, by intermodulation, of noise into a quiet slot created by the insertion of a band-stop filter between the noise generator and the network under test (Fig 9). The filter stopband width is equal to the width of the measurement channel.

Large-Signal Effects

Except for P_{-1dB} , the figures of merit discussed so far evaluate amplitude nonlinearity under small-signal conditions. At input powers that drive a network into gain compression and saturation, intermodulation products of odd orders higher than three become significant. Curves, dips and nulls appear in their characteristics (Fig 10). Phase shifts related to nonlinear (primarily voltage-dependent) capacitances in solid-state devices are one cause of these effects. Under such conditions a network may exhibit hysteresis, with its behavior at any given instant

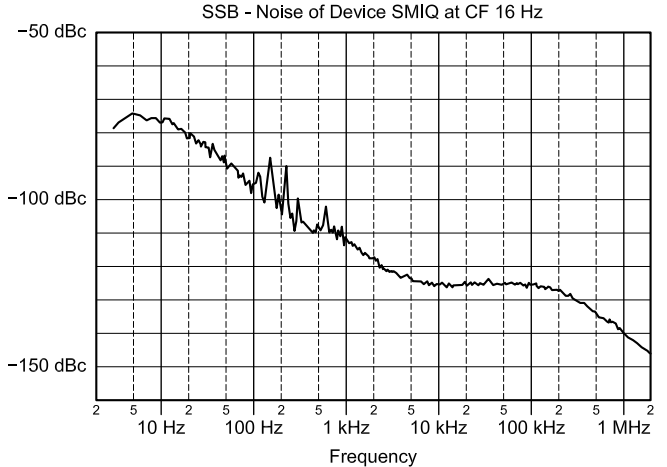


Fig 21—Measured phase noise of the Rohde & Schwarz SMIQ signal generator at 1 GHz. This signal generator is optimized for all digital modulation capabilities and can be configured via appropriate programming. Above 10 kHz, the influence of the wide-bandwidth loop becomes noticeable; above 200 kHz, the resonator Q takes over.

depending not only on the voltage or current applied to it, but also on its recent history.

AM-to-PM Conversion

The nonlinear distortion effects we've discussed so far can be termed *AM-to-AM distortion*. Such distortion, to a degree, depends on the amplitude of the signal(s) applied to the network and results in changes in the network's gain and/or production of signals at new frequencies. AM-to-PM distortion can also occur. As a network nears saturation, part of the driving signal shifts the bias point(s) of the active device(s). This changes their drive-dependent reactances and shifts the phase of the output signal relative to its value at input levels below compression (Figs 11 and 12). This effect, *AM-to-PM conversion*, can cause incidental phase modulation that degrades the performance of digital communication systems.

Spectral Regrowth and Adjacent-Channel Power Ratio

Spectral regrowth occurs largely because of third-, fifth- and seventh-order IMD in power amplifiers operated near or in compression. That is, at power levels where hysteretic intermodulation effects result in poor agreement between measured behavior and predictions based on

small-signal intermodulation figures of merit. We therefore evaluate the impact of spectral regrowth more directly, using a figure of merit called *adjacent-channel power ratio* (ACPR). ACPR measurement techniques that incorporate memory can be used to increase ACPR predictions for networks that exhibit saturation hysteresis. Fig 13 shows the critical relationship between compression, power-added efficiency and ACPR in a MESFET power amplifier.

Phase Response Issues and Figures of Merit

We have already seen how large-signal nonlinear distortion can result in amplitude-dependent phase shifts through AM-to-PM conversion. Because phase linearity is critical at *all* signal levels in PM systems, especially those using digital modulation, we must also consider linear distortion in evaluating networks used in wireless systems.

Differential Group Delay

Every frequency-selective network subjects signals passing through it to some degree of time delay. Ideally, this delay (also known as *group* or *envelope delay*) does not vary with frequency. That is, the network's phase-shift versus frequency response is monotonic and linear. In practice, a network's time delay varies across its passband, transition bands and stopbands, exhibiting curvature, ripple and transition-band peaks (Fig 14). The network's *differential* group delay—its group-delay spread—is therefore of considerable importance. This is especially so in digitally modulated systems, where the resulting phase distortion can cause errors in modulation and demodulation.

Effects of Phase Noise

The phase of an oscillator's output signal is subject to random phase variations (Figs 15 and 16). Called *phase noise*, this effect is often quantified as the decibel ratio of the phase-noise power in a single phase-noise sideband (a 1-Hz bandwidth centered at a specified frequency offset from the oscillator carrier) to the carrier power (Fig 17). Alternatively, it may be specified in degrees RMS. A microwave voltage-controlled oscillator, for instance, might exhibit an SSB phase noise of -95 dBc/Hz at 10 kHz. Oscillator phase noise may manifest itself, through a mechanism known as *reciprocal mixing*, as the emission of unacceptably strong noise outside a transmitter's occupied bandwidth or as an increase in receiver noise floor. Phase noise may also directly introduce phase errors that cause modulation and demodulation errors.

Because the oscillators used for frequency translation in wireless systems are usually embedded in phase-locked loops, their phase-noise characteristics differ from those of "bare" oscillators, as shown in Figs 18 and 19. Figs 20

and 21 show the measured phase noise of the Rohde & Schwarz SMY and SMIQ signal generators. The SMY is a low-cost signal source, while the SMIQ is a very high performance signal generator, which can be programmed for all digital modulations. Therefore, their PLL systems exhibit different phase-noise-versus-frequency responses as the measured results show.

Reciprocal Mixing

In reciprocal mixing, incoming signals mix with LO-sideband energy to produce an IF output (Fig 22). Because one of the two signals is usually noise, the resulting IF output is usually noise. Reciprocal-mixing effects are not limited to noise. Discrete-frequency oscillator sideband components, such as those resulting from crosstalk to, or reference energy on, a VCO control line, or the discrete-frequency spurious signals endemic to direct digital synthesis, can also mix incoming signals to IF. In practice, the resulting noise-floor increase can compromise the receiver's ability to detect weak signals and achieve a high IMD dynamic range. On the test bench, noise from reciprocal mixing may invalidate desensitization,

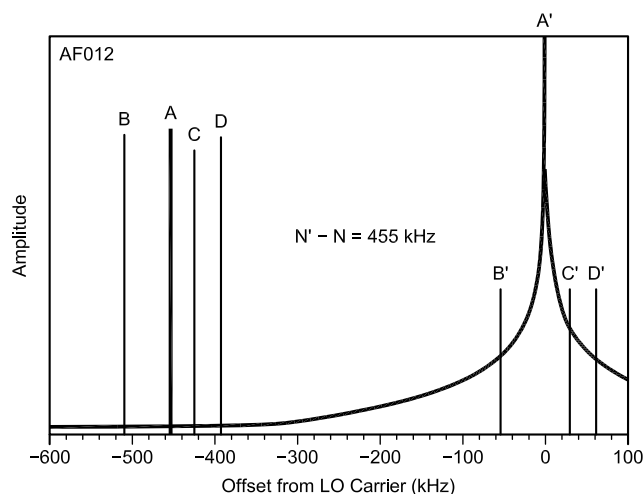


Fig 22—Reciprocal mixing occurs when incoming signals mix energy from an oscillator's sidebands to the IF. In this example, the oscillator is tuned so that its carrier, at A', heterodynes with the desired signal, A, to the 455-kHz IF as intended. At the same time, the undesired signals B, C and D mix the oscillator noise-sideband energy at B', C' and D', respectively, to the IF. Depending on the levels of the interfering signals and the noise-sideband energy, the result may be a significant rise in the receiver noise floor.

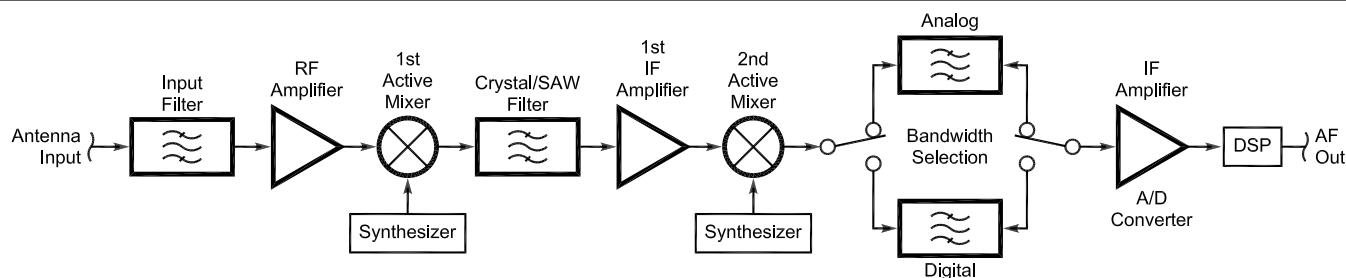


Fig 23—Block diagram of an analog/digital receiver showing the signal path from antenna to audio output. No AGC or other auxiliary circuits are shown. This receiver principle can be used for all types of modulation, since the demodulation is done in the DSP block.

cross-modulation and intermodulation testing by obscuring the weak signals that must be measured in these tests.

Fig 23 shows a typical arrangement of a dual-conversion receiver with local oscillators. The signal com-

ing from the antenna is filtered by an arrangement of tuned circuits referred to as providing *input selectivity*. For a minimum attenuation in the passband, an operating bandwidth must be

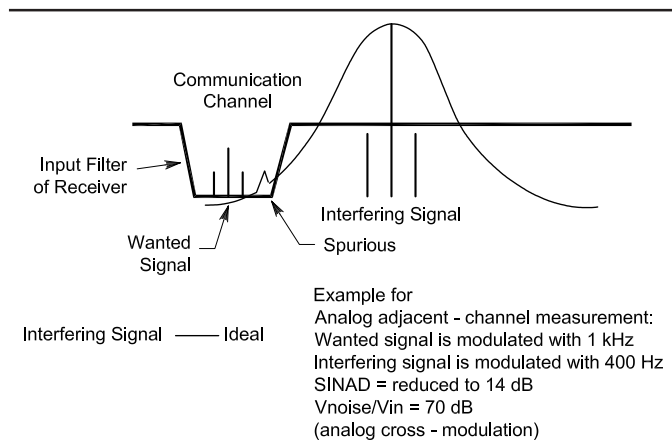


Fig 24—The principle of selectivity-measurement for analog receivers.

Fig 25—(right) The principle of selectivity-measurement for digital receivers.

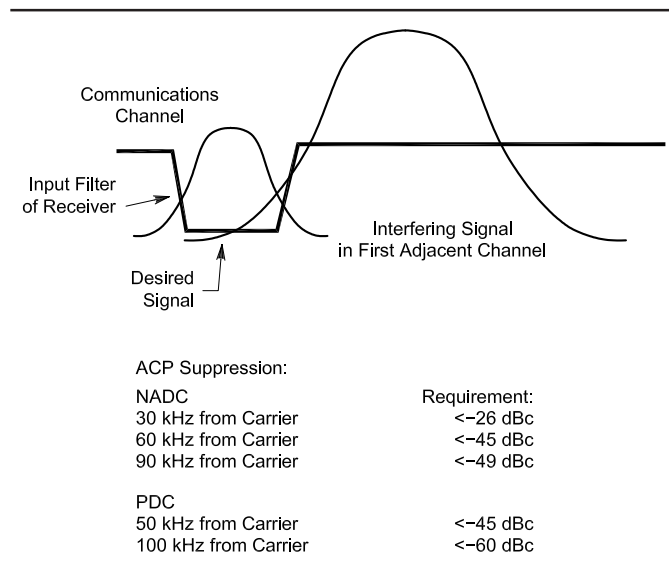


Table 2—Level Diagram of a 2.4-GHz Receiver

Calculation of IP_3

1. Module1: $IP_3 = \infty$
2. Module2: $IP_3 = 23.2 \text{ dBm} = 209 \text{ mW}$
3. Module3: $IP_3 = \infty$
4. Module4: $IP_3 = 31 - (-0.2 + 3.0 - 0.2) = 31.4 \text{ dBm} = 1380.384 \text{ mW}$
5. Module5: $IP_3 = \infty$
6. Module6: $IP_3 = 140 - (-0.2 + 3.0 - 0.2 - 6.0 - 0.2) = 143.6 \text{ dBm}$
 Input- $IP_3 = 2.29086E14 \text{ mW}$

$$IP_{3(2.4\text{GHz_Receiver})} = \frac{1}{\sum_{i=1}^6 \left(\frac{1}{IP_3(\text{module})} \right)}$$

$$= \frac{1}{\frac{1}{\infty} + \frac{1}{209} + \frac{1}{\infty} + \frac{1}{1380.384} + \frac{1}{\infty} + \frac{1}{2.29086E14}} = \frac{1}{0.0055091} = 181.51$$

$$= 181.51 \text{ mW} = 22.58 \text{ dBm}$$

Calculation of NF

1. Module1: NF=0.2 dB: F=1.04712
2. Module2: NF=1 dB: F=1.2589
3. Module3: NF=0.2 dB: F=1.04712
4. Module4: NF=6 dB: F=3.98107
5. Module5: NF=0.2 dB: F=1.04712
6. Module6: NF= 2 dB: F=1.58489

$$F_{\text{Total}} = F_1 + \frac{F_2 - 1}{G_1} + \frac{F_3 - 1}{G_1 G_2} + \frac{F_4 - 1}{G_1 G_2 G_3} + \dots$$

$$F = 1.04712 + 0.261 + 0.0001205 + 0.06 + 0.01 + 0.054 = 1.4322$$

$$NF = 1.56 \text{ dB}$$

$$BW = \frac{f}{\sqrt{2} \cdot Q_L} \quad (\text{Eq 20})$$

This approximation formula is valid for the insertion loss of about 1 dB due to loaded Q .

The filter in the first IF is typically either a SAW filter (from 500 MHz to 1 GHz) or a crystal filter (from 45 to 120 MHz) with a typical insertion loss of 6 dB. Since these

resonators have significantly higher Q s than LC circuits, the bandwidth for the first IF will vary from ± 5 kHz to ± 500 kHz. It is now obvious that the first RF filter does not protect the first IF because of its wider bandwidth. For typical communication receivers, IF bandwidths from 150 Hz to 1 MHz are found. For digital modulation, the bandwidth varies roughly from 30 kHz to 1 MHz. Therefore, the IF filter in the second IF must accommodate these bandwidths; other-

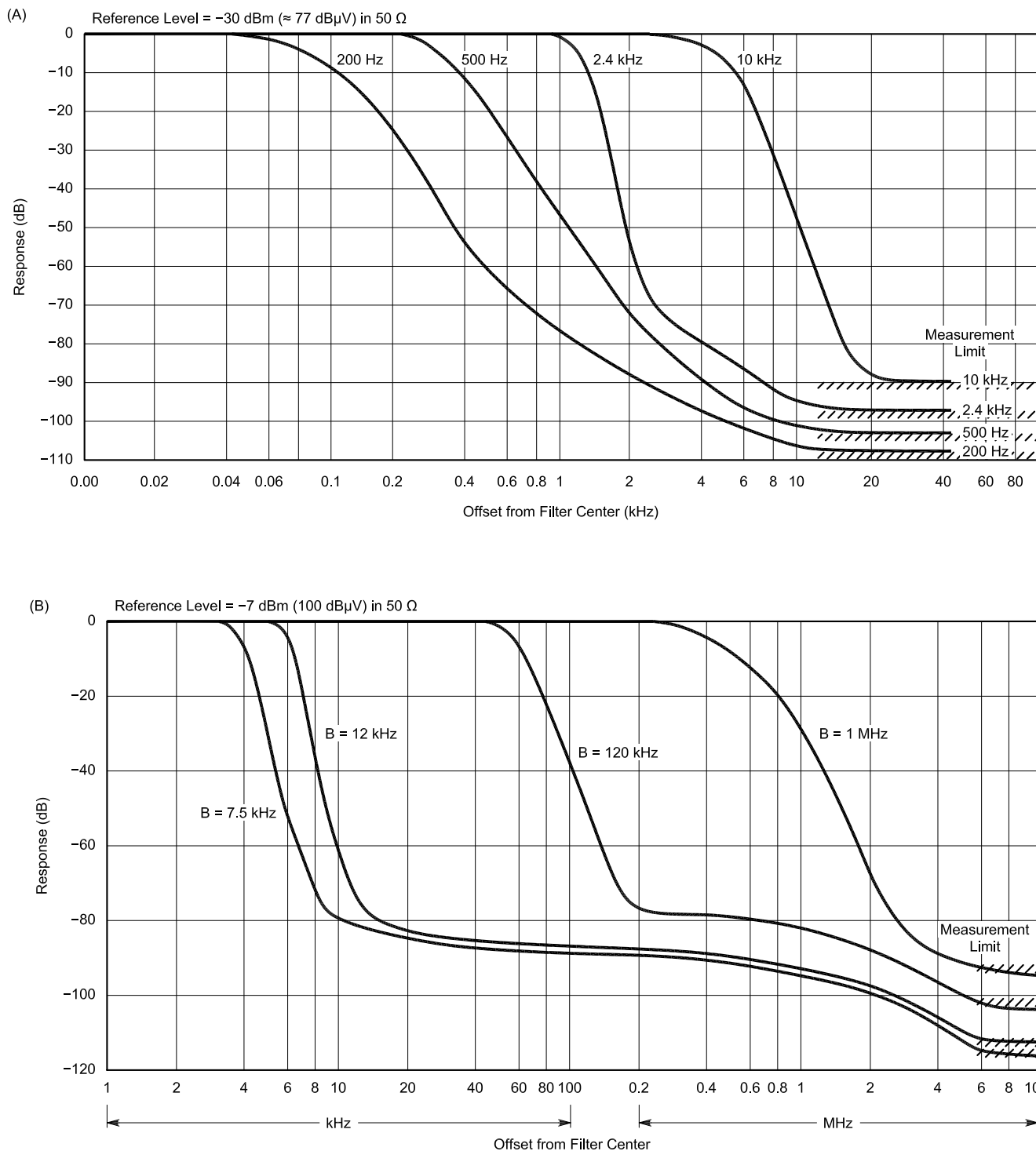
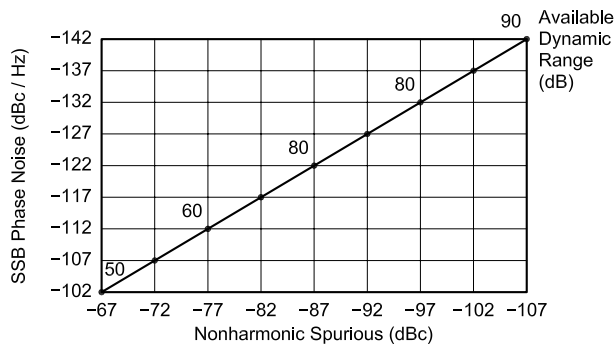


Fig 26—Dynamic selectivity versus IF bandwidth for (A) the Rohde & Schwarz ESH-2 test receiver (9 kHz to 30 MHz) and (B) the Rohde and Schwarz ESV test receiver (10 MHz to 1 GHz). Reciprocal mixing widens the ESH-2's 2.4 kHz response below -70 dB (-100 dBm) at (A) and the ESV's 7.5, 12 and 120 kHz responses below approximately -80 dB (-87 dBm) at (B).

wise, the second mixer is easily overloaded. This also means that both synthesizer paths must be designed for minimum noise and spurious emissions. The second IF of this arrangement (Fig 23) can be either analog or digital, or it may even be a zero-IF. There are good reasons for using IFs at 50/3 kHz (like the Walkman), with DSP using low-cost modules found in mass-market consumer products.

The following two pictures (Figs 24 and 25) show the principle of selectivity measurement for both analog and digital signals. The main difference is that the occupied bandwidth for the digital system can be significantly wider, and yet both signals can be interfered with either by a noise synthesizer/first LO or a synthesizer that has unwanted spurious frequencies. Such a spurious signal is shown in Fig 24. In the case of Fig 24, the analog adjacent-channel measurement has some of the characteristics of cross-modulation and intermodulation, while in the digital system the problem with the adjacent-channel power suppression in modern terms is more obvious. Rarely has the concept of adjacent-channel power (ACP) been used with analog systems. Also, to meet the standards, requires signal generators that are better, with some headroom, than the required dynamic measurement. We have therefore included in Fig 25 the achievable



6 dB Reserve for Errors Less than 1 dB
Carrier - to - Spurious Ratio for 14 dB SINAD = 11 dB
Carrier - to - Noise for 14 dB SINAD = 46 dB

Fig 27—This graph shows the available dynamic range, which is determined by either masking of the unwanted signal by phase noise or by discrete spuri. As far as the culprit synthesizer is concerned, it can be either the local oscillator or the effect of a strong adjacent-channel signal that takes over the function of the local oscillator.

performance for a practical signal generator—in this case, the Rohde & Schwarz SMHU58.

Because reciprocal mixing produces the effect of noise leakage around IF filtering, it plays a role in determining a receiver's dynamic selectivity (Fig 26). There is little value in using IF filters with stopband rejection more than 3 to 10 dB beyond that which results in an acceptable reciprocal mixing level. Although additional RF selectivity can reduce the number of signals that contribute to the noise, improving the LO's spectral purity is the only effective way to reduce reciprocal mixing noise from *all* signals present at a mixer's RF port.

Factoring in the effect of discrete spurious signals with that of oscillator phase noise can give us the useful dynamic range of which an instrument or receiver is capable (Fig 27).

An Example of a Receiver System

Fig 28 shows a level diagram of a high-performance receiver for analyzing the noise and gain distribution. This receiver consists of a band-pass filter centered at 2.4 GHz, an amplifier stage marked "two" (for two-port) with its electrical characteristics attached and another band-pass filter. The signal then is applied to a high-level mixer with a third-order intercept point of 25 dBm. The down-converter signal is filtered in a band-pass filter and applied to a broadband, high-gain amplifier chain. This is a typical front end, as we would expect it at a base station for CDMA applications.

The purpose of this block diagram is to show how the calculation of noise figure and intercept point is done properly. By applying the equations discussed earlier, the complete calculation is shown in Table 2 for the 2.4-GHz receiver. Here are the design steps:

1. Transfer all input intercept points to the system input, subtracting gains and adding losses decibel-for-decibel.
2. Convert intercept points to powers (dBm to milliwatts). We have IP_1, IP_2, \dots, IP_N for N elements.
3. Assuming all input intercept points are independent and uncorrelated, add powers in "parallel."
4. Convert IP_3 input from power (milliwatts) to dBm.

Notes

- ¹U. Rohde and D. Newkirk, *RF/Microwave Circuit Design for Wireless Applications*, (Indianapolis, Indiana: John Wiley & Sons, April 2000) ISBN 0-471-29818-2; customer@wiley.com.
- ²P. Vizmuller, *RF Design Guide—Systems, Circuits and Equations*, (Norwood, Massachusetts: Artech House, 1995) ISBN 0-89006-754-6.

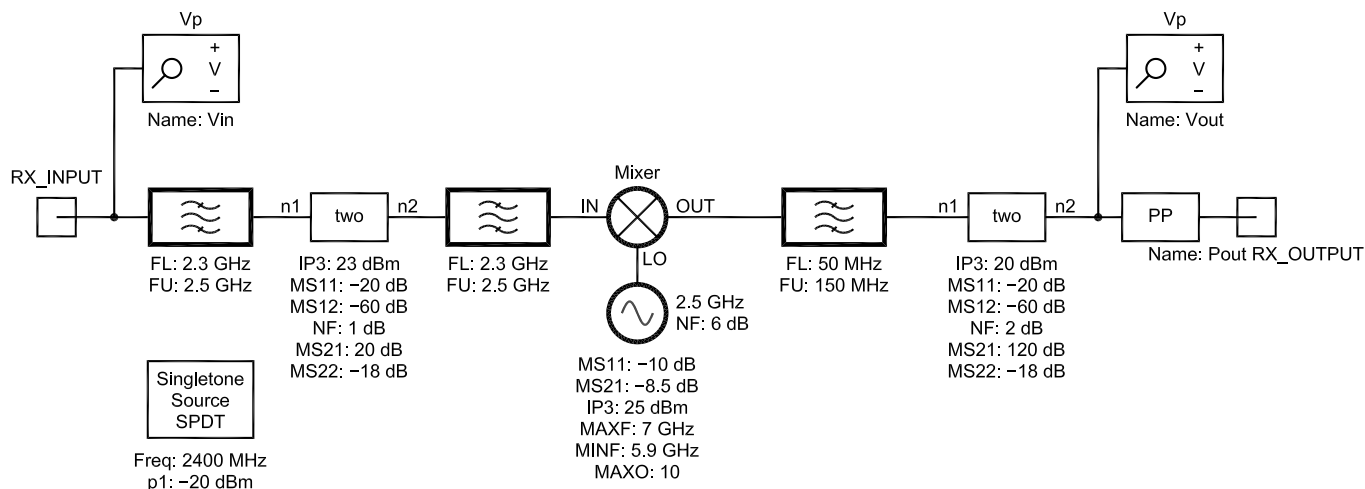


Fig 28—A level diagram of a high-performance 2.4-GHz receiver front-end.

A 700-W Switch-Mode Transmitter for 137 kHz

*This European project makes a lot of VLF power.
With our new allocation, it's adaptable for
US application, as well.*

By Andy Talbot, G4JNT

This project was inspired by the design of the transmitters used for the old Decca Navigator system operating in the 70-150 kHz bands. Decca was decommissioned in 1999, and the hardware from some of the UK-based transmitters became available to the amateur community a couple of years ago. Many of these units were adapted and retuned for use in the 137-kHz and 73-kHz bands, providing RF output of around 1 kW

15 Noble Rd
Hedge End, Southampton
SO30 0PH United Kingdom
g4jnt@thersgb.net

with high reliability under continuous operation for many hours.

The high-power design presented here is not meant purely as a constructional article. Rather, it describes the route I followed to come up with a successful design. It includes enough information and design detail so that experienced constructors can produce a similar unit. *Construction by those without experience in high-power, high-voltage circuitry is not advised.* Particularly, the unit contains some potentially dangerous circuit features such as direct connection to the ac mains and strong RF fields. It has quite a lot in common with modern switch-mode power sup-

plies, however, so anyone confident with these units should have no qualms about constructing this transmitter. Anyone who has built high-power tube amplifiers should be confident enough at these voltage levels.

Decca Transmitter Design

Decca navigation transmitters differ from traditional power amplifiers designed for amateur use in that the Decca units operated at one frequency each, transmitting a pulsed, unmodulated carrier. The constant amplitude of the unmodulated signal meant that a very high-efficiency switching power amplifier could be used. In this

type of design, the output devices are switched either fully on or fully off (saturated or cutoff) at the carrier frequency. This means that power losses in the circuit are minimal; the main loss mechanisms are device on-resistance and passive components.

The well-known class-C power amplifier used for FM operation is part way to being a switching design, and can sometimes achieve a dc power-to-RF conversion efficiency as high as 70%. As in all such nonlinear power amplifiers, the very high harmonic content of the generated waveform—a square wave—is removed by filtering. It is here that even higher efficiencies become possible by choosing a filtering system that returns harmonic energy, rectified and filtered, to the power amplifier to be used again. By optimizing the switching topology so that the devices switch at the optimum point in the conduction cycle, the zero-crossing point, efficiency can be improved to beyond 90%. Various measurements made on samples of the surplus Decca units showed efficiencies around 90-95%. In fact, one user even tried to claim the impossible value of 102%—so we can see that measurement accuracy has a lot to answer for!

The basic concept for the Decca transmitters is given in Fig 1. Three identical modules, each delivering up to 400 W, are combined in an output transformer that effectively connects all three in series for an output of 1200 W total. Each module contains four power MOSFETs in a full-bridge configuration, where diagonal pairs of devices are alternately switched on and off. The result is to alternately switch the polarity of the 50-V supply across the load, giving a 100-V pk-pk square wave. The FETs in each arm of the bridge are driven via a very simple transformer, wound on a ferrite pot core with multiple secondary windings, one for each gate. Direct gate drive with separate secondary windings gives the necessary voltage isolation for driving top and bottom devices and makes design of the driver circuitry straightforward.

The output is filtered by a single tank circuit, forming a series-resonant tuned circuit. An inductor-capacitor combination resonated at the desired frequency is placed in series with the connection from the bridge output terminal to the load, resulting in three tanks in series with each of the combining transformer primaries. Because the circuit is series-resonant,

only energy at the fundamental frequency can pass through to the load, and the current at harmonic frequencies is blocked. The effect is to cause the power-amplifier devices to switch at the zero-crossing point of the ac waveform, at current minimum, so reducing device dissipation. For optimum filtering of harmonics, the tank-circuit Q —the ratio of the reactance of C or L at resonance to series load resistance—must be as high as possible. However, the voltage across each element of the tuned circuit is magnified by the Q factor, meaning that some quite high voltages can easily appear. Information gleaned from members of the original Decca manufacturing team and examination of the units revealed that a loaded Q in the region of 5 to 6 was used.

If the switching devices were perfect, the design could be as simple as that shown in Fig 1, but the practicalities of MOSFETs require a more complex circuit configuration to avoid blowing up the transmitter. While power MOSFETs can be switched on very quickly after gate drive is suddenly applied, they do not switch off immediately when it is removed: There is a delay of a few nanoseconds. While this may not seem very

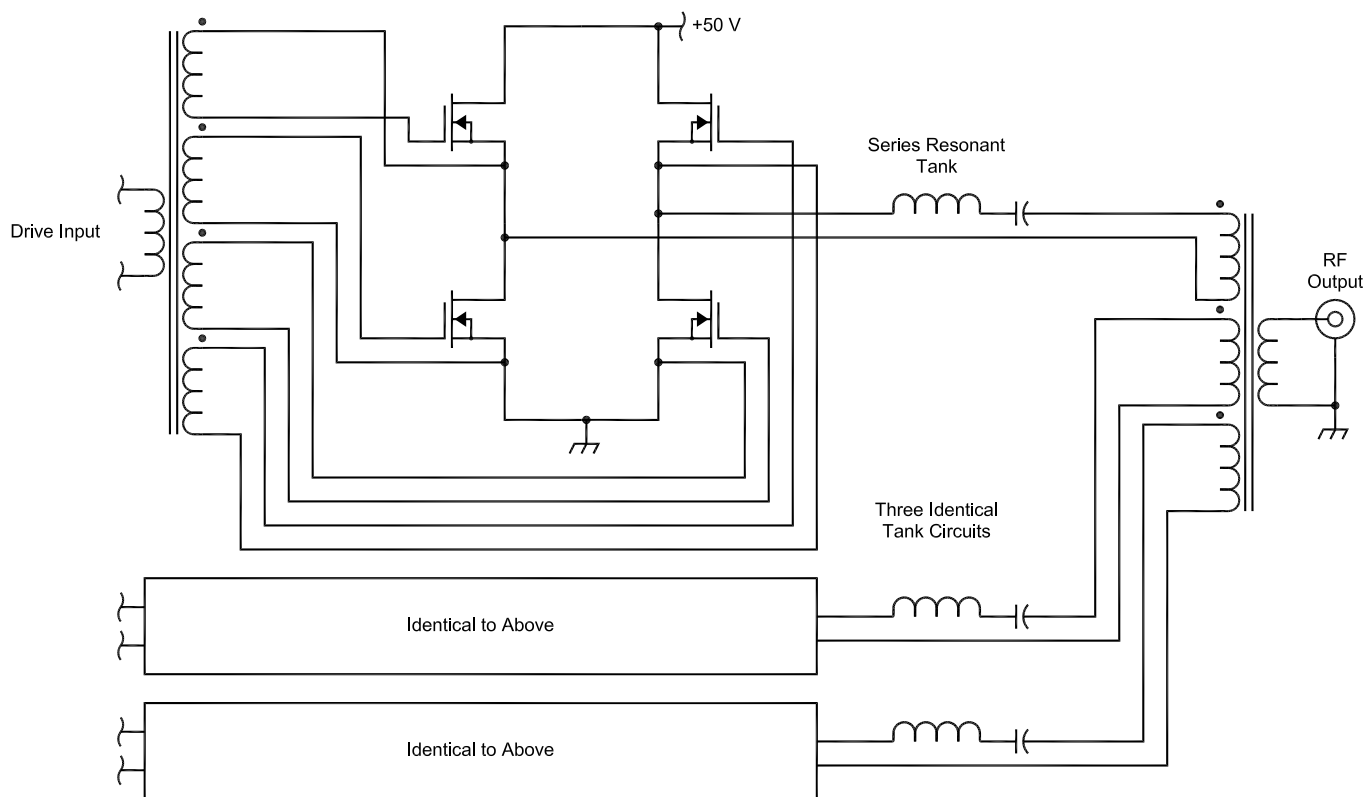


Fig 1—Decca Transmitter outline design.

long, it results in both pairs of devices being switched on for a few nanoseconds, shorting out the supply and leading quickly to device destruction. In switch-mode power supplies, this problem is overcome by allowing a period of dead time when both devices are off. This period is usually part of the voltage-regulation process in switchers anyway.

Allowing a dead period for the transmitter adds considerably to circuit complexity. The upper and lower devices now need separate drive waveforms as they are no longer both switched alternately, and another approach was adopted here. A small inductor is added between the upper and lower switching devices, as shown in the circuitry around the switching devices in Fig 2. Now, during the short time when both devices are on, the switching transient current merely causes a gradual buildup of stored energy in this inductor that is safely returned to the circuit when the transition is completed. A low-value damping resistor across this kills any high-voltage spikes that may appear should both devices be switched off simultaneously.

The final extra components are the diodes cross-connected from the ends of this inductor to the two power supply rails. The purpose of these is twofold: They return unused harmonic energy to the supply, contributing to the high efficiency of the power amplifier, and they clamp the maximum voltage across each device so that it cannot exceed that of the supply voltage. There is also a very crafty and elegant guard circuit to protect against output short circuits, but more about that later.

Extremely good reliability of the Decca transmitters was maintained by using 200-V-rated devices on a supply rail of 50-60 V, and by choosing devices with a very generous current rating. The design is vindicated by the Decca team statement that only one transmitter ever failed in service in 20 years of continuous operation! However, I had two main objections to using a surplus Decca unit. The main reasons were that I did not have one and all had been sold. The other criterion was the requirement for a high-current, 50-V power supply.

A 700-W Power Amplifier Design

A few years ago when the 73-kHz band became available, I tried making a transmitter based on switch-mode power-supply unit (SMPSU) practice. I directly rectified the mains to give approximately 340 V, then switched this using a half bridge (a

pair of 500-V MOSFETs) into a ferrite-core transformer for isolation and impedance matching. Filtering was performed by a conventional low-pass π -network. As I had never seen MOSFETs directly driven by a transformer without extra dc-restoration components, I instead used a proper high-side/low-side bridged MOSFET driver chip, again following SMPSU practice. The design did indeed work to an extent, but efficiency was only around 80% and I blew several FETs accompanied by loud bangs and flashes. While these devices were cheap, and I had plenty from dismantling old surplus SMPSUs, the driver chips that were destroyed each time a FET blew certainly were not! This project was rapidly shelved, and it remained there for several years.

Being taken by the Decca design, particularly the series-tuned tank concept, I decided to make a version powered directly from rectified mains. A very careful examination of the circuit followed, where I was determined to understand fully the precise functioning of every single component. The use of three identical modules was overkill; I did not need the super high reliability this would give, and having three tank circuits as well would just be silly! A few calculations soon showed that by making use of the 340 V possible by placing a bridge rectifier directly across the mains supply, some quite astronomical power levels could be theoretically achieved with just the one output stage. I already had a suitable PSU module on a PC board from an earlier abandoned 700-W SMPSU project. This was made up of a 10-A bridge rectifier, 1000 μF of supply decoupling and plenty of input-filtering and transient-suppres-

sion components. Most of these components came from dismantling old SMPSUs, so the design of mains input filtering was just lifted from these surplus units.

Now for a few back-of-envelope calculations to determine the major component values and their ratings. Initially, we will assume the use of low-cost 500-V MOSFETs in full bridge—such as the IRF840—which can switch 3A comfortably. A 340-V rail in the full-bridge configuration could give a 680-V peak square wave, and at 3 A this is nearly 2 kW! For a first breadboard design, even the thought of this was quite scary and I was sure my LF antenna and loading coil would not survive this sort of power without catching fire or melting.

So, how about a half-bridge design again? Here, the switching voltage is 340 V pk-pk; so again keeping to a current of 3 A, we can get theoretically over 900 W, which sounded rather safer. Refer to Fig 3 for the schematic for the complete transmitter.

Tank and Output-Circuit Design

Changing the supply voltage and going from full-bridge to half-bridge topology means the load impedance for the required output power changes from that in the Decca design, so the tank component values will be different. The load impedance is calculated as follows.

Peak-to-peak square-wave voltage across the load resistance, after allowing for voltage droop and losses in the PSU, will end up at around 320 V. The fundamental frequency component of a square wave has a peak amplitude greater than the peak square-wave voltage by a factor of $4/\pi$ —ie, 1.27 times higher—because of all those odd

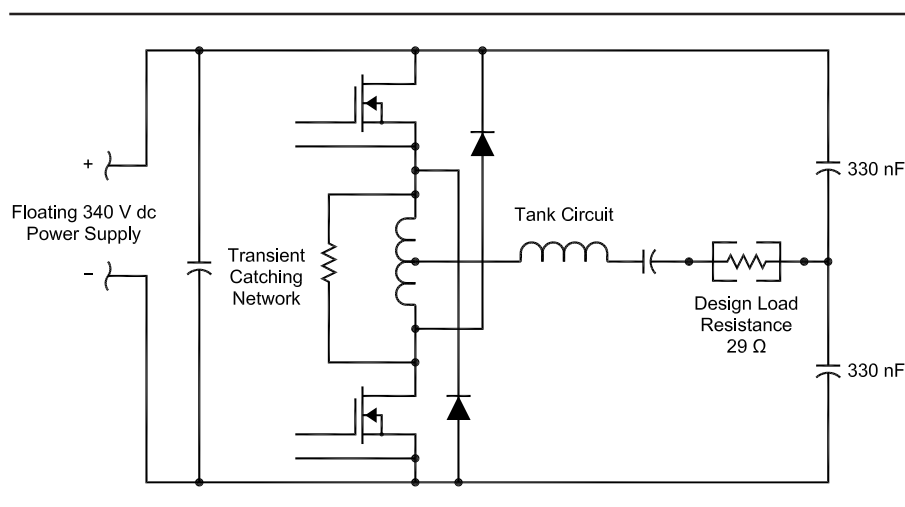


Fig 2—Circuitry around the switching devices.

harmonics combining to flatten the waveform. The resultant filtered sine wave across the load resistance therefore becomes 407 V pk-pk, or 144 V RMS. Having roughly estimated a potential maximum power of 900 W based on device switching capabilities, we need to reduce it a fair bit to allow for rectifier and PSU losses, so assume a power of 700 W maximum. This corresponds to an RMS load current of $700\text{ W} / 144\text{ V} = 4.86\text{ A}$ —again greater than that of the input square wave because of the $4/\pi$ factor. To achieve this value, a load resistance of $144 / 4.86 = 29.6\ \Omega$ would be required, which would be matched to the antenna impedance by a transformer.

For a Q in the region of six, the reactance of the capacitors and inductor making up the tank would need to be about $160\ \Omega$ each. At 137 kHz, this means around 7260 pF and 186 μH , respectively, and the voltage across each would be $(144)(6) = 864\text{ V RMS}$, or over 1.2 kV peak. This total capacitance was made up from a series-parallel combination of 1700-V, 3.3-nF polyester caps, with several 220-pF, 1-kV-rated disc ceramic capacitors added across half of the series legs to fine-tune the combination. The tank inductor was wound using PVC-covered Litz wire (obtained from the same source as the Decca transmitters), which could easily cope with 2 kV between windings. The coil form chosen was a piece of drain pipe approximately 44 mm in diameter; coil dimensions were estimated by applying Rayner's formula for single-layer coils:

$$L(\mu\text{H}) = \frac{(ND)^2}{(460D + 1020G)} \quad (\text{Eq 1})$$

Where D = diameter, G = coil length (both in millimeters) and N = number of turns. This suggests that around 200 turns would be needed for a single-layer coil, which was impractically long since the Litz wire was nearly 3 mm in diameter. So the coil was wound in three layers and the number of turns adjusted to get close to resonance with the calculated capacitance. The much shorter length and larger overall diameter of the multilayer coils meant that the total number of turns needed was now around only 120.

At this sort of power level, the output-transformer specification could have proved difficult. The largest SMPSU transformer core commonly available, the ETD49 shape using 3C85 material was tried. For SMPSU use, this core is rated to typically about 400 W, keeping temperature rise within acceptable limits. Here, how-

ever, the transformer is carrying a sine wave rather than the more usual switching waveform, so it will operate satisfactorily at significantly higher power levels. To calculate the number of turns needed on the primary, the standard equation used with all cored inductors used with sinusoidal waveforms was employed:

$$V(\text{RMS}) = 4.44 f n A_e B \quad (\text{Eq 2})$$

Where f = frequency in hertz, n = number of turns, A_e = core cross-sectional area in mm^2 , and B is the maximum permitted magnetic field strength for the ferrite used. With the core specified, A_e is $200\ \text{mm}^2$, and B is kept down to 0.1 tesla maximum—well below saturation, which usually occurs around 0.25 to 0.3 T. So for a full-power primary voltage of 144 V using this core, a minimum of 12 turns are needed; to allow a margin, 15 turns were used. The secondary must be tapped to match a range of impedances, from $50\ \Omega$ for testing purposes, up in stages to $150\ \Omega$ for my antenna in wet weather. Since the power amplifier wants to see a load of around $30\ \Omega$, the turns ratio needed to be in the range $(50/30)^{1/2}$ to $(150/30)^{1/2}$; that is, in the range of 1.3-2.3. So for 15 turns on the primary, the secondary was tapped at 19, 22, 25, 29 and 33 turns. A ceramic switch originally designed for HF ATU use was employed here to switch taps. Remember this item!

The small coil between the upper and lower devices to absorb switching transients came next on the design program. Looking at the coil on the Decca units, and plugging the measured dimensions into Rayner's formula, the value was estimated as $1\ \mu\text{H}$, shunted by $27\ \Omega$. Well, I was using a higher supply voltage by a factor of over six times, but with reduced current through the devices so the switching transients would not be so bad—let's try making it three times bigger. As I had a few of them, the damping resistor became two $56\text{-}\Omega$, 2-W carbon devices in parallel; although at this frequency, a wire-wound resistor would have been quite acceptable.

Driver Circuitry

The gate drive to the MOSFETs needs to be a square wave with very fast rise and fall times. It also has to be very near to a 50% duty cycle to ensure equal device dissipation and maximum efficiency. Fortunately, there are plenty of MOSFET driver chips around for just this sort of job, and since a transformer is used to

drive the gates, the chip would not be destroyed if (or when!) the FET devices blew. (Most driver chips contain a pair of devices, and it may be possible to use both in push-pull to get more drive capability. This has not been tried and is not needed for driving two FETs, but it may become necessary if four FETs are used in a full bridge.) With a transformer in this position, a capacitor becomes essential to remove the dc component from the 0-15 V output supplied from the driver chip. The drive transformer does not need to carry a lot of power, but as it provides the vital safety isolation barrier, it needs to be properly constructed. The windings need to be of well-insulated wire, so a larger core is needed for the turns and insulation than what would have been required to carry the drive power alone. I used an RM10 pot core made of 3C85 material. It turned out to be just large enough to accept $12 + 12$ turns of PTFE insulated wire for the secondary (the safety insulation) and 12 turns of normal enameled wire for the primary. This is all a bit tight and an RM12 size core would be better in this position.

Since I wanted binary phase-shift keying (BPSK) modulation as well as on-off keying for LF use, the MOSFET driver chip was controlled by TTL logic designed to provide four phase states—I had decided to include QPSK as well as BPSK. This necessitated an input drive at four times the output frequency, which came from one of my standard DDS modules,¹ which already had provision for driving at four times the wanted frequency. Any other source—such as VFO, crystal oscillator and so forth—is acceptable provided the drive waveform is TTL-compatible and close to a 1:1 ratio. Another drive circuit making use of a comparator and low-pass filter was tried, allowing use of any arbitrary waveform to drive the transmitter.

A schematic of this alternative drive circuit using a comparator to square up a sinusoidal drive signal is shown in Fig 4. The low-pass filter makes sure that the input to the comparator is a sine wave to force it to generate a symmetrical switching waveform in case a non-ideal drive waveform is applied to the transmitter.

Power Supply

In principle, this need consist only of a bridge rectifier and smoothing capacitors. A 10-A rated bridge rectifier gives ample margin for the

¹Notes appear on page 26.

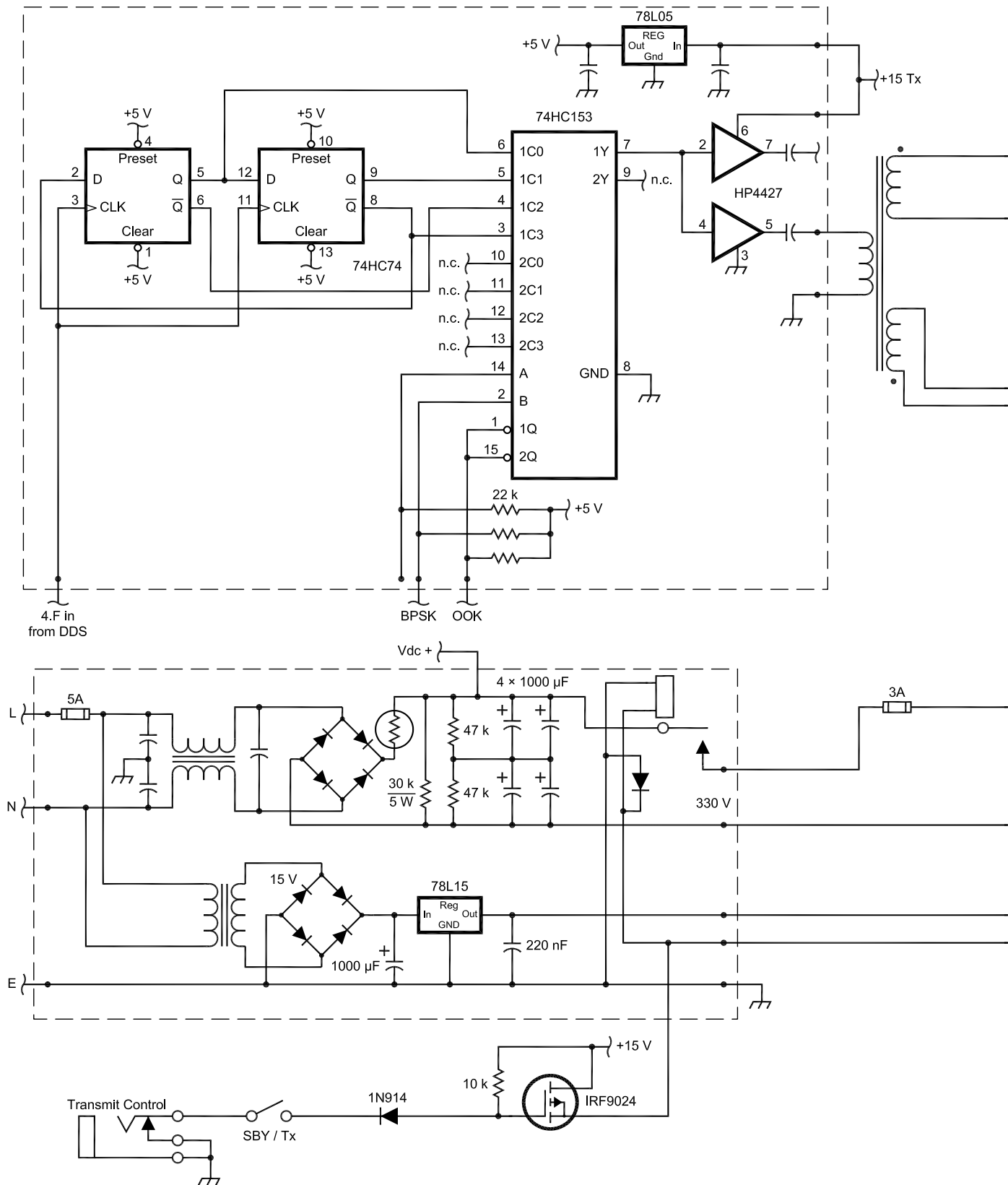


Fig 3—Full 700 W transmitter circuit diagram.

here gives 30 V ripple at a load current of 3 A. This corresponds to approximately 10% ripple, which means 10% AM with sidebands around 30 dB below the carrier. If this is considered too high, the values of smoothing capacitors can be raised. Capacitors rated at 400 V are widely available at values of 1000 μF and higher, but as I had a large surplus stock of 200-V-rated devices, the series-parallel combination shown in Fig 3 was employed.

EMC filtering on the mains input is advisable to prevent LF interference from being fed back along the supply. All switch-mode supplies incorporate such filtering, usually in the form of a dual-wound toroidal choke and mains-rated filter capacitors between the two conductors and from each to ground. The best source of these is often surplus computer power supplies. I also incorporated a thermistor to limit switch-on current. This, too, came from a surplus SMPSU. The last bit of the power supply needed is an isolated low-voltage supply for the driver circuitry and switching relays. Derived from a conventional transformer voltage-regulator assembly, it must supply up to 100 mA for the driver circuitry, plus whatever may be required for fans and relays—typically less than 1 A total.

Safety Notes

As will have become obvious by now, this is a potentially very dangerous project. All the power circuitry is connected directly to the 240-V mains, which, since it is full-wave rectified, means both rectified positive and negative supplies peak at 340 V above ground and average 170 V each. Fur-

thermore, the ac mains supply sometimes has transients on it which can reach kilovolt levels occasionally—albeit just for a few microseconds—because of switching and lightning strikes on some parts of the power network. To enable the FET driver circuitry to be connected to an isolated, ground-referenced source, a mains isolation barrier is essential to ensure there is no direct electrical connection whatsoever between the two circuit halves. This is very conveniently provided by the multi-tapped driver transformer. To ensure proper insulation standards, the windings are wound with good quality PVC- or PTFE-insulated wire rated for mains connections. Similarly, the output circuitry needs isolation. Here, the output transformer performs that function. The primary was wound with the same PVC covered Litz wire as used for the tank coil, which has a voltage rating far in excess of what is required for mains safety isolation.

The final safety issue is that of grounding. With such a large part of the circuitry being connected direct to mains, all metalwork surrounding the finished unit should be very firmly bonded to the mains earth. If a rack-mounted type of enclosure is used, check that each individual metal panel making up the mount is properly bonded. The electrical connection between the metal components is often poor because of their slide fit into anodized aluminum channels and the use of plastic captive nuts.

For all testing, use an isolation transformer! If you need to use a scope on the power-amplifier circuitry, it is essential.

First Tests

At this point, I was satisfied the design was sound and made the first lash-up breadboard on the workbench (Fig 5). The FETs used were surplus IRF840 devices, of which I had many—this fact was to prove extremely useful at this stage! I used a 3 A, 50-V PSU instead of the 340-V rectified mains supply, so I could check out the switching waveforms with a scope and ensure all the circuitry appeared to work as it should. The output load consisted of an old Navy dummy load made up of twelve carbon resistors and (allegedly) rated for 1-kW dissipation. With this 50-V supply, the power amplifier duly delivered the 18 W that would be expected from this voltage rail into the design load impedance, so I was satisfied all was correct. The next stage was the full voltage test. A 1:1 isolation transformer was used to allow direct scope measurements of all waveforms. This was followed by a Variac to allow the supply voltage to be slowly wound up to maximum. Drive was applied, the dummy load connected and (with some trepidation) the supply was slowly wound up while the output voltage waveform, supply voltage and current were continuously monitored. At 100% on the Variac, 320 V was measured as the supply and a sine wave in excess of 230 V peak was across the dummy load—it was working! After several minutes, it was still working and the dummy load was getting quite hot, but so was the heat sink on which the two switching FETs were mounted. Then suddenly, a loud bang and flash and the input fuse blew: Both FETs had shorted. These were replaced, the whole lot tested

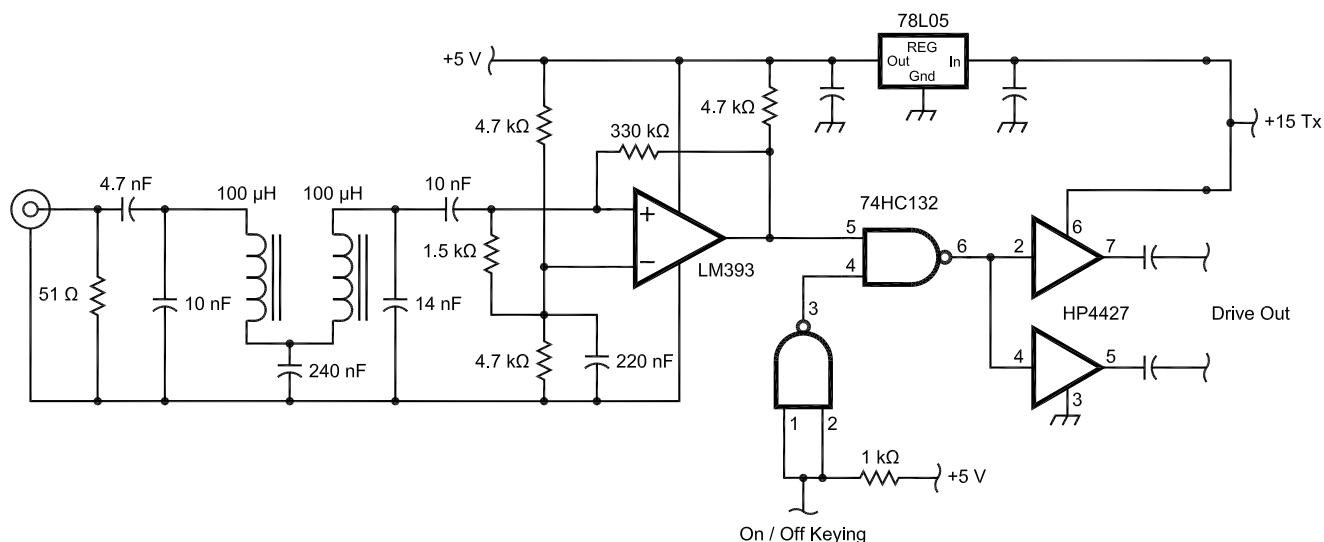


Fig 4—Alternative drive circuit for external input signal.

again by winding up the supply voltage slowly and all worked as before, until—you've guessed—another flash and bang.

It was obvious that the IRF840 devices were being overrun. I also noticed that when probing around the bridge connections with a scope probe, there were a few high-voltage transient pulses at the switching time. Perhaps insufficient decoupling was the problem? A few 10-nF, 1-kV ceramic capacitors were connected across the supply rails close to the FET connections. I also added a couple between $+V_e$ and $-V_e$ rails to the grounded heat sink just in case. Sure enough, the high-voltage transients were killed and by using a fan to cool the heat sink, over 600 W could now be produced for several hours. After this prolonged testing at full power, the output transformer was staying comfortably within its working temperature, so the choice of core and windings was justified, even though it was theoretically working significantly above its specified power rating. I was getting more confident that the transmitter may actually work out!

How about changing the transformer taps to increase power output? As I moved the output switch to its next tap setting while the transmitter was running, a loud flash and bang! I had failed to notice that the rather nice ceramic switch designed for ATUs was make-before-break. As the switch position was changed, there was a brief short circuit across the three turns between the tap positions and this momentary overload was more than sufficient to blow the devices.

At this point, morale fell and I was not too convinced that the design was going to be particularly reliable. The FETs could easily be upgraded to solve the heating problems, but if they were going to be blown by even the briefest of output overloads, this was completely unacceptable for a finished design. I considered various ideas for overload protection, such as supply-current trips, but none could really be considered perfect. It was only after mentioning this problem on the LF e-mail reflector that Jim Moritz, MOBMU, replied with "Have you looked at the Decca protection circuit?" It had never occurred to me that the Decca transmitters would have had exactly the same overload problem! No protection circuits were shown on the simplified diagrams of the Decca units I had examined. Jim had the full diagrams, having obtained one of the original units, and sent me the details. He had also worked out how the protection operates.

Overload Protection Circuitry

Refer to Fig 3. At first sight, this is a rather unusual bit of circuitry to see around a transmitter power amplifier. A second winding over the tank coil feeds via a capacitor to a bridge rectifier; the dc output from this feeds back to the supply rails. How can this provide overload protection?

The functioning of it is as follows. As RF output current through the tank coil rises, the resonant voltage across this rises proportionately: Remember that as the tank has a Q of around 6 in normal operation, the voltage is already in the kilovolt range. Now, arrange the turns ratio of the over winding to give a transformation ratio such that at maximum rated load, after full-wave rectification and smoothing, the dc voltage produced is equal to the supply voltage. The capacitor in series with the link winding is there to tune out its reactance, but operates with a very low loaded Q , in the region of one or two, so no adverse resonance effects are seen.

Now, if any attempt is made to draw any RF current through the tank exceeding the maximum design value, the rectified voltage would try to rise above the supply voltage. As this is directly connected to the dc supply, it obviously cannot rise above the nominal 340 V. Instead, the rectified power feeds back into the dc supply. This is where things get interesting. Power is now being taken from a component—an inductor—that ideally would not be dissipating anything. The effect of pro-

gressively taking more power from the tank is exactly as if a resistor were to be added in series, whose value increases as the overload goes up. The effect is nearly equivalent to operating the transmitter at a constant output current, equal to the maximum rating. Furthermore, by monitoring the dc current being fed back from the guard-circuit rectifier, the degree of overload can be measured.

Calculation of the link winding is not straightforward. If coupling between the two windings were perfect, that is, as if they formed a transformer, then for a tank-circuit loaded Q of 6 the turns ratio ought to be 1:6. However, for an air-core coil such as this, mutual coupling is never perfect and the only way to test the overload protection is to try various numbers of turns for the link coil and see what works. This was obviously not something to be done when operating at full power, so back to the 50-V, 3-A current-limited supply. I initially estimated (read "guessed") that coupling may be in the region of 40%, so I wound on a secondary winding with a turns ratio of 1:4. Overloading the output now did not cause excessive supply current, and the guard current did indeed rise: It worked. By altering the number of turns on the link, it was soon determined that coupling was a bit higher than I had estimated, at around 60%. It also became apparent that the presence of the extra wire around the main tank coil was detuning it, so the resonating capacitance had to be adjusted

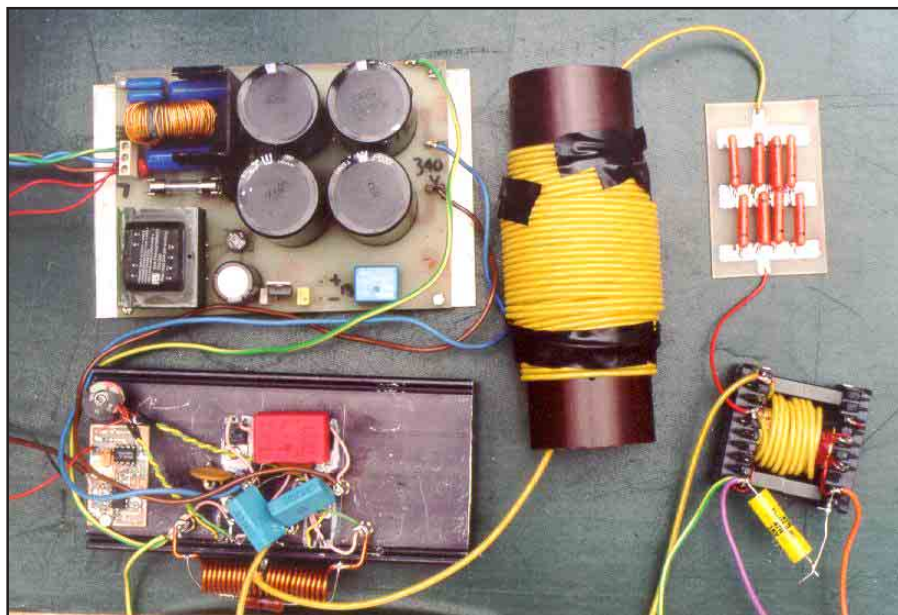


Fig 5—Transmitter components used for breadboarding: top-left, dc power supply; right-hand side, tank components and output matching / isolation transformer; bottom-left, driver and switching components.

by around 10 %. Now, we're ready for the full-power test.

Final Design

Again using the Variac and isolation transformer, power was increased to 600 W, and soak-tested for seven hours: No problems. The carbon resistors in the dummy load were glowing dull red (so much for their 1 kW rating!). The devices on the heat sink were at around 50°C, the output transformer about the same, and the tank coil was running at around 40°C. Those are all quite reasonable figures, especially during the middle of a UK summer. Shorting the output resulted in the devices surviving and only running slightly hotter than normal; guard current rose and supply current fell as expected. Now, to change the tap setting to increase power output. The power amplifier was supplying 700 W now, above my original estimated design value. The dummy load was getting so hot that I had to put it on a metal plate with a blower.

After an hour or so, I tried the next tap. The power amplifier briefly gave around 800 W then blew its output devices. I had finally tested it to its limits and the devices had just gotten too hot to carry on living. So, for reliability with these IRF840 devices, around 600 W should be considered the limit, with 400-500 W for continuous 100% duty-cycle operation. I replaced the IRF840 devices (stocks of these were by now getting low) and this time fired up the transmitter without the mains isolating transformer and Variac.

After another eight hours at 600 W all was still going well, so it was time for an on-air test. After connecting a beacon keyer module to the on-off-keying circuit to send my call sign periodically, the first beacon transmission was started. It operated flawlessly for several hours before I decided that the design was final. It was time to put it into a case to make the finished unit (see Fig 6).

I already had a surplus steel 19-inch rack-mount drawer that would take all the components comfortably. Mounting the tank coil was the biggest problem: It needed to be as far away from the metal case as possible to avoid reducing the Q and introducing additional losses. In the end, it was supported, horizontally, by spacers, still a bit near to the top of the unit. Some retuning of the tank was needed as the coil inductance had dropped a few percent from its proximity to metal surroundings.

A small fan was added, blowing directly onto the heat sink and metering was added to measure a number

of operating parameters. These included RF output voltage and current into the load, along with heat-sink temperature using a thermistor mounted by the switching devices. (The area is shown in Fig 7.) A resistor bridge circuit was used to give a zero-to-full-scale, almost linear range of 20-70°C. Another prolonged testing session proved the reliability, but I felt the devices were still running a bit too hot at 600 W for a fail-safe design. The intention had always been to replace the 5-A IRF840 devices with higher-current types when the design was proven, and now was the time to substitute more exotic IRF460 FETs. An-

other prolonged soak test showed that these, indeed, ran a lot cooler even with the output power increased to 700 W. Now, the top of the steel case above the tank coil was getting very hot—much hotter than any other component in the power amplifier!

Remembering how “lossy” magnetic materials can be at high frequencies and that this casing was in the magnetic field from the tank coil, a piece of aluminum was attached to the underside of the steel case over the coil to shield the steel from the field.² This was successful in preventing the case from heating up, and the coil Q went up slightly, necessitating a bit of re-

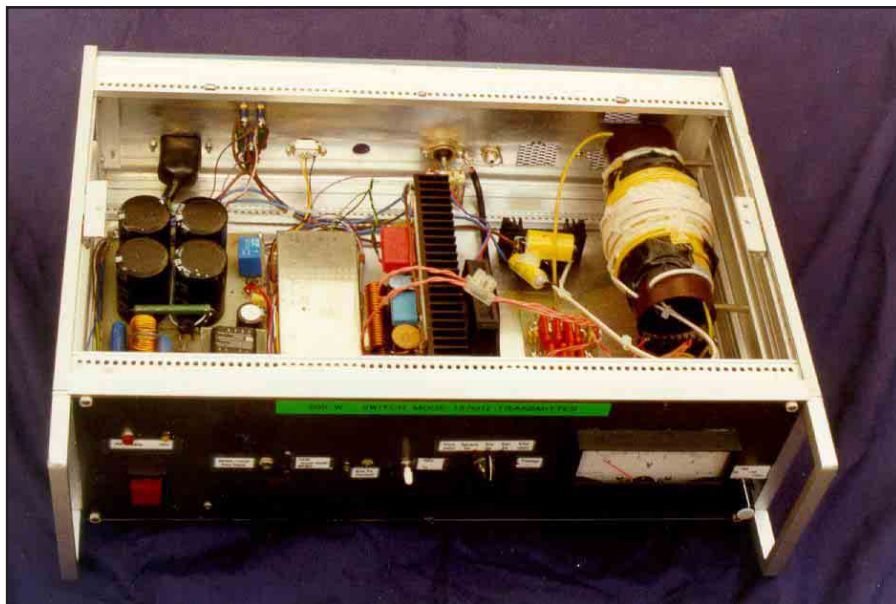


Fig 6—The completed transmitter.

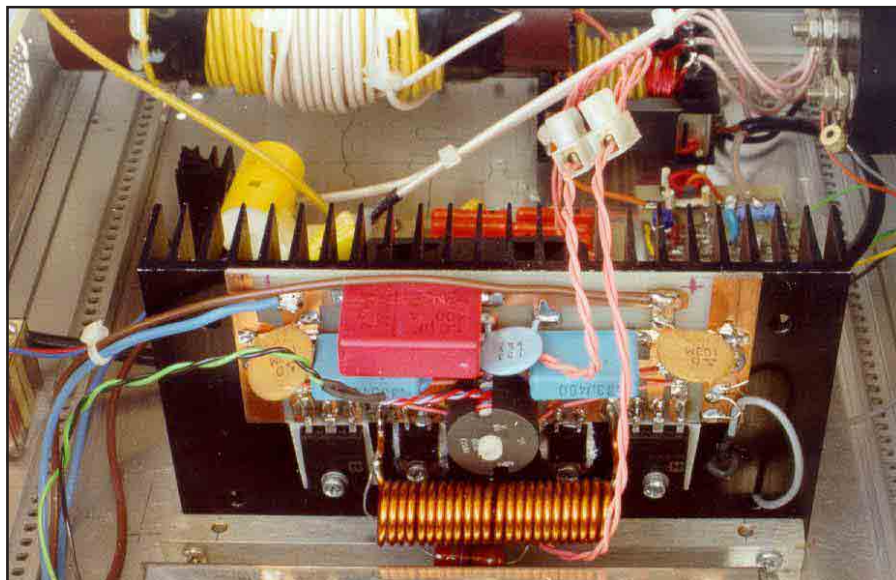


Fig 7—A close-up view of the active switching components.

tuning. A couple of turns had to be removed from the guard-circuit winding.

Operation

After over a year of operation, the work put into reliability and testing has proved worthwhile. There has been no failure of any component after many hours of operation, and I have managed to abuse the unit both deliberately and accidentally many times. I've disconnected it, shorted it, operated with a severe mismatch and once even at the completely wrong drive frequency—400 kHz—by mistake. This latter situation could have had unpleasant consequences as the tank, operating well away from resonance, could easily have allowed voltage or current overload, but fortunately didn't!

Also learned the hard way: Beware of removing the output connectors while the transmitter is operating. Transmitting into an open circuit is normally okay, since the transmitter is perfectly happy with a high-impedance load; but once I accidentally removed a BNC connector carrying 700 W of RF. The small arc, created as the inner contact broke connection, triggered a plasma arc between the center pin and the body of the plug, which developed into a sheet of flame spurting out of the plug as the pin vaporized. As I dropped the piece of coax in shock, the arc then proceeded to burn a hole in my floor covering before I was able to kill the power to the transmitter. The BNC plug was a blackened mess with a completely vaporized center pin and insulation. The moral of this story is: Don't under any circumstances remove connectors hot with high-power RF, and use something more substantial than BNC at this power level.

The transmitter has been used with on-off keyed signals such as CW and multitone Hellschreiber, as well as 100% duty-cycle transmissions of binary PSK. All passed through perfectly. In practice, although many parameters are metered, only two need to be monitored consistently during a long period of transmission. Supply current is the main reading to watch, as this is directly related to RF power out. It is immediately obvious when the load match changes. As weather affects the antenna performance, I tend to adjust the output transformer tap position to maintain a figure of around 2.5 A for high-duty-cycle modes, and up to 3 A for short-duration transmissions.

The other thing to watch is heat-sink temperature. At normal room



Fig 8—Another view of the complete transmitter

temperature, a relationship between dc load current and heat-sink temperature will become apparent after a few hours of experimentation with varying loads. If the antenna load is significantly reactive, though, the transmitter tends to run hotter than for a purely resistive load. This is caused by the FETs being forced to switch at a point other than zero current, giving rise to increased dissipation in the device on-resistance. Once you have gained practical experience in the supply current-temperature relationship, any discrepancy in this becomes obvious and it is time to check antenna tuning. It may even be worth installing an over-temperature LED or audible indication that trips at, say, 70°C.

Use with US Mains Supplies

The frequency difference of 50 Hz to 60 Hz is well-known and just means smoothing capacitors can be 1.2 times smaller for a given ripple at 60 Hz. In the UK and Europe, the ac main is a three-phase supply plus neutral along the street, with 415 V between phases and 240 V from phase to neutral. Other countries are a bit less than this, but rarely below 220 V. Domestic premises are supplied with one phase plus neutral and usually this neutral is connected to ground at many points along the supply route. Full-wave rectifying this gives around 340 V dc; but as one side of the ac feed is grounded, this 340 V is centered on ground, so each supply measures ± 170 V mean, but moving at mains frequency. My understanding of US supplies is that a center-tapped 240-V supply is available, giving 120 V for most low-power appliances and 240 V for high-power

use. This seems to be borne out by the seven wires I have seen on power-distribution poles.

So, for this transmitter, one option is merely to use the high-voltage, center-tapped supply, in which case the bridge rectification will give easier-to-visualize ± 165 V rails that do not oscillate with respect to ground potential. The other option is to use a full-bridge circuit with 120-V input only. Here the transmitter is operated from a 165-V rail, but now four FETs are used in a full bridge as was done in the original Decca design. The driver transformer now has to have four secondary windings, phased to switch diagonally opposite FETs together, and so will almost certainly end up physically larger. The full-bridge configuration has the effect of giving the same peak-to-peak voltage across the load as a half-bridge circuit does off twice the rail. So, load-impedance and tank-component calculations are the same, as are switching currents in each FET. There are just twice as many devices to blow up each time!

Conclusion

The unit described was an attempt to produce a low-cost, easy-to-build high-power transmitter for the 137-kHz band, using surplus components where possible. I was fortunate in having access to several scrap SMPSUs, typical of those used in older PCs, from which many of the power-supply components were recovered. I also had a large stock of IRF840 devices to destroy during the commissioning phases of this transmitter. However, once built and operated within its limits, the design is robust and reliable.

There is plenty of scope within this design for increasing output power. A full bridge running from 340 V will give well over 1 kW and doubling or tripling up the drive units as was done in the Decca design could yield many kilowatts.

Finally, I need to reiterate: *While working on this design, use an isolating transformer right until the end when it is finished and packaged. The voltages and currents can be lethal.* Construct it in a fully enclosed, well-grounded and bonded metal case and maintain good quality insulation and galvanic isolation between the power-

switching circuitry and the input-output connections. Also, a few hundred volts of 137 kHz, once it has started arcing, is very hot and creates a strong flame. Plasma-arc welders generate a similar type of waveform as that produced from this transmitter!

Late Note

Since writing this article, the announcement of the US 137-kHz band has been made. As it appears the permitted power is to be limited to 100 W of RF, this design can be used directly from a rectified 120-V supply. With a few changes to the tank-circuit values

and output transformer taps using the design guidelines specified, it will supply the maximum power output with ease.

Note

¹A. Talbot, G4JNT, "A Direct Digital Synthesiser Module for Radio Projects," *RadComm*, Nov 2000.

²Aluminum does not really "shield" the steel from the field, but it does intercept the field. The currents set up in the aluminum by the magnetic field tend to cancel that field near the aluminum, and therefore the field strength seen by the steel is much, much less than before. Note that the aluminum must be near but need not be in electrical contact with the steel to do its job. □□

Your FT-817 needs a Miracle!



The **Miracle Whip** lets you operate your new QRP rig with real freedom! It is a completely self-contained, all-band 50-inch telescoping whip antenna with integrated tuner for receiving and transmitting that mounts right on your radio. The Miracle Whip liberates your rig from coax, cables, mounts, tripods and trees, and gives you remarkable DX performance from desktop to picnic table, with no ground required. Take your portable transceiver anywhere and operate from 3.5 to 450 MHz with up to 20 W SSB. Only 13 inches collapsed. This quality product features gold plated rotor contacts and hand-formed solid brass contractors. Manufactured by Miracle Antenna of Montreal with three year limited warranty.

Order #3256 **\$148.95** (plus \$9.95 UPS)

Universal Radio
6830 Americana Pkwy.
Reynoldsburg, OH 43068
◆ Orders: 800 431-3939
◆ Info: 614 866-4267
www.universal-radio.com


universal radio inc.



ATOMIC TIME

1010 Jorie Blvd. #332 Oak Brook, IL. 60523

Tell time by the U.S. Atomic Clock -The official U.S. time that governs ship movements, radio stations, space flights, and warplanes. With small radio receivers hidden inside our timepieces, they automatically synchronize to the U.S. Atomic Clock (which measures each second of time as 9,192,631,770 vibrations of a cesium 133 atom in a vacuum) and give time which is accurate to 1 second every million years. Our timepieces even account automatically for daylight saving time, leap years, and leap seconds. Accept only the best, most precise, and reliable timepieces in the world, Atomic Time.

 <p>Atomic Time 0645R Digital Wall Stand for desk use Light/Dark Grey 12 or 24 hr. format day, date, month temperature, alarm 10.5" x 7.5" \$29.95</p>	<p>Junghans MEGA Carbon 016/2994 Carbon Fiber case, sapphire glass crystal lens, black leather band, LCD with day & date. Made in Germany. Stylish! \$239.20</p> 
 <p>Atomic Time W113 Digital Hour, minute, second, day, date, black polymer case-backlight, alarm & stopwatch. Wtproof. \$49.95</p>	<p>Atomic Time 12" Arabic Walnut German engineered wall clock updates time signal once daily. Automatically adjusts for daylight saving time, great gift! \$29.95</p> 

1-800-985-8463
www.atomictime.com
30 Day Money-Back Guarantee
Call for our FREE Brochure

All items add \$7.95 S/H
IL. res. add 6.75% sales tax

A Software-Defined Radio for the Masses, Part 3

Learn how to use DSP to make the PC sound-card interface from Part 2 into a functional software-defined radio.

We also explore a powerful filtering technique called FFT fast-convolution filtering.

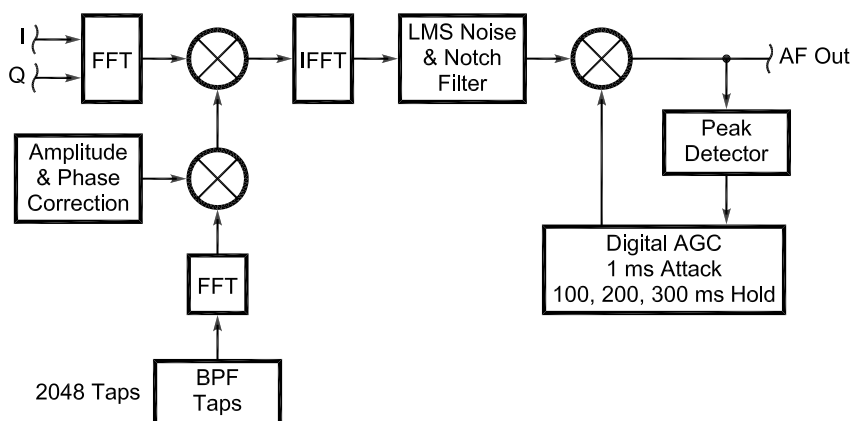
By Gerald Youngblood, AC5OG

Part 1¹ of this series provided a general description of digital signal processing (DSP) as used in software-defined radios (SDRs) and included an overview of a full-featured radio that uses a PC to perform all DSP and control functions. Part 2² described *Visual Basic* source code that implements a full-duplex quadrature interface to a PC sound card.

As previously described, *in-phase* (*I*) and *quadrature* (*Q*) signals give the ability to modulate or demodulate virtually any type of signal. The Taylor Detector, described in Part 1, is a simple method of converting a modulated RF signal to baseband in quadrature, so that it can be presented to the left and right inputs of a stereo PC

sound card for signal processing. The full-duplex DirectX8 interface, described in Part 2, accomplishes the input and output of the sampled

quadrature signals. The sound-card interface provides an input buffer array, *inBuffer()*, and an output buffer array, *outBuffer()*, through which the



¹Notes appear on page 36.

Fig 1—DSP software architecture block diagram.

DSP code receives the captured signal and then outputs the processed signal data.

This article extends the sound-card interface to a functional SDR receiver demonstration. To accomplish this, the following functions are implemented in software:

- Split the stereo sound buffers into *I* and *Q* channels.

- Conversion from the time domain into the frequency domain using a *fast Fourier transform* (FFT).
- Cartesian-to-polar conversion of the signal vectors.
- Frequency translation from the 11.25 kHz-offset baseband IF to 0 Hz.
- Sideband selection.
- Band-pass filter coefficient generation.

- FFT fast-convolution filtering.
- Conversion back to the time domain with an inverse fast Fourier transform (IFFT).
- Digital automatic gain control (AGC) with variable hang time.
- Transfer of the processed signal to the output buffer for transmit or receive operation.

The demonstration source code may

```

Public Const Fs As Long = 44100           'Sampling frequency in samples per
                                         'second
Public Const NFFT As Long = 4096         'Number of FFT bins
Public Const BLKSIZE As Long = 2048     'Number of samples in capture/play block
Public Const CAPTURESIZE As Long = 4096 'Number of samples in Capture Buffer
Public Const FILTERTAPS As Long = 2048  'Number of taps in bandpass filter
Private BinSize As Single                'Size of FFT Bins in Hz

Private order As Long                    'Calculate Order power of 2 from NFFT
Private filterM(NFFT) As Double          'Polar Magnitude of filter freq resp
Private filterP(NFFT) As Double          'Polar Phase of filter freq resp
Private RealIn(NFFT) As Double            'FFT buffers
Private RealOut(NFFT) As Double
Private ImagIn(NFFT) As Double
Private ImagOut(NFFT) As Double

Private IOverlap(NFFT - FILTERTAPS - 1) As Double 'Overlap prev FFT/IFFT
Private QOverlap(NFFT - FILTERTAPS - 1) As Double 'Overlap prev FFT/IFFT

Private RealOut_1(NFFT) As Double        'Fast Convolution Filter buffers
Private RealOut_2(NFFT) As Double
Private ImagOut_1(NFFT) As Double
Private ImagOut_2(NFFT) As Double

Public FHigh As Long                     'High frequency cutoff in Hz
Public FLow As Long                       'Low frequency cutoff in Hz
Public Fl As Double                       'Low frequency cutoff as fraction of Fs
Public Fh As Double                       'High frequency cutoff as fraction of Fs
Public SSB As Boolean                     'True for Single Sideband Modes
Public USB As Boolean                     'Sideband select variable
Public TX As Boolean                       'Transmit mode selected
Public IFShift As Boolean                  'True for 11.025KHz IF

Public AGC As Boolean                     'AGC enabled
Public AGCHang As Long                    'AGC AGCHang time factor
Public AGCMode As Long                    'Saves the AGC Mode selection
Public RXHang As Long                     'Save RX Hang time setting
Public AGCLoop As Long                    'AGC AGCHang time buffer counter
Private Vpk As Double                     'Peak filtered output signal
Private G(24) As Double                   'Gain AGCHang time buffer
Private Gain As Double                    'Gain state setting for AGC
Private PrevGain As Double                'AGC Gain during previous input block
Private GainStep As Double                'AGC attack time steps
Private GainDB As Double                  'AGC Gain in dB
Private TempOut(BLKSIZE) As Double        'Temp buffer to compute Gain
Public MaxGain As Long                    'Maximum AGC Gain factor

Private FFTBins As Long                   'Number of FFT Bins for Display
Private M(NFFT) As Double                 'Double precision polar magnitude
Private P(NFFT) As Double                 'Double precision phase angle
Private S As Long                          'Loop counter for samples

```

Fig 2—Variable declarations.

be downloaded from *ARRLWeb*.³ The software requires the *dynamic link library (DLL)* files from the Intel Signal Processing Library⁴ to be located in the working directory. These files are included with the demo software.

The Software Architecture

Fig 1 provides a block diagram of the DSP software architecture. The architecture works equally well for both transmit and receive with only a few lines of code changing between the two. While the block diagram illustrates functional modules for *Amplitude and Phase Correction* and the *LMS Noise and Notch Filter*, discussion of these features is beyond the scope of this article.

Amplitude and phase correction permits imperfections in phase and amplitude imbalance created in the analog circuitry to be corrected in the frequency domain. LMS noise and notch filters⁵ are an adaptive form of *finite impulse response (FIR)* filtering that accomplishes noise reduction in the time domain. There are other techniques for noise reduction that can be accomplished in the frequency domain such as *spectral subtraction*,⁶ *correlation*⁷ and *FFT averaging*.⁸

Parse the Input Buffers to Get I and Q Signal Vectors

Fig 2 provides the variable and constant declarations for the demonstration code. The code for parsing the *inBuffer()* is illustrated in Fig 3. The left and right signal inputs must be parsed into *I* and *Q* signal channels before they are presented to the FFT input. The 16-bit integer left- and right-channel samples are interleaved, therefore the code shown in Fig 3 must be used to split the signals. The arrays *RealIn()* and *RealOut()* are used to store the *I* signal vectors and the arrays *ImagIn()* and *ImagOut()* are used to store the *Q* signal vectors. This corresponds to the nomenclature used in the complex FFT algorithm. It is not critical which of the *I* and *Q* channels goes to which input because one can simply reverse the code in Fig 3 if the sidebands are inverted.

The FFT: Conversion to the Frequency Domain

Part 1 of this series discussed how the FFT is used to convert discrete-time sampled signals from the time domain into the frequency domain (see Note 1). The FFT is quite complex to derive mathematically and somewhat tedious to code. Fortunately, Intel has provided performance-optimized code in DLL form that can be called from a

single line of code for this and other important DSP functions (see Note 4).

The FFT effectively consists of a series of very narrow band-pass filters, the outputs of which are called *bins*, as illustrated in Fig 4. Each bin has a magnitude and phase value representative of the sampled input signal's content at the respective bin's center frequency. Overlap of adjacent bins resembles the output of a *comb filter* as discussed in Part 1.

The PC SDR uses a 4096-bin FFT. With a sampling rate of 44,100 Hz, the bandwidth of each bin is 10.7666 Hz (44,100/4096), and the center frequency of each bin is the bin number times the bandwidth. Notice in Fig 4 that with respect to the center fre-

quency of the sampled quadrature signal, the upper sideband is located in bins 1 through 2047, and the lower sideband is located in bins 2048 through 4095. Bin 0 contains the carrier translated to 0 Hz. An FFT performed on an analytic signal $I + jQ$ allows positive and negative frequencies to be analyzed separately.

The Turtle Beach Santa Cruz sound card I use has a 3-dB frequency response of approximately 10 Hz to 20 kHz. (Note: the data sheet states a high-frequency cutoff of 120 kHz, which has to be a typographical error, given the 48-kHz maximum sampling rate). Since we sample the RF signal in quadrature, the sampling rate is effectively doubled (44,100 Hz times

```

Erase RealIn, ImagIn
For S = 0 To CAPTURESIZE - 1 Step 2
  RealIn(S \ 2) = inBuffer(S + 1)
  ImagIn(S \ 2) = inBuffer(S)

```

'Copy I to RealIn and Q to ImagIn
'Zero stuffing second half of
'RealIn and ImagIn Next S

Fig 3—Parsing input buffers into *I* and *Q* signal vectors.

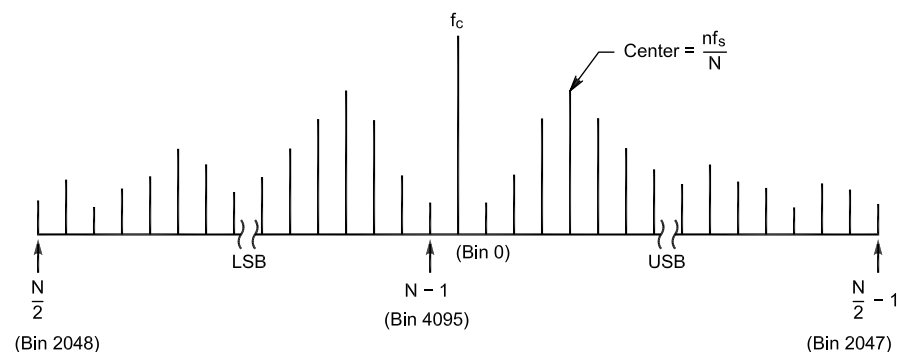


Fig 4—FFT output bins.

```

nspzrFftNip RealIn, ImagIn, RealOut, ImagOut, order, NSP_Forw
nspdbrCartToPolar RealOut, ImagOut, M, P, NFFT 'Cartesian to polar

```

Fig 5—Time domain to frequency domain conversion using the FFT.

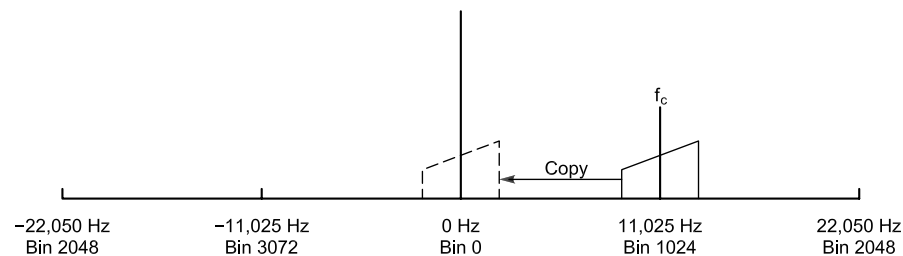


Fig 6—Offset baseband IF diagram. The local oscillator is shifted by 11,025 kHz so that the desired-signal carrier frequency is centered at an 11,025-Hz offset within the FFT output. To shift the signal for subsequent filtering the desired bins are simply copied to center the carrier frequency, f_c , at 0 Hz.

two channels yields an 88,200-Hz-effective sampling rate). This means that the output spectrum of the FFT will be twice that of a single sampled channel. In our case, the total output bandwidth of the FFT will be 10.7666 Hz times 4096 or 44,100 Hz. Since most sound cards roll off near 20 kHz, we are probably limited to a total bandwidth of approximately 40 kHz.

Fig 5 shows the DLL calls to the Intel library for the FFT and subsequent conversion of the signal vectors from the Cartesian coordinate system to the Polar coordinate system. The `nspzrFftNip` routine takes the time domain `RealIn()` and `ImagIn()` vectors and converts them into frequency domain `RealOut()` and `ImagOut()` vectors. The order of the FFT is computed in the routine that calculates the filter coefficients as will be discussed later. `NSP_Forw` is a constant that tells the routine to perform the forward FFT conversion.

In the Cartesian system the signal is represented by the magnitudes of two vectors, one on the *Real* or *x* plane and one on the *Imaginary* or *y* plane. These vectors may be converted to a single vector with a magnitude (*M*) and a phase angle (*P*) in the polar system. Depending on the specific DSP algorithm we wish to perform, one coordinate system or the other may be more efficient. I use the polar coordinate system for most of the signal processing in this example. The `nspdbrCartToPolar` routine converts the output of the FFT to a polar vector consisting of the magnitudes in *M*() and the phase values in *P*(). This function simultaneously performs Eqs 3 and 4 in Part 1 of this article series.

Offset Baseband IF Conversion to Zero Hertz

My original software centered the RF carrier frequency at bin 0 (0 Hz). With this implementation, one can display (and hear) the entire 44-kHz spectrum in real time. One of the problems encountered with direct-conversion or zero-IF receivers is that noise

increases substantially near 0 Hz. This is caused by several mechanisms: $1/f$ noise in the active components, 60/120-Hz noise from the ac power lines, microphonic noise caused by mechanical vibration and local-oscillator phase noise. This can be a problem for weak-signal work because most people tune CW signals for a 700-1000 Hz tone. Fortunately, much of this noise disappears above 1 kHz.

Given that we have 44 kHz of spectrum to work with, we can offset the digital IF to any frequency within the FFT output range. It is simply a matter of deciding which FFT bin to designate as the carrier frequency and then offsetting the local oscillator by the appropriate amount. We then copy the respective bins for the desired sideband so that they are located at 0 Hz for subsequent processing. In the PC SDR, I have chosen to use an offset IF of 11,025 Hz, which is one fourth

of the sampling rate, as shown in Fig 6.

Fig 7 provides the source code for shifting the offset IF to 0 Hz. The carrier frequency of 11,025 Hz is shifted to bin 0 and the upper sideband is shifted to bins 1 through 1023. The lower sideband is shifted to bins 3072 to 4094. The code allows the IF shift to be enabled or disabled, as is required for transmitting.

Selecting the Sideband

So how do we select sideband? We store zeros in the bins we don't want to hear. How simple is that? If it were possible to have perfect analog amplitude and phase balance on the sampled *I* and *Q* input signals, we would have infinite sideband suppression. Since that is not possible, any imbalance will show up as an image in the passband of the receiver. Fortunately, these imbalances can be cor-

```
IFShift = True 'Force to True for the demo

If IFShift = True Then 'Shift sidebands from 11.025KHz IF
  For S = 0 To 1023
    If USB Then
      M(S) = M(S + 1024) 'Move upper sideband to 0Hz
      P(S) = P(S + 1024)
    Else
      M(S + 3072) = M(S + 1) 'Move lower sideband to 0Hz
      P(S + 3072) = P(S + 1)
    End If
  Next
End If
```

Fig 7—Code for down conversion from offset baseband IF to 0 Hz.

```
If SSB = True Then 'SSB or CW Modes
  If USB = True Then
    For S = FFTBins To NFFT - 1 'Zero out lower sideband
      M(S) = 0
    Next
  Else
    For S = 0 To FFTBins - 1 'Zero out upper sideband
      M(S) = 0
    Next
  End If
End If
```

Fig 8—Sideband selection code.

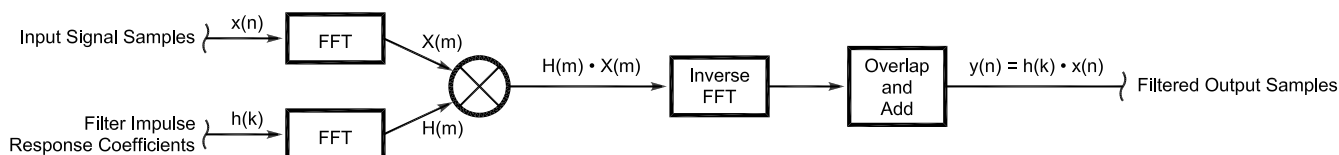


Fig 9—FFT fast-convolution-filtering block diagram. The filter impulse-response coefficients are first converted to the frequency domain using the FFT and stored for repeated use by the filter routine. Each signal block is transformed by the FFT and subsequently multiplied by the filter frequency-response magnitudes. The resulting filtered signal is transformed back into the time domain using the inverse FFT. The Overlap/Add routine corrects the signal for circular convolution.

rected through DSP code either in the time domain before the FFT or in the frequency domain after the FFT. These techniques are beyond the scope of this discussion, but I may cover them in a future article. My prototype using INA103 instrumentation amplifiers achieves approximately 40 dB of opposite sideband rejection *without* correction in software.

The code for zeroing the opposite sideband is provided in Fig 8. The lower sideband is located in the high-numbered bins and the upper sideband is located in the low-numbered bins. To save time, I only zero the number of bins contained in the *FFTBins* variable.

FFT Fast-Convolution Filtering Magic

Every DSP text I have read on single-sideband modulation and demodulation describes the IF sampling approach. In this method, the A/D converter samples the signal at an IF such as 40 kHz. The signal is then quadrature down-converted in software to baseband and filtered using finite impulse response (FIR)⁹ filters. Such a system was described in Doug Smith's *QEX* article called, "Signals, Samples, and Stuff: A DSP Tutorial (Part 1)."¹⁰ With this approach, all processing is done in the time domain.

For the PC SDR, I chose to use a very different approach called *FFT fast-convolution filtering* (also called *FFT convolution*) that performs all filtering functions in the frequency domain.¹¹ An FIR filter performs convolution of an input signal with a filter impulse response in the time domain. Convolution is the mathematical means of combining two signals (for example, an input signal and a filter impulse response) to form a third signal (the filtered output signal).¹² The time-domain approach works very well for a small number of filter taps. What if we want to build a very-high-performance filter with 1024 or more taps? The processing overhead of the FIR filter may become prohibitive. It turns out that an important property of the Fourier transform is that convolution in the time domain is equal to multiplication in the frequency domain. Instead of directly convolving the input signal with the windowed filter impulse response, as with a FIR filter, we take the respective FFTs of the input signal and the filter impulse response and simply multiply them together, as shown in Fig 9. To get back to the time domain, we perform the inverse FFT of the product. FFT convolution is often faster than direct convolution for filter kernels longer than

64 taps, and it produces exactly the same result.

For me, FFT convolution is easier to understand than direct convolution because I mentally visualize filters in the frequency domain. As described in Part 1 of this series, the output of the complex FFT may be thought of as a long bank of narrow band-pass filters aligned around the carrier frequency

(bin 0), as shown in Fig 4. Fig 10 illustrates the process of FFT convolution of a transformed filter impulse response with a transformed input signal. Once the signal is transformed back to the time domain by the inverse FFT, we must then perform a process called the *overlap/add method*. This is because the process of convolution produces an output signal that is

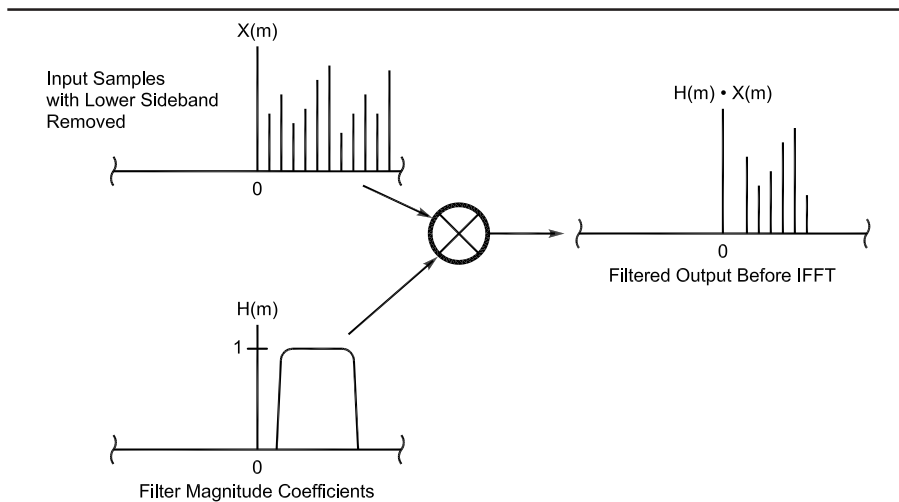


Fig 10—FFT fast convolution filtering output. When the filter-magnitude coefficients are multiplied by the signal-bin values, the resulting output bins contain values only within the pass-band of the filter.

```
Public Static Sub CalcFilter(FLow As Long, FHigh As Long)
    Static Rh(NFFT) As Double           'Impulse response for bandpass filter
    Static Ih(NFFT) As Double           'Imaginary set to zero
    Static reH(NFFT) As Double          'Real part of filter response
    Static imH(NFFT) As Double          'Imaginary part of filter response

    Erase Ih

    Fh = FHigh / Fs                      'Compute high and low cutoff
    Fl = FLow / Fs                        'as a fraction of Fs
    BinSize = Fs / NFFT                   'Compute FFT Bin size in Hz

    FFTBins = (FHigh / BinSize) + 50     'Number of FFT Bins in filter width

    order = NFFT                           'Compute order as NFFT power of 2
    Dim O As Long

    For O = 1 To 16                         'Calculate the filter order
        order = order \ 2
        If order = 1 Then
            order = 0
            Exit For
        End If
    Next

    'Calculate infinite impulse response bandpass filter coefficients
    'with window
    nspdFIRBandpass Fl, Fh, Rh, FILTERTAPS, NSP_WinBlackmanOpt, 1

    'Compute the complex frequency domain of the bandpass filter
    nspzrFftNip Rh, Ih, reH, imH, order, NSP_Forw
    nspdbrCartToPolar reH, imH, filterM, filterP, NFFT

End Sub
```

Fig 11—Code for the generating bandpass filter coefficients in the frequency domain.

equal in length to the sum of the input samples plus the filter taps minus one. I will not attempt to explain the concept here because it is best described in the references.¹³

Fig 11 provides the source code for producing the frequency-domain band-pass filter coefficients. The CalcFilter subroutine is passed the low-frequency cutoff, *FLow*, and the high-frequency cutoff, *FHigh*, for the filter response. The cutoff frequencies are then converted to their respective fractions of the sampling rate for use by the filter-generation routine, *nspdFirBandpass*. The FFT order is also determined in this subroutine, based on the size of the FFT, *NFFT*. The *nspdFirBandpass* computes the impulse response of the band-pass filter of bandwidth *FL()* to *Fh()* and a length of *FILTERTAPS*. It then places the result in the array variable *Rh()*. The *NSP_WinBlackmanOpt* causes the impulse response to be windowed by a Blackman window function. For a discussion of windowing, refer to the DSP Guide.¹⁴ The value of “1” that is passed to the routine causes the result to be normalized.

Next, the impulse response is converted to the frequency domain by *nspzrFftNip*. The input parameters are *Rh()*, the real part of the impulse response, and *Ih()*, the imaginary part that has been set to zero. *NSP_Forw* tells the routine to perform the forward FFT. We next convert the frequency-domain result of the FFT, *reH()* and *imH()*, to polar form using the *nspdbrCartToPolar* routine. The filter magnitudes, *filterM()*, and filter phase, *filterP()*, are stored for use in the FFT fast convolution filter. Other than when we manually change the band-pass filter selection, the filter response does not change. This means that we only have to calculate the filter response once when the filter is first selected by the user.

Fig 12 provides the code for an FFT fast-convolution filter. Using the *nspdbMpy2* routine, the signal-spectrum magnitude bins, *M()*, are multiplied by the filter frequency-response magnitude bins, *filterM()*, to generate the resulting in-place filtered magnitude-response bins, *M()*. We then use *nspdbAdd2* to add the signal phase bins, *P()*, to the filter phase bins, *filterP()*, with the result stored in-place in the filtered phase-response bins, *P()*. Notice that FFT convolution can also be performed in Cartesian coordinates using the method shown in Fig 13, although this method requires more computational resources. Other uses of the frequency-domain magnitude values include FFT aver-

aging, digital squelch and spectrum display.

Fig 14 shows the actual spectral output of a 500-Hz filter using wide-

bandwidth noise input and FFT averaging of the signal over several seconds. This provides a good picture of the frequency response and shape of

```
nspdbMpy2 filterM, M, NFFT      'Multiply Magnitude Bins
nspdbAdd2 filterP, P, NFFT      'Add Phase Bins
```

Fig 12—FFT fast convolution filtering code using polar vectors.

```
'Compute: RealIn(s) = (RealOut(s) * reH(s)) - (ImagOut(s) * imH(s))
nspdbMpy3 RealOut, reH, RealOut_1, NFFT
nspdbMpy3 ImagOut, imH, ImagOut_1, NFFT
nspdbSub3 RealOut_1, ImagOut_1, RealIn, NFFT 'RealIn for IFFT

'Compute: ImagIn(s) = (RealOut(s) * imH(s)) + (ImagOut(s) * reH(s))
nspdbMpy3 RealOut, imH, RealOut_2, NFFT
nspdbMpy3 ImagOut, reH, ImagOut_2, NFFT
nspdbAdd3 RealOut_2, ImagOut_2, ImagIn, NFFT 'ImagIn for IFFT
```

Fig 13—Alternate FFT fast convolution filtering code using cartesian vectors.

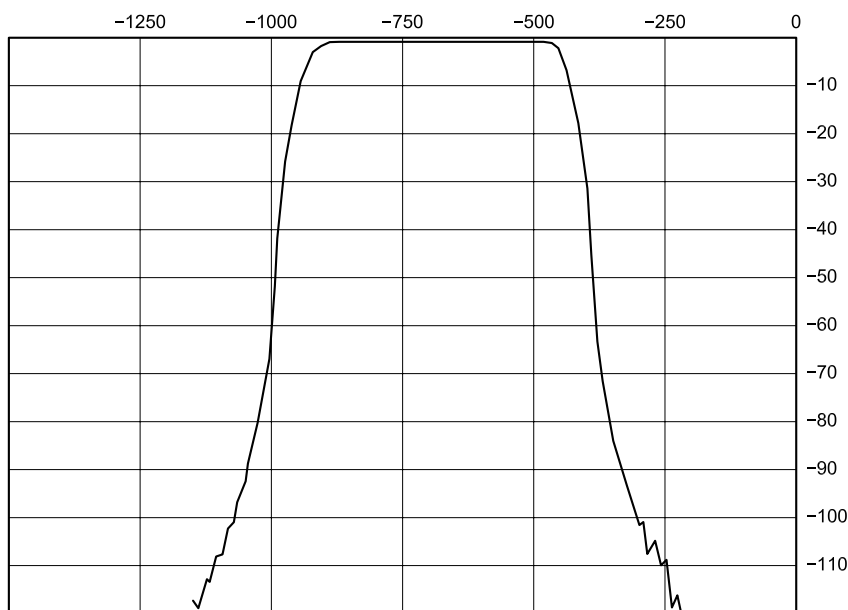


Fig 14—Actual 500-Hz CW filter pass-band display. FFT fast-convolution filtering is used with 2048 filter taps to produce a 1.05 shape factor from 3 dB to 60 dB down and over 120 dB of stop-band attenuation just 250 Hz beyond the 3 dB points.

```
'Convert polar to cartesian
nspdbrPolarToCart M, P, RealIn, ImagIn, NFFT

'Inverse FFT to convert back to time domain
nspzrFftNip RealIn, ImagIn, RealOut, ImagOut, order, NSP_Inv

'Overlap and Add from last FFT/IFFT: RealOut(s) = RealOut(s) + Overlap(s)
nspdbAdd3 RealOut, IOverlap, RealOut, FILTERTAPS - 2
nspdbAdd3 ImagOut, QOverlap, ImagOut, FILTERTAPS - 2

'Save Overlap for next pass
For S = BLKSIZE To NFFT - 1
    IOverlap(S - BLKSIZE) = RealOut(S)
    QOverlap(S - BLKSIZE) = ImagOut(S)
Next
```

Fig 15—Inverse FFT and overlap/add code.

the filter. The shape factor of the 2048-tap filter is 1.05 from the 3-dB to the 60-dB points (most manufacturers measure from 6 dB to 60 dB, a more lenient specification). Notice that the stop-band attenuation is greater than 120 dB at roughly 250 Hz from the 3-dB points. This is truly a brick-wall filter!

An interesting fact about this method is that the window is applied to the filter impulse response rather than the input signal. The filter response is normalized so signals within the passband are not attenuated in the frequency domain. I believe that this normalization of the filter response removes the usual attenuation asso-

ciated with windowing the signal before performing the FFT. To overcome such windowing attenuation, it is typical to apply a 50-75% overlap in the time-domain sampling process and average the FFTs in the frequency domain. I would appreciate comments from knowledgeable readers on this hypothesis.

The IFFT and Overlap/Add—Conversion Back to the Time Domain

Before returning to the time domain, we must first convert back to Cartesian coordinates by using `nspdbrPolarToCart` as illustrated in Fig 15. Then by setting the `NSP_Inv`

flag, the inverse FFT is performed by `nspzrFftNip`, which places the time-domain outputs in `RealOut()` and `ImagOut()`, respectively. As discussed previously, we must now overlap and add a portion of the signal from the previous capture cycle as described in the DSP Guide (see Note 13). `Ioverlap()` and `Qoverlap()` store the in-phase and quadrature overlap signals from the last pass to be added to the new signal block using the `nspdbAdd3` routine.

Digital AGC with Variable Hang Time

The digital AGC code in Fig 16 provides fast-attack and -decay gain

```

If AGC = True Then

    `If true increment AGCLoop counter, otherwise reset to zero
    AGCLoop = IIf(AGCLoop < AGCHang - 1, AGCLoop + 1, 0)

    nspdbrCartToPolar RealOut, ImagOut, M, P, BLKSIZE `Envelope Polar Magnitude

    Vpk = nspdMax(M, BLKSIZE) `Get peak magnitude

    If Vpk <> 0 Then `Check for divide by zero
        G(AGCLoop) = 16384 / Vpk `AGC gain factor with 6 dB headroom
        Gain = nspdMin(G, AGCHang) `Find peak gain reduction (Min)
    End If

    If Gain > MaxGain Then Gain = MaxGain `Limit Gain to MaxGain

    If Gain < PrevGain Then `AGC Gain is decreasing
        GainStep = (PrevGain - Gain) / 44 `44 Sample ramp = 1 ms attack time
        For S = 0 To 43 `Ramp Gain down over 1 ms period
            M(S) = M(S) * (PrevGain - ((S + 1) * GainStep))
        Next
        For S = 44 To BLKSIZE - 1 `Multiply remaining Envelope by Gain
            M(S) = M(S) * Gain
        Next
    Else
        If Gain > PrevGain Then `AGC Gain is increasing
            GainStep = (Gain - PrevGain) / 44 `44 Sample ramp = 1 ms decay time
            For S = 0 To 43 `Ramp Gain up over 1 ms period
                M(S) = M(S) * (PrevGain + ((S + 1) * GainStep))
            Next
            For S = 44 To BLKSIZE - 1 `Multiply remaining Envelope by Gain
                M(S) = M(S) * Gain
            Next
        Else
            nspdbMpy1 Gain, M, BLKSIZE `Multiply Envelope by AGC gain
        End If
    End If

    PrevGain = Gain `Save Gain for next loop

    nspdbThresh1 M, BLKSIZE, 32760, NSP_GT `Hard limiter to prevent overflow

End If

```

Fig 16 – Digital AGC code.

control with variable hang time. Both attack and decay occur in approximately 1 ms, but the hang time may be set to any desired value in increments of 46 ms. I have chosen to implement the attack/decay with a linear ramp function rather than an exponential function as described in DSP communications texts.¹⁵ It works extremely well and is intuitive to code. The flow diagram in Fig 17 outlines the logic used in the AGC algorithm.

Refer to Figs 16 and 17 for the following description. First, we check to see if the AGC is turned on. If so, we increment *AGCLoop*, the counter for AGC hang-time loops. Each pass through the code is equal to a hang time

of 46 ms. PC SDR provides hang-time loop settings of 3 (fast, 132 ms), 5 (medium, 230 ms), 7 (slow, 322 ms) and 22 (long, 1.01 s). The hang-time setting is stored in the *AGCHang* variable. Once the hang-time counter resets, the decay occurs on a 1-ms linear slope.

To determine the AGC gain requirement, we must detect the envelope of the demodulated signal. This is easily accomplished by converting from Cartesian to polar coordinates. The value of *M()* is the envelope, or magnitude, of the signal. The phase vector can be ignored insofar as AGC is concerned. We will need to save the phase values, though, for conversion back to Cartesian coordinates later. Once we

have the magnitudes stored in *M()*, it is a simple matter to find the peak magnitude and store it in *Vpk* with the function *nspdMax*. After checking to prevent a divide-by-zero error, we compute a gain factor relative to 50% of the full-scale value. This provides 6 dB of headroom from the signal peak to the full-scale output value of the DAC. On each pass, the gain factor is stored in the *G()* array so that we can find the peak gain reduction during the hang-time period using the *nspdMin* function. The peak gain-reduction factor is then stored in the *Gain* variable. Note that *Gain* is saved as a ratio and not in decibels, so that no log/antilog conversion is needed.

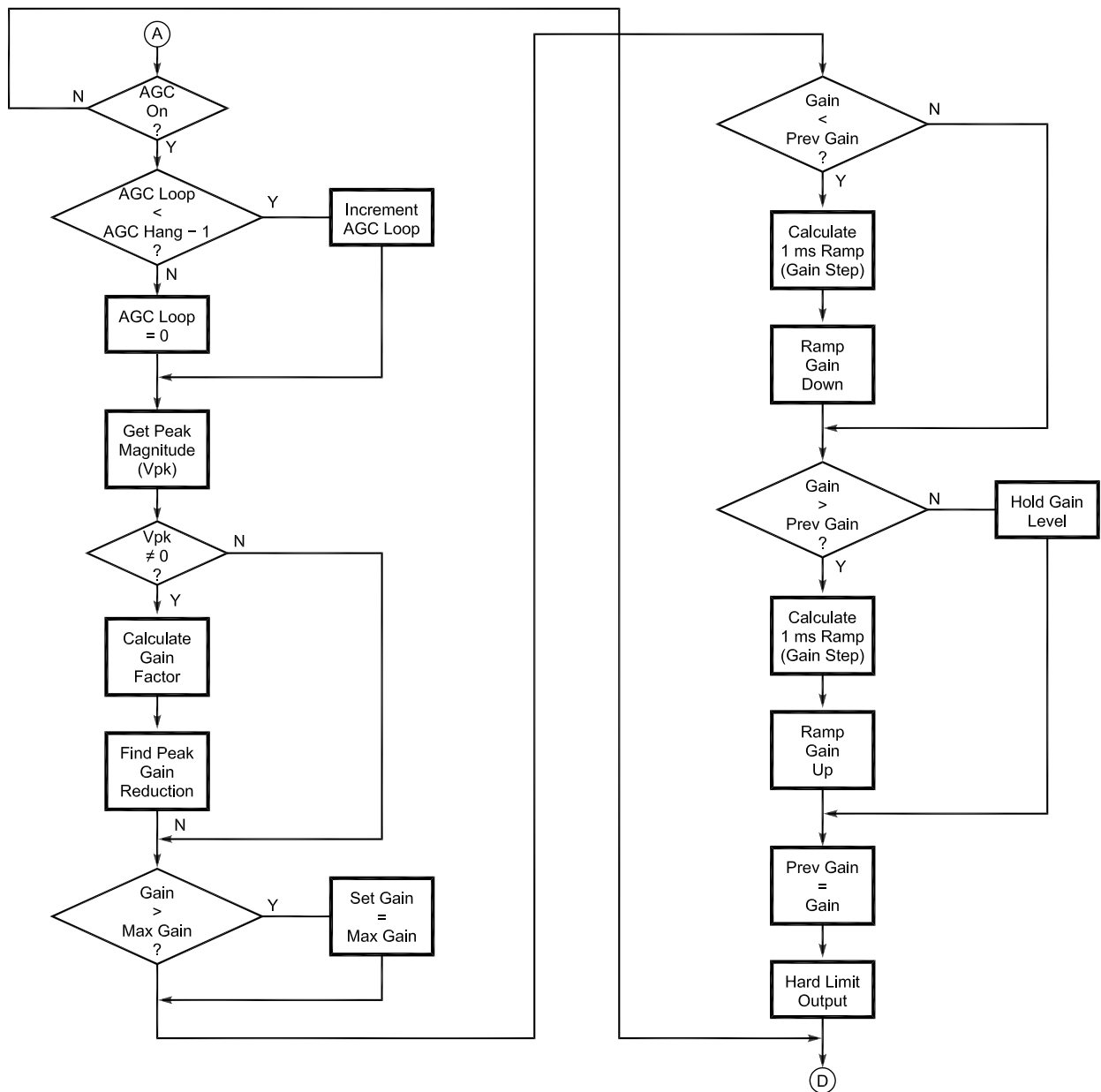


Fig 17—Digital AGC flow diagram.

The next step is to limit *Gain* to the *MaxGain* value, which may be set by the user. This system functions much like an IF-gain control allowing *Gain* to vary from negative values up to the *MaxGain* setting. Although not provided in the example code, it is a simple task to create a front panel control in *Visual Basic* to manually set the *MaxGain* value.

Next, we determine if the gain must be increased, decreased or left unchanged. If *Gain* is less than *PrevGain* (that is the *Gain* setting from the signal block stored on the last pass through the code), we ramp the gain down linearly over 44 samples. This yields an attack time of approximately 1 ms at a 44,100-Hz sampling rate. *GainStep* is the slope of the ramp per sample time calculated from the *PrevGain* and *Gain* values. We then incrementally ramp down the first 44 samples by the *GainStep* value. Once ramped to the new *Gain* value, we multiply the remaining samples by the fixed *Gain* value.

If *Gain* is increasing from the *PrevGain* value, the process is simply reversed. If *Gain* has not changed, all samples are multiplied by the current *Gain* setting. After the signal block has been processed, *Gain* is saved in *PrevGain* for the next signal block. Finally, *nspdbThresh1* implements a hard limiter at roughly the maximum output level of the DAC, to prevent overflow of the integer-variable output buffers.

Send the Demodulated or Modulated Signal to the Output Buffer

The final step is to format the processed signal for output to the DAC. When receiving, the *RealOut()* signal is copied, sample by sample, into both the left and right channels. For transmitting, *RealOut()* is copied to the right channel and *ImagOut()* is copied to the left channel of the DAC. If binaural receiving is desired, the *I* and *Q* signal can optionally be sent to the right and left channels respectively, just as in the transmit mode.

Controlling the Demonstration Code

The SDR demonstration code (see [Note 3](#)) has a few selected buttons for setting AGC hang time, filter selection and sideband selection. The code for these functions is shown in Fig 18. The code is self-explanatory and easy to modify for additional filters, different hang times and other modes of operation. Feel free to experiment.

The Fully Functional SDR-1000 Software

The SDR-1000, my nomenclature for the PC SDR, contains a significant amount of code not illustrated here. I have chosen to focus this article on the essential DSP code necessary for modulation and demodulation in the frequency domain. As time permits, I hope to write future articles that delve into other interesting aspects of the software design.

Fig 19 shows the completed front-panel display of the SDR-1000. I have had a great deal of fun creating—and modifying many times—this user interface. Most features of the user interface are intuitive. Here are some interesting capabilities of the SDR-1000:

- A real-time spectrum display with one-click frequency tuning using a mouse.
- Dual, independent VFOs with database readout of band-plan allocation. The user can easily access and modify the band-plan database.
- Mouse-wheel tuning with the ability to change the tuning rate with a click of the wheel.
- A multifunction digital- and analog-readout meter for instantaneous and average signal strength, AGC gain, ADC input signal and DAC output signal levels.
- Extensive VFO, band and mode control. The band-switch buttons also provide a multilevel memory on the same band. This means that by pressing a given band button

```
Private Sub cmdAGC_Click(Index As Integer)

    MaxGain = 1000                                'Maximum digital gain = 60dB

    Select Case Index

        Case 0
            AGC = True
            AGCHang = 3                            '3 x 0.04644 sec = 139 ms
        Case 1
            AGC = True
            AGCHang = 7                            '7 x 0.04644 sec = 325 ms
        Case 2
            AGC = False                            'AGC Off
    End Select

End Sub

Private Sub cmdFilter_Click(Index As Integer)

    Select Case Index

        Case 0
            CalcFilter 300, 3000                    '2.7KHz Filter
        Case 1
            CalcFilter 500, 1000                    '500Hz Filter
        Case 2
            CalcFilter 700, 800                     '100Hz Filter
    End Select

End Sub

Private Sub cmdMode_Click(Index As Integer)

    Select Case Index

        Case 0
            SSB = True
            USB = True                              'Change mode to USB
        Case 1
            SSB = True
            USB = False                             'Change mode to LSB
    End Select

End Sub
```

Fig 18 – Control code for the demonstration front panel.

multiple times, it will cycle through the last three frequencies visited on that band.

- Virtually unlimited memory capability is provided through a Microsoft Access database interface. The memory includes all key settings of the radio by frequency. Frequencies may also be grouped for scanning.
- Ten standard filter settings are provided on the front panel, plus independent, continuously variable filters for both CW and SSB.
- Local and UTC real-time clock displays.
- Given the capabilities of *Visual Basic*, the possibility for enhancement of the user interface is almost limitless. The hard part is “shooting the engineer” to get him to stop designing and get on the air.

There is much more that can be accomplished in the DSP code to customize the PC SDR for a given application. For example, Leif Åsbrink, SM5BSZ, is doing interesting weak-signal moonbounce work under *Linux*.¹⁶

Also, Bob Larkin, W7PUA, is using the DSP-10 he first described in the September, October and November 1999 issues of *QST* to experiment with weak-signal, over-the-horizon microwave propagation.¹⁷

Coming in the Final Article

In the final article, I plan to describe ongoing development of the SDR-1000 hardware. (Note: I plan to delay the final article so that I am able to complete the PC board layout and test the hardware design.) Included will be a tradeoff analysis of gain distribution, noise figure and dynamic range. I will also discuss various approaches to analog AGC and explore frequency control using the AD9854 quadrature DDS.

Several readers have indicated interest in PC boards. To date, all prototype work has been done using “perfboards.” At least one reader has produced a circuit board, that person is willing to make boards available to other readers. If you e-mail me, I will

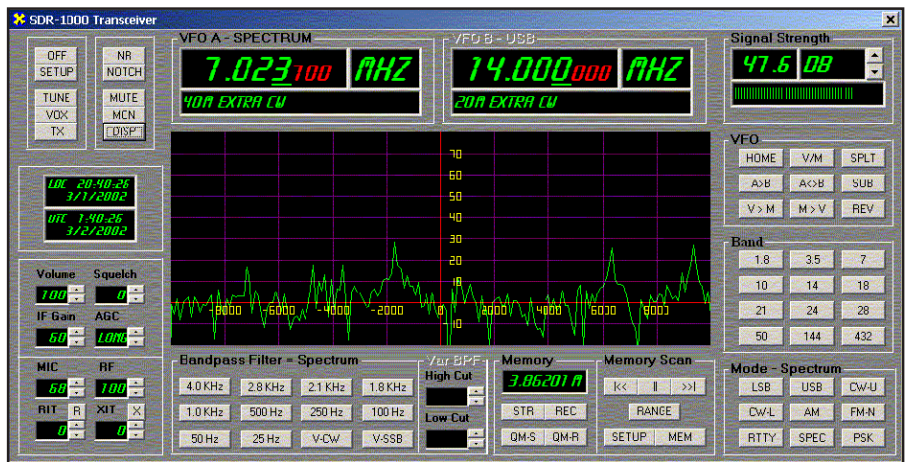


Fig 19—SDR-1000 front-panel display.

gladly put you in contact with those who have built boards. I also plan to have a Web site up and running soon to provide ongoing updates on the project.

Notes

- ¹G. Youngblood, AC5OG, “A Software Defined Radio for the Masses, Part 1,” *QEX*, Jul/Aug 2002, pp 13-21.
- ²G. Youngblood, AC5OG, “A Software Defined Radio for the Masses, Part 2,” *QEX*, Sep/Oct 2002, pp 10-18.
- ³The demonstration source code for this project may be downloaded from *ARRL Web* at www.arrl.org/qexfiles/. Look for 1102Youngblood.zip.
- ⁴The functions of the Intel Signal Processing Library are now provided in the Intel Performance Primitives (Version 3.0, beta) package for Pentium processors and Itanium architectures. An evaluation copy of IPP is available free to be downloaded from developer.intel.com/software/products/ipp/ipp30/index.htm. Commercial use of IPP requires a full license. Do not use IPP with the demo code because it has only been tested on the previous signal processing library.
- ⁵D. Hershberger, W9GR, and Dr S. Reyer, WA9VNU, “Using The LMS Algorithm For QRM and QRN Reduction,” *QEX*, Sep 1992, pp 3-8.
- ⁶D. Hall, KF4KL, “Spectral Subtraction for Eliminating Noise from Speech,” *QEX*, Apr 1996, pp 17-19.
- ⁷J. Bloom, KE3Z, “Correlation of Sampled Signals,” *QEX*, Feb 1996, pp 24-28.

⁸R. Lyons, *Understanding Digital Signal Processing* (Reading, Massachusetts: Addison-Wesley, 1997) pp 133, 330-340, 429-430.

⁹D. Smith, KF6DX, *Digital Signal Processing Technology* (Newington, Connecticut: ARRL, 2001; ISBN: 0-87259-819-5; Order #8195) pp 4-1 through 4-15.

¹⁰D. Smith, KF6DX, “Signals, Samples and Stuff: A DSP Tutorial (Part 1),” *QEX* (Mar/Apr 1998), pp 5-6.

¹¹Information on FFT convolution may be found in the following references: R. Lyons, *Understanding Digital Signal Processing*, (Addison-Wesley, 1997) pp 435-436; M. Frerking, *Digital Signal Processing in Communication Systems* (Boston, Massachusetts: Kluwer Academic Publishers) pp 202-209; and S. Smith, *The Scientist and Engineer’s Guide to Digital Signal Processing* (San Diego, California: California Technical Publishing) pp 311-318.

¹²S. Smith, *The Scientist and Engineer’s Guide to Digital Signal Processing* (California Technical Publishing) pp 107-122. This is available for free download at www.DSPGuide.com.

¹³Overlap/add method: *Ibid*, Chapter 18, pp 311-318; M. Frerking, pp 202-209.

¹⁴S. Smith, Chapter 9, pp 174-177.

¹⁵M. Frerking, *Digital Signal Processing in Communication Systems*, (Kluwer Academic Publishers) pp 237, 292-297, 328, 339-342, 348.

¹⁶See Leif Åsbrink’s, SM5BSZ, Web site at ham.te.hik.se/homepage/sm5bsz/.

¹⁷See Bob Larkin’s, W7PUA, homepage at www.proaxis.com/~boblark/dsp10.htm.

Linrad: *New Possibilities for the Communications Experimenter, Part 1*

Discussion opens with analog versus digital RF-input techniques and attendant performance considerations.

By Leif Åsbrink, SM5BSZ

In the old days, amateurs built their own equipment. Experiment was a natural part of the hobby. Inspired by what others did, one had to try to use the parts from one's own junk box to do something similar—or better.

With the commercial availability of modern amateur SSB transceivers, the need for experimentation declined. It is not easy to design and build equipment that can compete with commercial units. The best way to get a well-performing station has long been to buy a SSB transceiver. Only very few real enthusiasts build their own receivers and transmitters.

Today, the situation is changing. By use of simple equipment well suited for home building, radio signals can be moved into the digital world. Once a signal is available in digital form, a whole new field of experimentation is opened. A computer can do everything that we did before using analog electronics. Experimenting with different filter characteristics, AGC (automatic gain control) and AFC (automatic frequency control) can be done in soft-

ware at little cost—except the cost of the experimenter's time.

New possibilities in interference reduction treat different kinds of interference as separate signals, each one received with a digital receiver that optimizes the signal-to-noise ratio (SNR) for the particular interference. That brings with it a wide world of experiments with radio receivers, allowing reception of signals that cannot be received at all with a conventional SSB transceiver.

Linrad is a computer program that works under the *Linux* operating system on a standard PC (IBM-compatible, x86). This program receives an IF passband in digital form using simple read statements. Performance is determined by the hardware; the program just analyses the digital data. *Linrad* can be used to process the audio output from a conventional SSB radio or any other linear receiver with a bandwidth that can be handled by the sound card of the computer. *Linrad* can also use two audio channels (stereo) to process the *I/Q* pair produced by a quadrature mixer (direct-conversion radio). *Linrad* is designed for use with radio A/D converters in the future when boards and device drivers for *Linux* become available. The

Linrad program package is an ongoing development project.

In this first part of a series, I cover general receiver design philosophy. Part 2 will illustrate practical aspects of bringing radio signals into a computer via soundboards while subsequent articles will take up the specifics of *Linrad*, how to install it, what the special features are and how to use them to improve reception of weak signals.

Fundamental Receiver Operation

Fundamentally, there is no difference between analog and digital receivers. Both have the same basic problems with dynamic range and spurious responses. All the new digital methods for interference fighting have their equivalent analog counterparts. Let's begin with a general discussion of radio receivers intended to resolve common misunderstandings and explain how one can make sure a receiving system is properly optimized. The well-known problems of noise and dynamic range are central.

Linear Receivers

The ideal receiver for weak signals is the linear receiver. It uses linear processes only, and it may be imple-

mented in analog or digital hardware or by some combination thereof. The ideal receiver is completely quiet. That is, the output should be zero if a resistor at a temperature of zero kelvins (-273°C) were connected to the input. When something else is connected (an antenna), the ideal receiver selects a narrow part of the frequency spectrum, amplifies it and converts it to audio. That is all!

Linear processes may be split into several linear processes and applied after each other in any order. Because of the limitations of the available building blocks, one must use many linear processes to realize something that is near an ideal linear receiver.

Below is a list of the most important building blocks of a receiver for 144 MHz (see Fig 1). It is probably the most difficult band, in that very low noise figure is useful at the same time that very strong interference may be present, both in band and out of band. Notice that the goal is to come as close as possible to an ideal receiver so there are no compromises—just in case. If compromises are required, they should be made with full awareness of what the conflicting desires are, so no performance is thoughtlessly discarded.

For EME (moonbounce, reflecting signals off the moon) it is essential to have a receiver with performance close to that of an ideal receiver. When CW messages are received at a level where many repetitions are required, a small degradation in SNR will have large effects. Improving SNR by as little as 0.2 dB may be the difference between success and failure.

In “normal” communications, an improvement of 1 dB in SNR can barely be noticed. Degrading the noise floor by a single decibel makes it much easier to obtain good resistance against cross modulation and overload.

Noise Temperatures

Noise is best expressed as a noise temperature because noise temperatures are additive. A resistor that is kept at a temperature T will deliver the power $P = kT$ to another resistor with the same resistance for each hertz of bandwidth. (Where k is Boltzmann's

constant, 1.38×10^{-23} and T is in kelvins.) At room temperature, $kT = -174$ dBm/Hz. Two resistors having the same temperature are in thermal equilibrium and deliver the same power to each other. If one resistor is at 0 K, it will be heated by the power from the other resistor at temperature T according to the formula. The associated voltage is $V = \sqrt{kTBR}$, where B is the bandwidth in hertz and R is the source resistance in ohms. The equation is valid for normal temperatures and frequencies. For infinitely high bandwidths, V does not go to infinity because of quantum-mechanical effects.

The noise temperature of an amplifier is defined by a thought comparison with an ideal amplifier having exactly the same gain. It is the temperature that a resistor at the input of the ideal amplifier would have to produce the same noise power as the actual amplifier produces when connected to a resistor at 0 K.

In a system of amplifiers and other signal-processing hardware, the noise contribution from each stage can be expressed as a temperature component at the input. These temperature components are additive, and their sum is the system noise temperature.

The Input Amplifier

The input amplifier should not add significant amounts of noise to the signal received from the antenna, and it should not saturate from strong signals that may be present.

To obtain near-ideal noise performance from a receiver while maintaining good resistance to cross-modulation and overloading requires a good understanding of the problems involved. Look at ham.te.hik.se/~sm5bsz/pcdsp/preamp.htm, which mainly discusses the input circuitry and the tradeoffs between noise figure, selectivity and how they relate to the L/C ratio. The discussion is relevant to higher bands where too often, low impedance levels are chosen for the input filters. A 50- Ω transmission-line high-Q resonator may provide unnecessarily good filtering while it degrades the noise temperature too much. A higher impedance for the input filter

yields less noise and should be a good choice at 432 and 1296 MHz, where the low sky temperature makes system noise particularly important.

Once the compromise between noise performance and overload characteristics has been achieved, one should be sure the preamplifier is as close to ideal as possible. The famous Murphy's Law says something we should not forget: “Anything that can go wrong, will go wrong.” It is a good idea to place an overload detector at the output of all amplifiers that are followed by filters. The need for a filter directly after the preamplifier is discussed below.

The Second RF Amplifier

The gain of the preamplifier is usually insufficient to overcome the noise floor of the first conversion process, which is a frequency mixer in today's technology; but sometime in the future, it will probably be an A/D converter. Although it's possible to make broadband amplifiers with enough power output to preclude saturation by RF from the preamplifier, it is generally a good idea to insert some selectivity between the preamplifier and the second RF stage. Since this filter is mainly a precaution, there is no reason to make it complicated or to allow it to cause much attenuation in the passband.

The preamplifier is normally located very close to the antenna, while the rest of the receiver is placed indoors, so there is an attenuator in the form of a long cable between the preamplifier and the second RF stage. High preamplifier gain, low noise figure of the second RF amplifier and modest losses are required for nearly ideal performance. Table 1 shows data for 144 MHz. The noise figure of the second RF amplifier includes all losses between the preamplifier and the second amplifier. Attenuators inserted before an amplifier degrade the noise figure with their attenuation.

Table 1 shows degradation caused by the second RF amplifier, which is treated including the NF degradation caused by cable and filter losses. T is the temperature associated with the NF at the second amplifier input. $T(\text{ant})$ is the same noise contribution

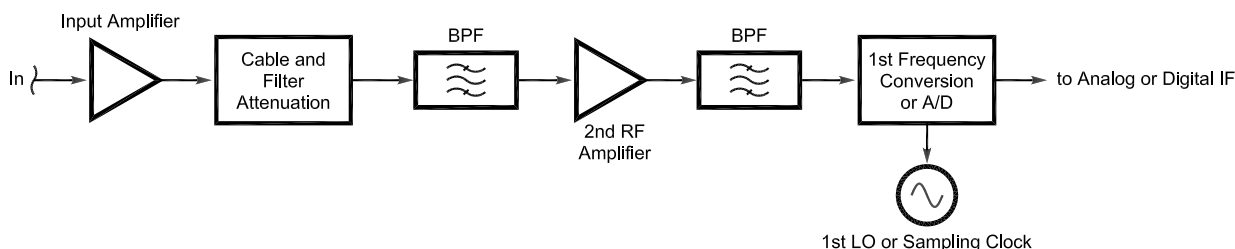


Fig 1—A block diagram of a typical receiver front end to feed a sound card for DSP.

when referenced to the input of the first preamplifier.

The noise temperature caused by antenna and preamplifier are assumed as shown in Table 2, with two alternatives. To obtain good dynamic range farther down the signal path, it will be necessary to allow some contributions to system noise from other amplifier stages. To keep the total excess noise low, the contributions must be very small. An inspection of Table 1 shows that even on 144 MHz, where the antenna temperature is not very low, the gain of the preamplifier must be about 20 dB.

To allow 3-dB of cable/filter loss and a second RF amplifier noise figure (NF) of 2 dB, preamplifier gain must be 25 dB. A neutralized GASFET with power-matched output has a gain on the order of 30 dB, and it allows 8 dB of combined filter and cable attenuation if the second amplifier has a NF of 2 dB.

Such a receiver front end does not have an optimum third-order intercept point (IP3) for in-band signals, but performance is usually good enough for practical purposes. A two-tone test of such an amplifier with an MGF1801 shows a mediocre IP3 of 0 dBm at the input. Signals up to about -30 dBm can be allowed without serious problems, since two -30-dBm signals give third-order IM spurs (IMD3) corresponding to -90 dBm at the input. For in-band signals, IM3 at such levels is not likely to be a problem. The noise floor is at -174 dBm/Hz, and so as not to destroy weak-signal operation, the interfering stations must have their noise sidebands below -145 dBc/Hz. Amateur Radio equipment is not quite that good as far as I know, so desensitization dynamic range (DDR) will be the limiting factor.

Should it turn out to be desirable, it is not difficult to improve the in-band IMD3 performance of the preamplifier by using so-called noiseless feedback stages and a second preamplifier using a device running at higher power, also with feedback. Table 3 shows the characteristics of a nearly ideal receiver based on the output-power matched, neutralized, MGF1801.

From the data in Table 3, we can get the noise temperature at the input of the second RF amplifier, referenced to the antenna input: $T_{rx} = 34231 / (0.315 \times 500) = 217.3$ K. The contribution from the second stage is 2.3 K.

The amount of gain required in the second RF amplifier will depend strongly on the noise figure of the next stage. The gain and output intercept point required for the second RF amplifier is listed in Table 4 for

different assumptions of the noise figure for the next stage, usually a Schottky-diode mixer.

Amplifiers having noise figures of 2 dB and power outputs up to 2 W are not difficult to design. Gain and saturation power level depends on the noise figure and maximum input power for the first frequency-conversion stage.

The RF Band-Pass Filter

The first conversion, be it an A/D converter or a diode mixer, has spurious responses. A filter with adequate suppression for signals on the spurious frequencies must be inserted in the signal path before the first conversion stage.

If necessary, the RF band-pass filter can be made very narrow with rela-

tively high attenuation in the pass-band. Any attenuation caused by the band-pass filter adds to the noise figure of the third stage, which leads to a bigger transistor in the second RF stage, as shown in Table 3.

When using RF A/D converters with today's technology, the sampling speed is typically 50 to 100 MHz. All frequencies between 0 and 200 MHz fall between zero and half the sampling frequency. The RF band-pass filter must allow only one set of alias frequencies, in a bandwidth of half the sampling frequency, to reach the A/D converter.

When using a local oscillator and a frequency mixer for the first conversion, the RF filter must suppress not only the mirror frequency but also frequencies that would mix with the LO overtones and give an output at the

Table 1—Degradation from a Second RF Amplifier Including Cable and Filter Losses

T is the temperature associated with the *NF* at the second-amplifier input. *T*(ant) is the same noise contribution when referenced to the input of the first preamplifier.

Preamp Gain (dB)	Second Amplifier + Loss			S/N Loss	
	NF (dB)	<i>T</i> (K)	<i>T</i> (ant) (K)	At 215 K (dB)	At 272 K (dB)
15	1	75	2.4	0.04	0.03
15	2	170	5.4	0.11	0.09
15	3	290	9.2	0.18	0.13
15	4	439	14	0.27	0.22
15	5	627	20	0.39	0.31
15	6	870	28	0.53	0.41
20	1	75	0.8	0.01	0.01
20	2	170	1.7	0.03	0.03
20	3	290	2.9	0.06	0.05
20	4	439	4.4	0.09	0.07
20	5	627	6.3	0.12	0.10
20	6	870	8.7	0.17	0.14
20	10	2610	26	0.50	0.40
25	1	75	0.2	0.00	0.00
25	2	170	0.5	0.01	0.01
25	3	290	0.9	0.02	0.02
25	4	439	1.4	0.03	0.02
25	5	627	2.0	0.04	0.03
25	6	870	2.8	0.06	0.05
25	10	2610	8.2	0.16	0.13
30	10	2610	2.6	0.05	0.04

Table 2—Noise Temperature Assumptions

Source	Noise 1	Noise 2
Sky	167 K	167 K
Sidelobes	15 K	40 K
Antenna losses	5 K	5 K
Cable + relay	13 K (0.2 dB loss)	30 K (0.4 dB loss)
Preamplifier	15 K (0.22 dB NF)	30 K (0.4 dB NF)
Total	215 K	272 K

IF. A narrow RF filter will also suppress false responses caused by spurs that may be present in the LO signal. There are more reasons for a narrow RF filter below.

The First Conversion: A/D Converter or Diode Mixer

Someday, an A/D converter will be the first mixer in receivers up to many hundreds of megahertz. Today's technology allows 65-MHz sampling at 14-bit resolution using, for example, the AD6644 from Analog Devices. Such a chip offers typically 74 dB of SNR at a bandwidth of 32 MHz, corresponding to 149 dBc/Hz. The peak-to-peak amplitude such a device needs for full range is 2.2 V, corresponding to about 11 dBm into a 50-Ω load. The noise floor is at -138 dBm/Hz, which corresponds to a noise figure of 37 dB, all referenced to a 50-Ω load. The input impedance of the AD6644 is 1 kΩ, so the power actually consumed by the chip is -2 dBm for full scale. If a lossless impedance transformer were used at the AD6644 input, rather than a 50-Ω termination resistor, the noise floor would be at -151dBc/Hz, with an associated noise figure of about 23 dB.

The AD6644 receives noise from nearly 10 times more bandwidth than represented by the digital bandwidth. It is not possible to lower the noise figure by more than about 6 dB without using a selective amplifier or degrading the dynamic range. Allowing 3 dB of loss for the RF filter, Table 4 (extrapolated) shows that the AD6644 will need 39.6 dB of gain in the second RF stage if the AD6644 is terminated in a 50-Ω resistor. Saturation of the AD6644 will occur at 14 dBm, 38.6 dB below the level where the MGF1801 saturates.

High-level Schottky-diode mixers (level-23 from Mini-Circuits) have IP3s around 30 dBm and 1-dB compression points of around 15 dBm. Consider a 10-dB gain second RF amplifier using some transistor that can deliver 200 mW (23 dBm) through the RF filter with an impedance-matching network required by the mixer. This will make a level-23 mixer saturate just before the preamplifier, with an IP3 around -2 dBm at the input. Since mixers attenuate by about 8 dB and the noise figure at the mixer input has to be maximum 10.4 dB, the amplifier after the mixer must be very quiet lest it degrade the system noise figure. Compensating a poor IF-amplifier noise figure with more gain in the second RF amplifier will degrade system intercept point.

It follows from the discussion above that the MGF1801 power matched and neutralized amplifier is good

enough when it comes to power-handling capabilities. A 10-dB improvement is not difficult by noiseless feedback, but to utilize the improvement one must design very special low-noise, high-level mixer/IF combinations. In cases where signals well outside the desired passband cause the preamplifier to go nonlinear, noiseless feedback and additional filters and amplifiers may be needed.

The A/D converter has superb linearity. IP3 is only about 8 dB lower than a well designed level-23 diode mixer. A diode mixer can be driven into the nonlinear region by a single very strong interfering signal without any serious degradation of a desired weak signal, while the D/A converter produces useless data when saturated. Saturation occurs about 36 dB earlier in an AD6644, so if there is only one interfering signal, the diode mixer allows about 30 dB more interference signal. It is quite clear already that today's A/D

technology is extremely attractive.

The First Local Oscillator

If the first conversion is an A/D converter, the first LO is the sampling clock, which has a fixed frequency. The first LO will be at a fixed frequency also were a diode mixer used in conjunction with a broadband IF. Typically, an LO frequency of 116 MHz is used to convert 144 MHz to 28 MHz.

Fixed-frequency oscillators using crystals can be made with very little phase noise. It may seem very simple to use a 12.88888-MHz crystal and two frequency triplers to produce 116 MHz. Good filtering is required, though, because the thirteenth overtone of 12.88888 MHz is at 167.55 MHz, which may cause a spurious response at 139.55 MHz that may not be suppressed much by the RF filters. Good filters, with two L-C circuits, to make the output of all frequency-multiplier stages pure will prevent this problem.

Table 3—Typical Output-Power Matched MGF1801 Preamplifier (Negligible System Noise Degradation)

Preamplifier

Antenna temperature = 200 K
 Preamplifier NF = 0.2 dB = 15 K
 Preamplifier gain = 27 dB = 500 times in power
 Noise temperature at output of preamplifier = (200 + 15) × 500 = 107500 K
 Input intercept point = 0 dBm
 Saturated power output = 18 dBm

Cable/Filter

Losses = 5 dB (gain = 0.315 times in power)
 Output noise temperature = 0.315 × 107500 + (1 - 0.315) × 290 = 34061 K

Second RF Amplifier

NF = 2 dB = 170 K
 Noise temperature at input = 34061 + 170 = 34231 K
 Preamplifier intercept point at input = 0 + 27 - 5 = 22 dBm
 Saturated power input = 18 - 5 = 13 dBm

Table 4—RF Amplifier 2 Requirements

Gain, Output Power and Output IP3 required of RF Amplifier 2 for different Noise Figures of the Third Stage to make the Third Stage Contribute 2 K at the Antenna Input. This table is based on the data of Table 3.

Saturated Minimum Output				
NF (dB)	Temp (K)	Gain (dB)	Power Output (dBm)	IP3 (dBm)
6	865	4.4	17.4	26.4
9	2013	8.1	21.1	30.1
12	4307	11.4	24.4	33.4
15	8880	14.5	27.5	36.5
18	18009	17.6	30.6	39.6
21	36221	20.6	33.6	42.6

When the first IF is routed to a narrow filter at typically 9 MHz or 10.7 MHz, the first LO must produce a variable frequency. It is very difficult to make good oscillators with variable frequency. The first LO is usually the limiting factor for receiver dynamic range in well-designed receivers having a first IF of narrow bandwidth. Many articles in the amateur literature describe the design of low-noise frequency synthesizers for LO use.

It is not easy to select a good frequency for the first local oscillator. There are many problems. For example, using 116 MHz to convert 144 MHz to 28 MHz has the following problem: A signal at 145.3 MHz will produce its main signal from the IF port at 29.3 MHz. If the signal were very strong, the third overtone of the IF signal at 87.9 MHz would be present inside the mixer. There, it would be mixed with 116 MHz to produce a false signal at 28.1 MHz that, in turn, would cause interference for signals at 144.1 MHz. There will always be combinations of overtones of the IF signal and the LO or its overtones that would fall within the IF passband, causing spurs at some frequencies. To avoid such problems, it is a good idea to avoid LO/IF combinations that give spurs like this of low order, and it is a good idea not to make the RF passband wider than necessary.

Broadband IF Filters and Amplifiers

The problem of amplifying and filtering the signal present at the output of the first mixer is identical to the problem of designing the RF amplifier and RF filter section. The noise figure need not be as low: The only reason to have a very low noise figure is to get good dynamic range in earlier stages, because their gain can be made lower.

If the IF amplifier had a noise figure of 0.6 dB (= 43 K), the stage limiting the in-band dynamic range will be allowed to contribute with 127 K for the IF noise figure to become 2 dB. If the IF amplifier has a noise figure of 1.6 dB (= 130 K) the gain of the IF amplifier must be increased by 5 dB to keep the IF noise figure at 2 dB. That would be a bad idea: It is better to increase RF gain and accept a worse IF noise figure.

The purpose of the broadband IF filter is to suppress the mirror frequency and the spurious responses of the next frequency conversion. The first broadband IF filter may also be used to shape the pulse response of the receiver, to allow an efficient noise blanker. A wide bandwidth with roughly Gaussian frequency response makes interference pulses very short

and allows an efficient noise blanker.

Conversion to Baseband

The conversion to baseband is normally incomplete in analog receivers. The baseband signal is a complex signal that has two components, in-phase (*I*) and quadrature (*Q*). The two signals, *I* and *Q*, contain the same frequencies and their phase relation contains information about whether the signal at baseband is above or below the frequency of the last LO (the BFO). In analog filter-based SSB receivers, one uses a narrow filter—the last IF filter—to ensure that no signal is present on one side of the last LO (undesired sideband). Thus, one is sure that any signal present at baseband must be from the desired sideband. Consequently, there is no need to produce both *I* and *Q* because their phase relationship will give no new information.

An analog receiver for AM may convert the IF signal to a baseband signal with both *I* and *Q*. If the frequency of the LO were very close to the carrier of the AM signal, the *Q* signal could be used to control the last LO frequency through a low-pass filter. This way, the LO becomes phase locked to the carrier and the modulation is in the *I* signal only. The noise in the *Q* channel will not contribute and some improvement of SNR is possible.

Digital-signal processing is easier and more efficient at baseband with complex signals. There are several different ways to go from RF to the digital baseband *I-Q* pair. When the RF signal is fed to an AD6644 sampling at 65 MHz, a 144-MHz signal will be at 14 MHz in the digital data stream. A general-purpose DSP or a modern PC is not fast enough to process data at 65 MHz. There is a chip, the AD6620 (Analog Devices), that mixes frequencies to baseband by multiplying the input samples by a sine/cosine function at a frequency specified by the user.

The AD6620 is normally used to sample the RF signal directly so the input data stream is real data. To listen to 144 MHz for weak signals, one would make the internal digital oscillator of the chip operate at 144.15 MHz, typically. The 14.000-MHz signal corresponding to 144.00 MHz is then converted to two signals at 150 kHz, with a phase shift of 90° between them. A signal at 14.300 MHz, corresponding to 144.3 MHz, would also be converted to two signals at 150 kHz; but with the opposite phase shift. Because of the precise phase and amplitude relations possible in digital circuits, these two signals can be completely separated in later processing stages.

The AD6620 contains decimating

filters that gradually bring the sampling speed down. Unfortunately, these filters do not allow very steep cutoff so the spur-free bandwidth becomes very limited in relation to the re-sampled data speed. There are better data decimation chips, for example the GC4016 from Graychip, which will allow extremely steep filters and an output data stream that is not over-sampled but still spur-free.

I have no practical experience with AD6644 and AD6620 or GC4016. These chips would allow more bandwidth and better dynamic range compared to most sound-card-based solutions.

When using an audio board to convert from analog to digital, there are two ways to go. One is to filter a well-defined passband by means of an IF filter with steep skirts that will allow very good suppression of the image frequency on the other side of the LO. In this case, a single mixer and one A/D converter channel is required for each RF channel. With a standard audio board, sampling at 44.1 kHz, one can receive two independent signals this way at bandwidths up to about 20 kHz. Unless great care is taken, overtones in the audio range (IM2) cause strong spurs that can easily be avoided by allowing only a 10-kHz bandwidth, in which case the audio range is placed typically from 10 to 20 kHz.

When the A/D converter is sampling real data (the filter method), the conversion to complex data is made in the computer. The other way is to produce the baseband complex pair (*I* and *Q*) in analog hardware (direct-conversion radio), in which case two audio channels are needed for each RF signal.

Creating the baseband signal in analog hardware saves some computer time and gives more bandwidth—twice as much—because of the use of two audio channels. It is advantageous to eliminate sophisticated IF filters, but direct conversion has the problems of audio overtones and requires great care for extremely good linearity of mixers and audio amplifiers. The local oscillator must be extremely stable, because modulation on it will be detected (mixed with the LO carrier) to produce interference in the audio range.

Summary

This article has concerned itself with the broad issues involved in receiver design. In my next segment, I shall discuss details in design of the hardware required to move radio signals into the computer by use of sound-cards. □□

A Guy-Wire-Interaction Case Study

One ham's antennas and guys interacted more than he expected. Do yours? Learn how he discovered the problem and what he did about it.

By Dick Weber, K5IU

I've written this article to discuss an unexpected interaction I had between an HF Yagi and the insulated steel guy wires on a tower 125 feet away. The interaction was strong enough to cause the SWR to go from 1.05 to 1.35:1 when the beam was pointed at the guys. After the interaction was discovered, I used *NEC2* models to see if the interaction could be predicted.¹ The models clearly show a strong interaction and provided a good prediction of the SWR. An interesting aspect of the NEC modeling was examining the magnitudes of the guy-segment currents predicted by these models. Segments that you wouldn't

expect to have high currents did have, while segments that you would expect to have high currents didn't have. Although this interaction was experienced with a 17-meter Yagi, the conclusions and issues raised are applicable to tower installations with antennas for any HF band. Overall, guys appear to act as an array of parasitic elements with coupling among themselves, and interactions with nearby antennas can't be mitigated by following existing guidelines for guy-segment lengths. Therefore, published guidelines for using conductive guys need to be revised.

Observed Guy Interaction

For several years, I've been building and experimenting with HF Yagi antennas using a 56-foot self-supporting tower as the host for these antennas. Prior to 2000, I experimented with

numerous designs including three 17-meter beams. Some of these were later installed on my 140-foot rotating tower after I was happy with their performance, while some were used for extended periods on the test tower. One thing I noticed while testing these antennas on the test tower was that some of them had slightly higher SWRs when they were pointed toward my rotating tower, about 125 feet away. This was not surprising because I had Yagis for 40, 20, 15 and 10 on it. The SWR increase was not very much for some. For the others, none was seen. I didn't record the SWRs because the increases weren't of any significance.

Up to that time, 17-meter beams I built had no SWR bumps as they were rotated through 360° on the test tower. These were three-element beams with T matches on 18- to 24-foot booms with

¹Notes appear on [page 48](#).

typical SWRs in the 1.2-1.3:1 range. Based on this, I didn't expect any SWR bumps to show up with a new four-element, 17-meter beam that I built in the spring of 2000 (see the "YO7 Yagi Designs" sidebar²). As it turns out, I did experience a drastic change in SWR as it was rotated past my rotating tower.

When I first set the hairpin match on the new 17-meter antenna, it was pointed about 90° clockwise from the heading toward the rotating tower. As it turns out, this was fortunate because the guy interaction was not very strong in this direction. After setting the hairpin match and rotating the beam to observe its pattern, I decided to see if there were any slight SWR bumps, although I didn't expect any. After I saw the SWR go from 1.1 to 1.3:1, I rocked the antenna back and forth to find the peak SWR. This produced another unexpected result. The SWR peaked when the beam was

pointed at one set of guy wires on the rotating tower, not when pointed at the tower itself as shown in Fig 1.

I then did a search to find the worst and best SWRs at the band edges and at mid-band. These and the SWR at the original heading I used to set the matching network are shown in Fig 2.

The data in the figure show that the worst SWR was at the bottom of the band. In view of this, I made additional SWR measurements at the lower band edge for 360° of antenna rotation. These are shown in Fig 3. After these tests, the rotating tower was turned through 360° with the 17-meter beam

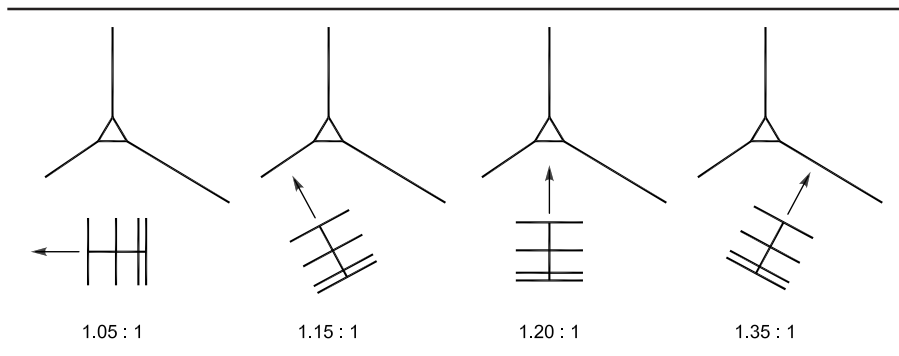


Fig 1—SWR peaked with beam pointed at one guy set.

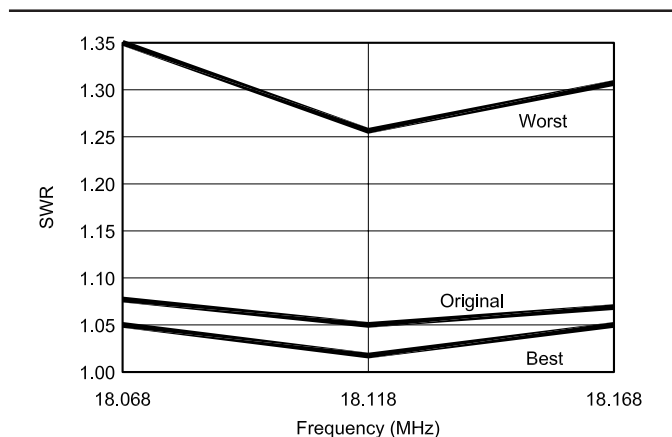


Fig 2—SWR at best, worst and original headings.

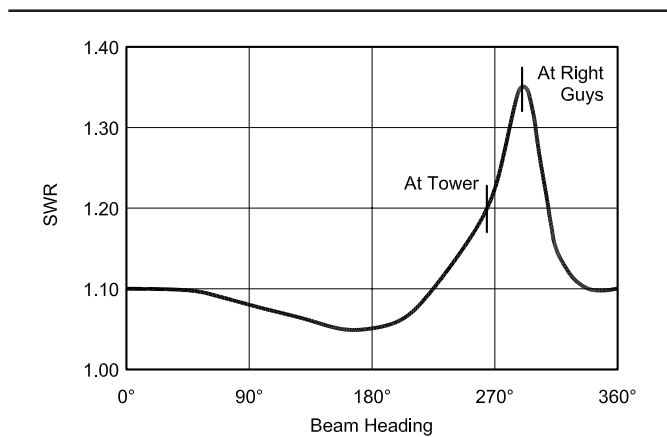


Fig 3—SWR at lower band edge for different beam headings.

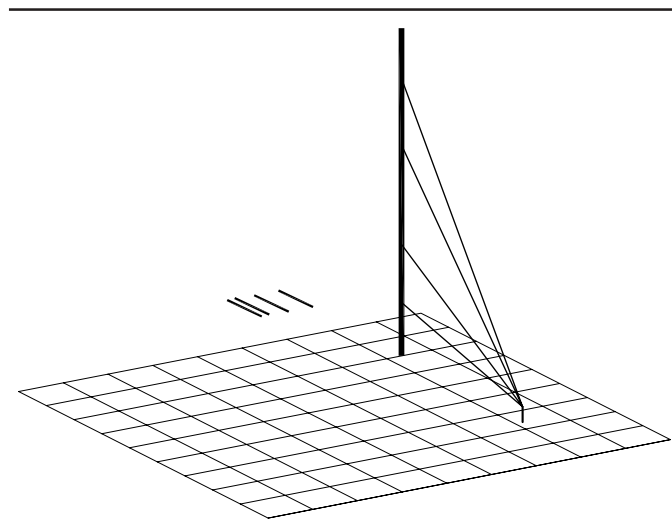


Fig 4—NEC2 model of 17-meter Yagi with the guys to the right of the tower.

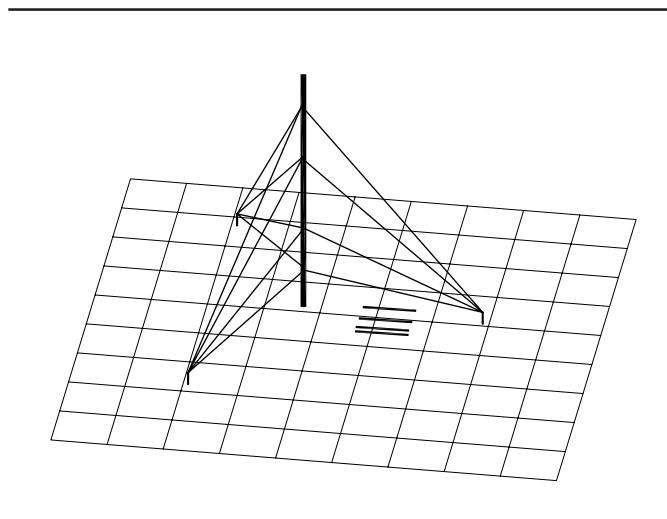


Fig 5—NEC2 model of 17-meter Yagi with all guys.

pointed first at the tower and then in the direction of the worst SWR. No change in SWR was seen in either case. Clearly, a guy-wire interaction was present. In view of this and the fact that I planned to put a 17-meter beam on the rotating tower in the future, the steel guys were replaced with nonconductive guys. After the new guys were installed, I checked the 17-meter Yagi SWR. I found that the SWR was now no more than 1.05:1 across the band at all beam headings. The data shown in Figs 1, 2 and 3 were taken using a Bird ThruLine, Model 43 wattmeter at the end of a 105-foot length of LMR 400.

NEC SWR Predictions

With the old guys on the ground, I measured and recorded the insulated segment lengths. In doing this, I found that similar segments of each guy set were within 1 to 3 inches of each other. Using the measured lengths, two NEC2 models of the guying system and the Yagi were constructed as shown in Figs 4 and 5. The first model had only the guys in the direction of the worst SWR and the second model had all the guys. A 1-inch gap was put between the guy segments and the model used average ground with a conductivity of 0.005 S/m and a relative permittivity of 13.0. The tower-end of the guys had a 24-inch EHS section from the first insulator to where it secured to the tower. The ground end of the guys secured to 7-foot-tall elevated guy posts 90 feet from the base of the tower.

The NEC2 models were first used to see how well predicted SWR would correlate to measured values. To do this, the models were used to find the input impedance of the Yagi driven element as a function of beam heading at 18.068 MHz. This was done with all guys present and again with only those guys to the right of the tower. The predicted impedances are listed in Table 1.

To find the corresponding SWRs for the impedance values shown in Table 1, a simple matching network was defined and applied to the listed impedances. The matching network was based on the driven element's predicted impedance with the antenna pointed in the direction at which the beam's hairpin match was set. Since the beam was initially adjusted for the best SWR at 18.118 MHz, the matching network was defined to give a 1:1 SWR at 18.118 MHz. The driven-element impedance at 18.118 MHz was found to be $15.26 - j23.15 \Omega$ with all guys present. The driven-element impedance was almost the same when

only the guys to the right of the tower were used. To transform this to 50Ω , the matching network used a series reactance of 23.15Ω at 18.118 MHz and a perfect matching transformer with an impedance ratio of 3.28:1. Using the transformed impedances and the loss of the transmission line, SWRs at the end of the transmission line were calculated. These are shown in Fig 6 along with the measured values.

There are two interesting features in Fig 6. First, the best alignment of a predicted SWR curve and the measured curve is for the NEC model where only the guys to the right of the tower are considered. At this heading, the antenna is beaming directly at the

guys as shown in the extreme right portion of Fig 1. This is not surprising because only one guy set is used in the model to generate this curve. Second, the best agreement for the maximum measured and maximum predicted SWR levels is with the beam pointed at the tower. The direction of the predicted maximum is not surprising either, because the guys to the left and right of the tower are essentially symmetric about a line between the two towers. What remains surprising, though, is the fact that the worst-case measured SWR was in the direction shown in Fig 1.

To understand the misalignment of the plots in Fig 6, two things were done. First, both NEC models were run

Table 1—NEC Predicted Input Impedances at 18.068 MHz with Guys

Heading	1 Guy Set		3 Guy Sets	
	R	X	R	X
0.0°	14.28	-23.64	14.25	-23.64
22.5°	14.27	-23.61	14.28	-23.56
45°	14.28	-23.62	14.39	-23.59
67.5°	14.28	-23.63	14.39	-23.65
90°	14.33	-23.61	14.36	-23.62
112.5°	14.38	-23.57	14.39	-23.56
135°	14.29	-23.55	14.28	-23.54
157.5°	14.24	-23.62	14.24	-23.63
180°	14.28	-23.64	14.15	-23.81
202.5°	14.28	-23.61	13.39	-24.51
225°	14.14	-23.54	12.15	-25.06
247.5°	13.63	-23.73	11.52	-24.70
270°	13.03	-24.84	11.84	-24.84
292.5°	13.02	-25.79	12.69	-25.64
315°	13.71	-25.18	13.68	-25.16
337.5°	14.21	-24.01	14.21	-24.02
360°	14.28	-23.64	14.25	-23.64

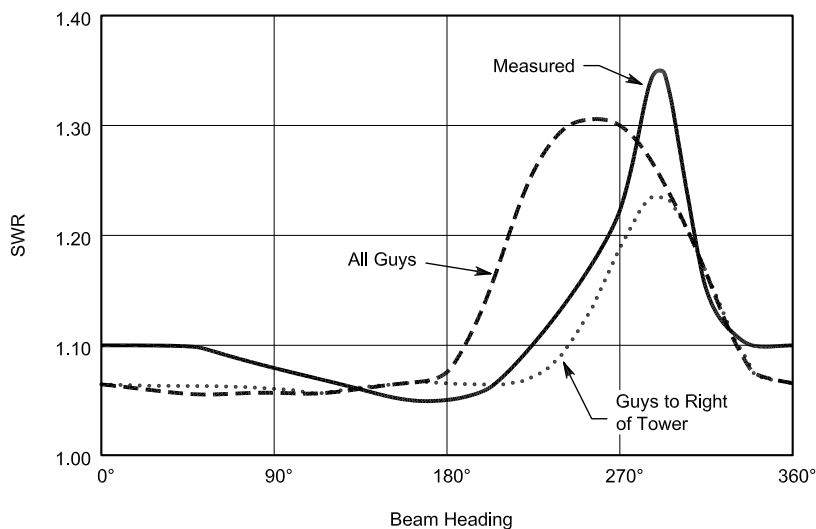


Fig 6—Predicted and measured SWR as a function of beam heading.

with the tower removed. This made no difference in the predicted driven element impedances. Second, a third NEC model was generated that included an 80-meter elevated-radial ground-plane antenna behind the guys that were in the direction of the worst case measured SWR. This antenna hangs 35 feet from the tower using a support wire. The feed point is 12 feet above ground with the radial ends 7 feet above ground. This is the only conductive structure within 140 feet of the rotating tower other than the test tower. The NEC model with the elevated-radial ground plane showed essentially no difference in the driven element's impedances as compared to when the 80-meter antenna was absent. This was not surprising because the actual SWR interaction ceased when non-conductive guys were installed while the 80-meter elevated-radial ground plane remained.

I'm not able to account for the misalignment of the plots in Fig 6. Similar guy segments are within several inches of each other and the test tower is almost in line with the back guy wire. This means the guy layout is symmetric to the left and right and that there is no asymmetry overall. It may be that minor differences in actual guy segment lengths can cause drastic changes in the overall interaction of the guys. Or, perhaps the small amount of capacitive coupling between segments from the guy insulators in combination with slightly different guy-segment lengths can lead to a strong interaction by one set of guys.

Regardless, the SWR prediction is quite good overall, but there must be some effects for which my NEC2 model does not account.

Guy-Segment Currents

The NEC2 model with the guys to the right of the tower while the four-element Yagi was beaming at them was used to better understand the guy interaction. It was used because it showed the best SWR alignment with the measured data as shown in Fig 6. It was used to see how the predicted currents in the guy segments compared to each other. Fig 7 shows the predicted current levels after they have been normalized to the largest current within the set of segments. The segment

with the largest current is within the guy that goes to the 48-foot level as indicated by the box. Normalized currents are listed below the corresponding guy segments and guy-segment lengths are listed above. The currents in the guy segments that are secured to the grounded elevated guy posts are shown in parentheses. These values should not be considered because of inaccuracies in using NEC2 to connect a conductor to ground.

It is interesting to compare the currents in the lengths of the guy segments shown in Fig 7 to each other. It is especially interesting to look at the currents while comparing the guy-segment lengths to those *The ARRL Antenna Book* suggests avoiding for 17 meters. *The Antenna*

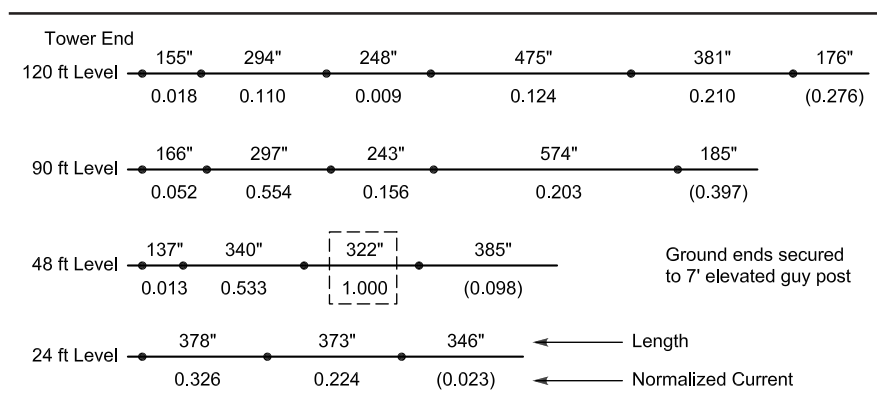


Fig 7—Normalized segment currents from NEC2 model at 18.068 MHz.

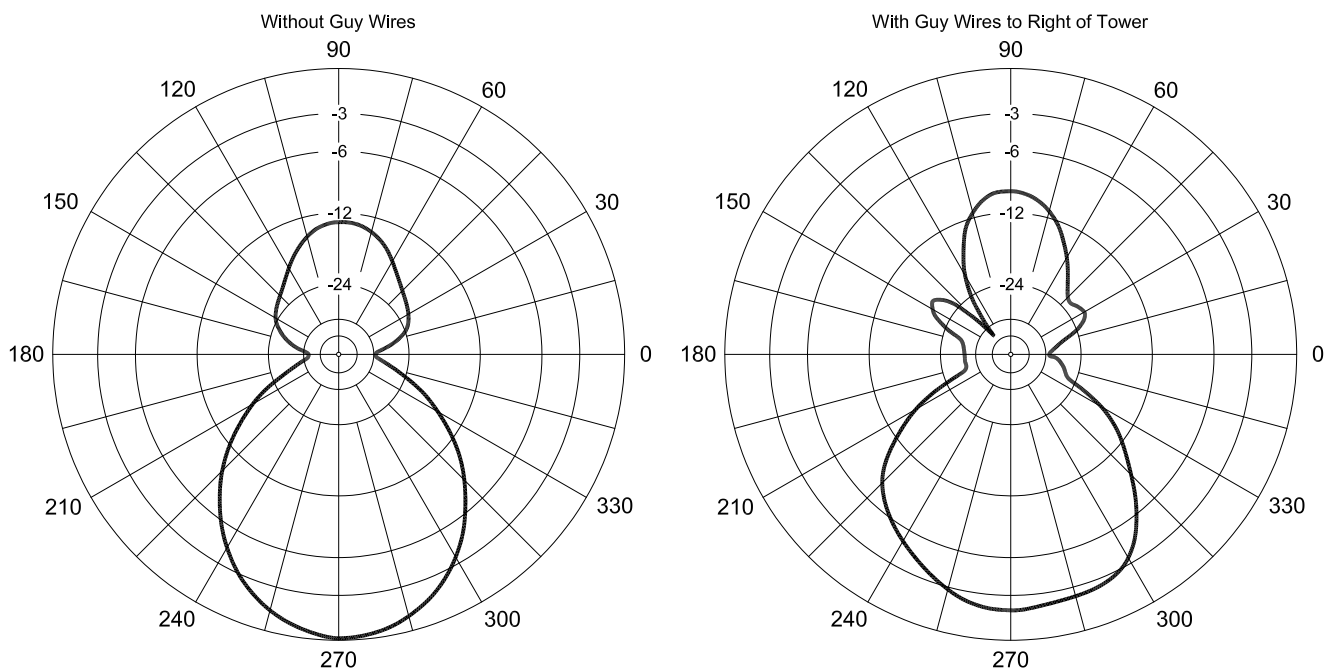


Fig 8—Azimuth patterns at 12° elevation, without and with guys (four-element Yagi beaming at guys).

Book shows that lengths between 270 and 336 inches (near a half wavelength) and between 558 and 696 inches (near a full wavelength) should not be used.³ As might be expected, the segments that are near a half wavelength (317 inches at 18.068 MHz) have the highest currents.

It is also interesting to note that there are relatively high currents in some guy segments that are longer than 336 inches. Segments of the lowest guy show this. The 378-inch section at the tower end of the guy at the 24-foot level has appreciable current. It is also interesting that the adjacent 373-inch segment has less current, although it is five inches closer to a half wavelength. You might expect these currents to be about the same or for the current in the 373-inch segment to be somewhat higher.

Another interesting case is the current in the 340-inch section of the guy going to the 48-foot level. It has significant current, although it is longer than the segment length to be avoided as recommended by *The ARRL Antenna Book*.

Probably the most interesting anomaly is the 5:1 ratio of predicted currents between the 297-inch segment near the tower at the 90-foot level and the 294-inch segment of the top guy just above it. This is curious because you would expect the currents in these two guy segments to be similar. It appears as though guy segments

can act together as an array. From this it is prudent to not treat guy segments as isolated components. This implies that a more rigorous approach to defining inappropriate guy-segment lengths is needed.

Effect on Gain when Beaming through Conductive Guys

The NEC model used to generate the currents shown in Fig 7 was also used to predict the antenna's radiation patterns with and without the guys on the tower with the 17-meter Yagi on the test tower. Again, this was with the guys to the right of the tower while the Yagi was beaming directly at them. These are shown in Fig 8 at 18.118 MHz for an elevation of 12°, which is the elevation angle for the peak of the lowest lobe. The pattern with the guys to the right of the tower is distorted, with a 1.9-dB gain reduction at the peak of the beam relative to the pattern without the guys present. This appreciable gain reduction is about the same as changing to a two-element Yagi in the clear. This issue will be discussed again.

I mentioned that prior to building the four-element, 17-meter beam discussed above, I had built three other beams for this band. They were three-element designs on 18- to 24-foot booms with T matches. Unlike the four-element design, they were not highly optimized for minimum SWR with maximum gain. These had SWRs in the 1.2 to 1.3:1 range and had about 0.5 to 1.0 dB less gain. Because of their lower gains and higher SWRs, I believe the guy interaction was masked. As I remember, there were no SWR changes as these antennas were pointed at the guy system. In reality there may have been, but they certainly weren't significant enough to be noteworthy. Although the guys did not noticeably affect the SWRs of the three-element designs, their patterns most likely were.

The plots in Fig 9 show patterns for a three-element design with and without the guys to the right of the tower. These are the same conditions used for the plots in Fig 8. This design was on an 18-foot boom (see the "YO7 Yagi Designs" sidebar). The plots of Fig 9

Table 2—Gain of 17-Meter Yagis at 12° Elevation

	Gain (dBi)		
	2 Element	3 Element	4 Element
Without Guys	12.5	13.7	14.8
With Guys to Right of Tower	na	11.8	12.9

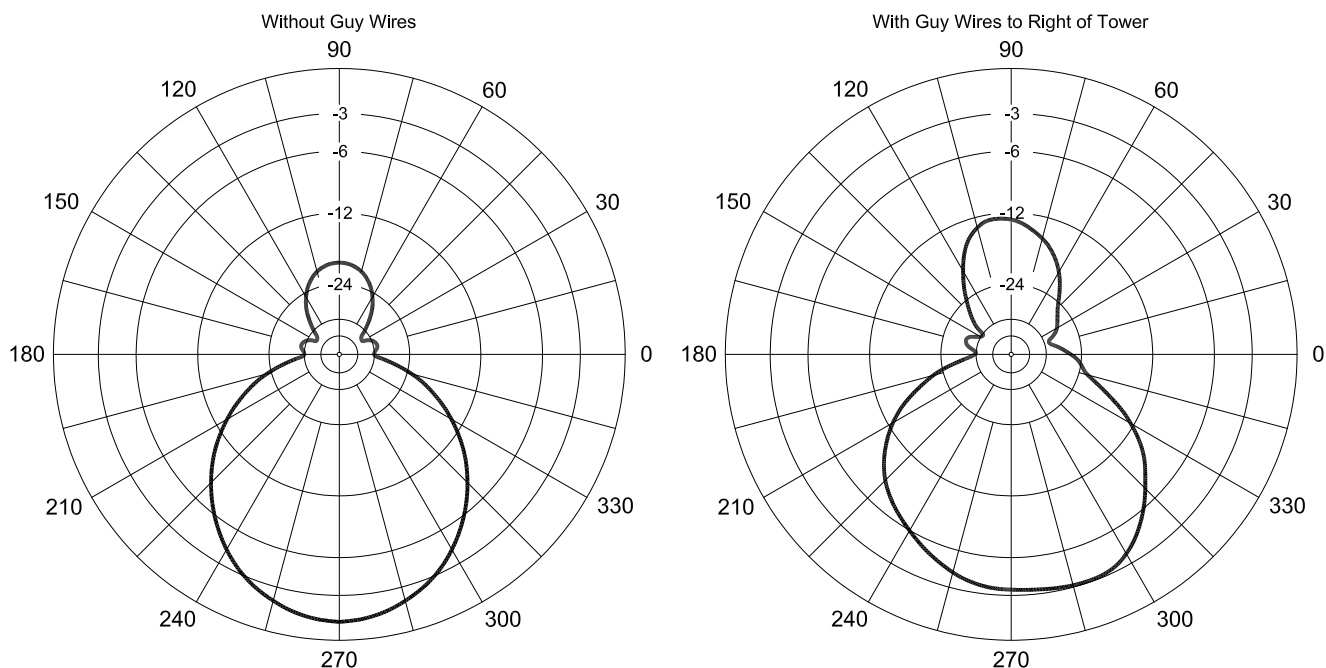


Fig 9—Azimuth patterns at 12° elevation, without and with guys (three-element, 18-Foot-Boom design).

coincidentally show a reduction in forward gain of 1.9 dB at the peak of the beam relative to the pattern without the guys present. As a further comparison, *YO7* was used to generate a two-element Yagi for 17 meters (also shown in the sidebar). The design was then modeled in *NEC2* with the guys absent and its gain predicted. This model also used the same conditions as the plots

in Fig 8. The gain of the two-element Yagi at the peak of its lower major lobe and the gains of the three- and four-element Yagis, with and without guys, are listed in Table 2.

Table 2 shows that the conductive guys lower the gain of the four-element Yagi to almost that of the two-element design. It also shows that the gain of the three-element beam drops

below that of the two-element version. In view of this, I suggest that you make sure you don't have a guy interaction with a Yagi as it beams through the guys or another tower. You may not be getting full performance from your antennas, and you may not get the full benefit of a new, higher-gain antenna over an appreciable portion of antenna rotation.

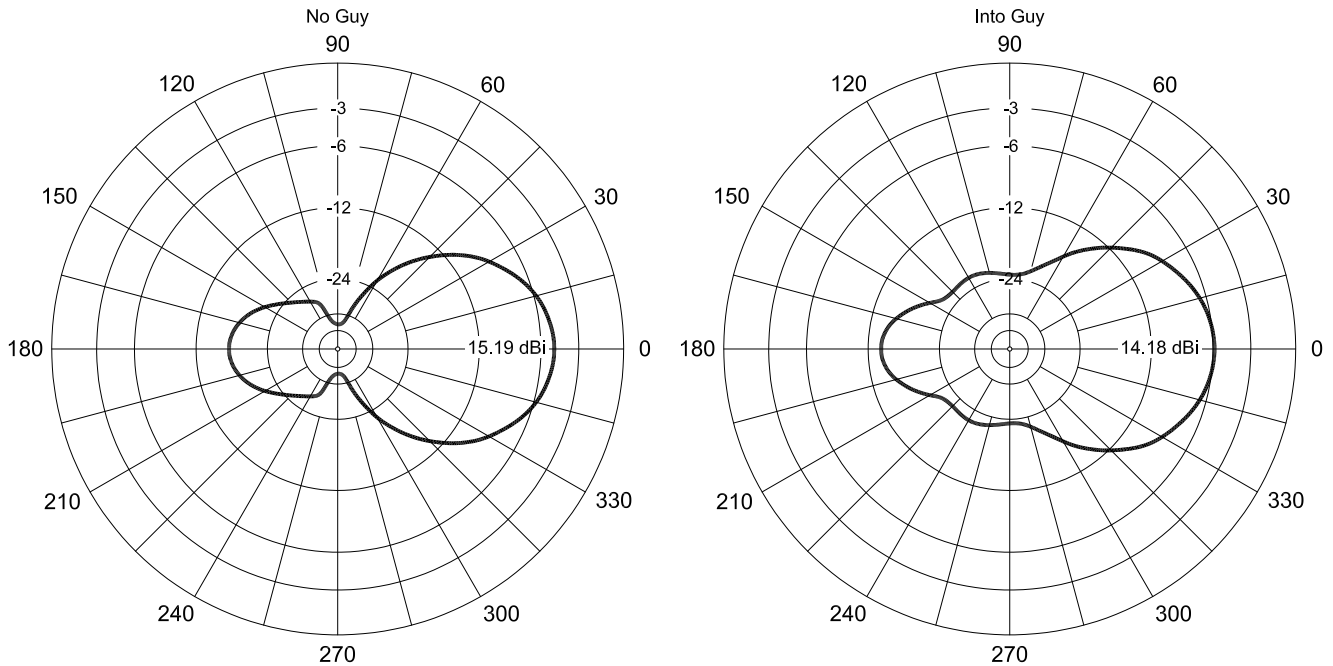


Fig 10—17-meter Yagi patterns with conductive guys.

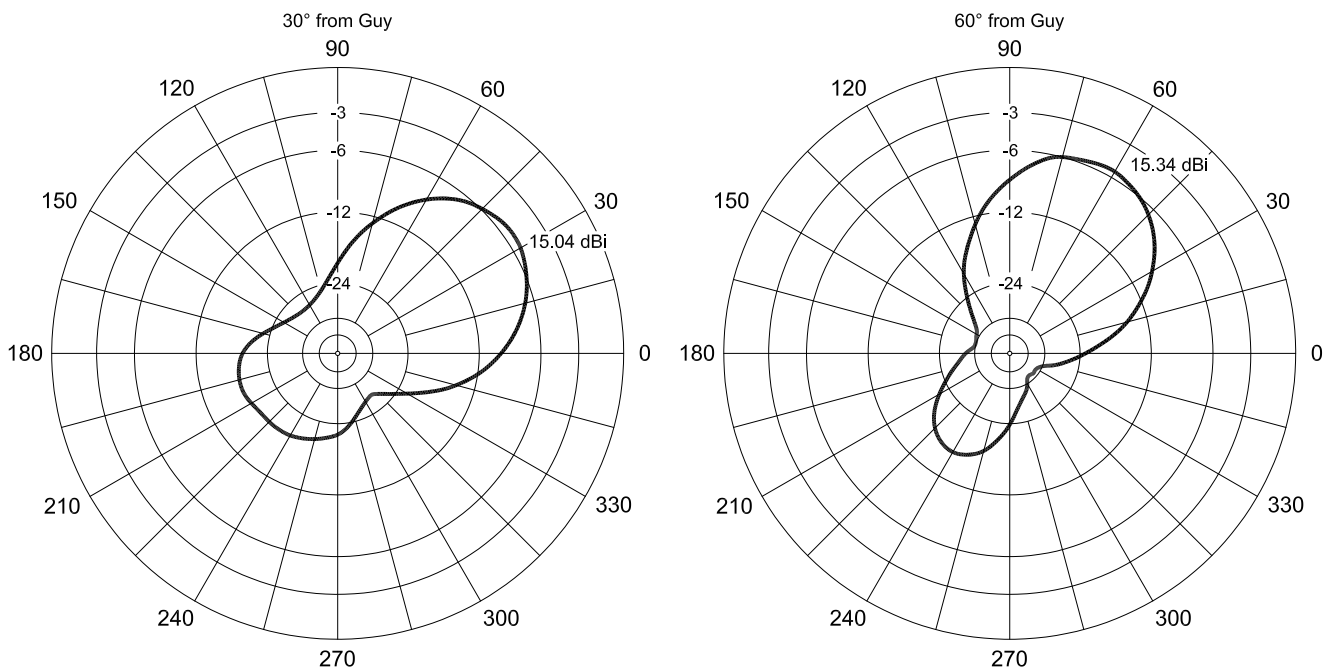


Fig 11—17-meter Yagi patterns with conductive guys.

Effect on Gain when Mounted on Tower with Conductive Guys

The steel guys on the 140-foot rotating tower were originally installed when I did not anticipate mounting a 17-meter beam on it. Twelve years later, this changed with the aim to move the 17-meter beam from the test tower to the 92-foot level on the rotating tower. In view of this, it is interesting to see what might have happened to the pattern of the 17-meter Yagi if it had been installed while the steel guys were in place. An additional *NEC2* model was set up with the four-element 17-meter Yagi mounted on the rotating tower at the 92-foot level and predictions made with and without the steel guys. Three cases with the guys were considered: One had the boom in line with one set of guys. The second had the boom rotated 30° from being in line with a guy. The last was with the boom rotated 60° from being in line with a guy. At 60°, the boom was midway between two guys. The patterns shown in Figs 10 and 11 are at 18.118 MHz for an elevation of 8°, which is the elevation angle for the peak of the lowest lobe.

The patterns shown in Figs 10 and 11 indicate that the guys do have an effect. They show that the gain is reduced by about 1 dB compared to the case where conductive guys are absent. This is about the same reduction in gain as when going from the four-element design to a shorter-boom design with three elements. An interesting result of these *NEC2* runs is for the case where the Yagi is beaming midway between two guys. For this case, *NEC2* shows a slight increase in gain. This outcome is obviously caused by the unique lengths entered into the *NEC2* model. No doubt, this result would change if the insulated guy segments were 10-20% different in length. Segments that were acting as reflectors might then act as directors, and *vice versa*. Similarly, I suggest that you take measures to be sure you don't have an interaction between a Yagi and the guys of the tower on which it is mounted. You may not be getting all the performance your antenna is capable of providing. This issue becomes more complex as antennas for multiple bands are used.

Guying Issues and Guidelines

According to current guidelines, the only appropriate guy-segment lengths for a tower with a single antenna or several antennas covering 20, 17, 15, 12 and 10 meters (inclusive) are in the 10-13 foot range. For 20- through 10-meter installations, the cost of in-

Antenna Designs from YO7

The four-element Yagi is optimized to give a near-flat SWR curve and maximum gain across the band. The measurements shown are for untapered 0.875-inch-diameter elements.

Four-Element Yagi

Element	Position (inches)	Half Length (inches)
Reflector	0.00	161.79
Driven	38.97	153.29
Director 1	147.07	151.25
Director 2	284.00	149.11

Two-Element Yagi

Element	Position (inches)	Half Length (inches)
Reflector	0.00	158.83
Driven	71.55	158.55

Three-Element Yagi

Element	Position (inches)	Half Length (inches)
Reflector	0.00	162.59
Driven	82.00	150.75
Director 1	212.00	146.10

ulators and the hardware to install them could easily become very high. Therefore, nonconductive guys may be the more economical solution and, by default, they would provide the best electrical solution overall. Some installations use short, insulated guy segments near a tower and longer segments farther out as a way to economically use conductive guys. This approach may or may not mitigate an interaction. If an antenna with a SWR greater than 1.2:1 is used, it is quite probable an interaction would go undetected. In addition, it is essentially impossible to know if there's a 1-2 dB gain reduction from your guys. Most amateurs can't do A/B tests with their guys.

Conclusions

So where does this leave us? One obvious answer is not to use conductive guys. This is probably the only economical way to ensure there are no interactions for 20-through 10-meter installations. For installations with a single monobander or a stack of monobanders for 20 or 40-meters, nonconductive guys will ensure the best possible performance. Although in this case, it is likely that conductive guys with insulators can be successfully used and may be more economical than nonconductive guys. The remaining issue then is whether antennas on another tower will beam through these guys. Will the insulated guys interact with the antennas on the other tower? In view of these and potentially other issues, better guidelines are required before you can select appropriate guy-segment lengths. If you plan a tower installation to sup-

port antennas for multiple bands, it's probable that a tower with nonconductive guys and less expensive antennas will do better than one with big antennas and interacting guys.

As an interim step, the range of lengths shown in *The ARRL Antenna Book* should be increased to further reduce guy-segment currents. This is a reasonable approach for installations with antennas for one or two lower-HF bands. To accurately define inappropriate guy segments and guy system designs in the long term, an investigation of considerable effort would be required. Such an undertaking would require rigorous NEC modeling and careful testing to verify model predictions.

I fully expect that new guidelines for conductive guys will only be of value for tower installations that have monobanders for one or two lower-HF bands, where appropriate guy segments can be implemented economically. I also fully expect that guidelines for 20- through 10-meter installations will show that nonconductive guys are a less-expensive solution. In my own case, when I put up towers at a new home in a few years, I'll be using only nonconductive guys and my towers will be as far apart as possible.

Notes

¹*NEC-Win Plus+*, Version 1.1, Nittany Scientific, Inc., 1733West 12600 South, Suite 420, Riverton, UT, 84065.

²YO7 is a Yagi optimization program by Brian Beezley, K6STI, 3532 Linda Vista Dr, San Marcos, CA 92069.

³R. D. Straw, N6BV, Ed., *ARRL Antenna Book*, 19th edition (Newington, Connecticut: ARRL) Fig 29, p 22-17. □□

Using the HP Z3801A GPS Frequency Standard

*Learn how to apply surplus GPS receivers for
weak-signal work at VHF and higher frequencies.*

By Bill Jones, K8CU

The Hewlett Packard Z3801A is a GPS-based frequency standard that tracks global-positioning satellites to get accurate timing data to adjust the long-term frequency of an internal oven oscillator. It was originally used for synchronizing CDMA cellular land network wireless base stations. It provides highly accurate timing. If a satellite signal is lost, the receiver automatically switches to holdover mode, which ensures system synchronization for up to 24 hours with reduced accuracy. You get the best of both worlds: crystal-oven oscillator short-term stability, and GPS long-term stability.

5411 Spruce Ln
Westerville, OH 43082
k8cu@realhamradio.com

This type of frequency standard is roughly comparable to a rubidium standard without the maintenance issues of the rubidium lamp. The frequency accuracy is several parts per billion. This is an exceptional piece of test equipment for a home workshop and ham station. These units have a Hewlett-Packard double-oven oscillator, the HP 10811D/E, with one-part-per-billion stability per day. The frequency output of this GPS receiver is 10 MHz. This is a necessary component in an Amateur Radio station equipped for weak-signal detection at VHF frequencies and above, such as low-power EME work. If you aren't listening on *exactly* the right frequency, you can't pull a weak signal from below the noise level. The 10-MHz output drives an external frequency

synthesizer that generates the radio's operating frequency.

This frequency standard is also useful as a home-workshop reference for test-equipment maintenance. I use it to drive a Tektronix frequency multiplier that makes handy marker signals up to 500 MHz.

These GPS receivers are surplus equipment. I'm not aware of the technology change that has placed them into this category. It appears that many cellular-telephone sites have used GPS receivers, judging from the outside GPS antennas visible on the cellular buildings. Look for these antennas. They look like three-inch-tall cone shaped white mushrooms that are mounted on the building roof and not on the cell tower. Nearly every cellular site that I have seen has one of these antennas. This

implies that many of these receivers have been made.

GPS frequency standards are expensive if purchased new. *QST* has a remarkable article by Brooks Shera, W5OJM, about making your own GPS standard using a surplus commercial oven oscillator, Motorola GPS boards and a custom-designed embedded PIC controller.¹ I first considered building one of these, but I was able to purchase a ready-made HP GPS standard at a cost comparable to the homemade version.

The HP receiver is a basic OEM unit and has only a simple front panel (see Fig 1). Detailed control is provided via a rear-panel RS-422 serial-control port. I built an RS-422/EIA232 converter into the DB25 connector as shown in Fig 2. An external power supply (Fig 3) and external outside GPS antenna (Fig 4) are also required. My unit needed 48 V dc. This unit runs 24 hours a day, usually unattended.

The HP Z3801A has these rear-panel connectors:

- One 25-pin female DB25 connector. This connector provides two 1-pps timed outputs, two 10-MHz frequency outputs and an RS-422 serial-interface port.
- A 10-MHz output with a BNC connector.
- A remote-antenna N connector.
- A power input connector.²

HP supplies a program called *SatStat* that serves as a front panel and control interface for the receiver. I leave the serial cables connected to

my PC and check on the receiver sometimes. With my particular antenna mounting method, the receiver always reports a minimum of four to six separate satellites as being actively tracked. Fig 5 is a screen capture of *Satstat* that shows typical operation of the receiver.

Common Questions

Q: Where can I buy one of these GPS receivers?

A: The surplus receivers are available on E-bay. That's where mine came from. I looked recently, and prices vary from \$200 to \$300. They are also available from other sources. Just do an Internet search on the word Z3801A.

Q: What antenna do I need to make this receiver work?

A: The Motorola antenna (ANT62301A/B) of the era when the Z3801A was built included a preamplifier with 24-dB gain, a noise figure of around 2.5 dB and expected 6-10 dB of cable loss. If you can get the original Motorola antenna, use it. The currently available Motorola Antenna97 will probably work as an alternative.³ Make sure the antenna you use has a preamplifier that will run from the +5-V source the Z3801A provides on the antenna coax center conductor. One site on the Internet claims a homemade helix antenna with no preamplifier will work. Save your time—it doesn't. Other designs that give a desirable omnidirectional pattern use patch antennas, but these have no preamplifier. An amplified exterior mobile-GPS antenna mounted in the clear with a good view of the sky (preferably in all directions,

to the horizon) will give you the best results.

I mounted an external Magellan GPS mobile antenna (with an internal preamplifier) on a PVC pipe mount that clamps to a roof stack vent on my home (Fig 4). I used a six-inch square aluminum plate as a ground plane to simulate the vehicle's roof. I spliced a length of RG-58 coax to the smaller cable on the mobile antenna to give me enough length to bring the coax into the workshop. Cable length and coax attenuation aren't very critical. The GPS receiver system expects about 10 dB of loss in the cable. The L1 frequency band used is around 1.5 GHz, so take care if you are using "lossy" cable or a very long cable length. Try to keep the cable loss between 6 and 10 dB. I used 20-feet of RG-58 with no problems.⁴

Q: I just got my unit. My receiver appears physically okay, it powers up correctly, the antenna is probably good and is connected, but the Z3801A never reports a GPS Lock on the front panel LED, even after hours of power on time. What's wrong?

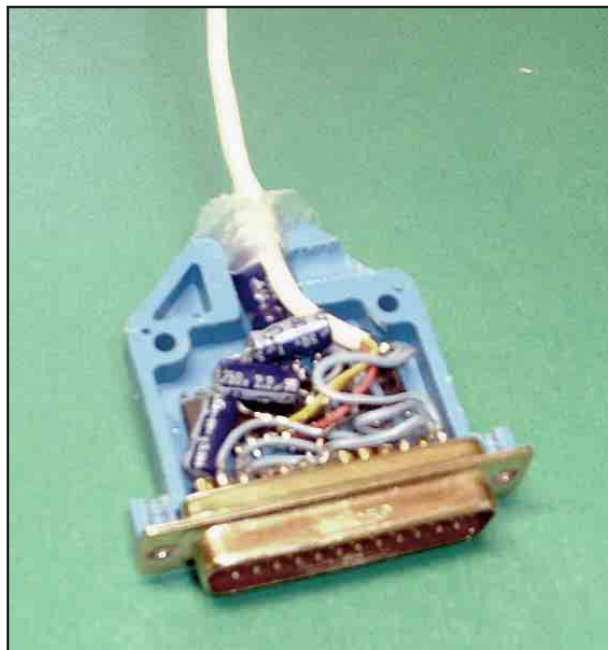
A: The Z3801A receiver thinks it is still at the location where power was last turned off. This may have been thousands of miles away. You must initiate a Survey command to the receiver. This instructs the Z3801A to determine its present location. Once this is done, the unit will probably function properly. The Survey command is issued using the *Satstat* software. (Refer to the user manual for details.) Hint: After you first hook up your receiver, the GPS location re-

¹Notes appear on page 51.



Fig 1—Front view of Z3801A receiver.

Fig 2—A homemade serial RS422 to RS232 converter, using the circuit of Fig 6B.



ported to *Satstat* is the *old* location where the unit was in service. Write these numbers down before the receiver determines its new location. It's interesting to see where your unit came from and learn its old elevation. My particular unit lived the first four years of its life in a cell-telephone site in Florida along highway A1A. The internal memory told me its exact location when it was last turned off. I have heard of one militarized unit from a government surplus sale that had a prior elevation of 50,000 feet.⁵

Q: I need a manual, power supply details, *Satstat* software or interface details on RS422 to RS232. Where can I get these?

A: Many of the people on the TACS-GPS reflector that were getting HP receivers like this one were buying regulated power supplies and commercial RS-422-to-RS-232 converters. I decided to design and build my own, for cost savings. The schematic diagrams give all the details. Three different options for the RS-422 to RS232 converter are offered in Fig 6. A reliable 48-V dc power supply is shown in Fig 3. Power supply reliability and safety is an issue with full-time operation. In use, the power supply is bolted underneath the workbench out of sight.

The following are available for downloading from author's Web site www.realhamradio.com.

- A two-page interface and power-supply schematic in PDF format (Figs 3 and 6 here)
- *SatStat* GPS receiver software in a ZIP file (500 kB)
- A Z3801A manual in PDF format (1 MB)

Visit the Web site for the latest application information.

Two good application note links exist about the technology used in the Z3801A. The first is an HP application note about Smartclock Technology. It goes into the theory behind GPS-disciplined oscillators: literature.agilent.com/litweb/pdf/5966-0431E.pdf. The second one also from HP; it explains basic GPS concepts and delves into precision-timing applications with GPS: literature.agilent.com/litweb/pdf/5965-2791E.pdf.

Notes

¹Brooks Shera, "A GPS-Based Frequency Standard," *QST*, July 1998. Brooks has a Web site dedicated to this project at www.rt66.com/~shera/index_fs.htm.

²The J4 power connector is a three-terminal Amp MATE-N-LOCK connector, Mouser #571-7700181. Two socket pins are also required, #571-7702513.

Fig 5—(right) A screen capture of *Satstat* software in operation with a Z3801A.

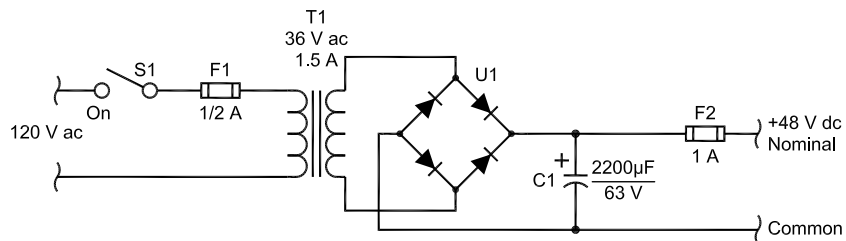


Fig 3—A schematic of the receiver power supply. The output is 54-V dc with no load, 47 V during warm up, 48-50 V during normal operation. This meets the Hewlett-Packard specifications for the 54-V version Z3801A. A regulated supply is not necessary. C1—2200 μF 63 V; use more capacitance if available. T1—120 V primary, 36 V 1.5 A secondary (Jameco #104416). U1—Diode bridge, 100 PIV 1 A, minimum; 10 A suggested.

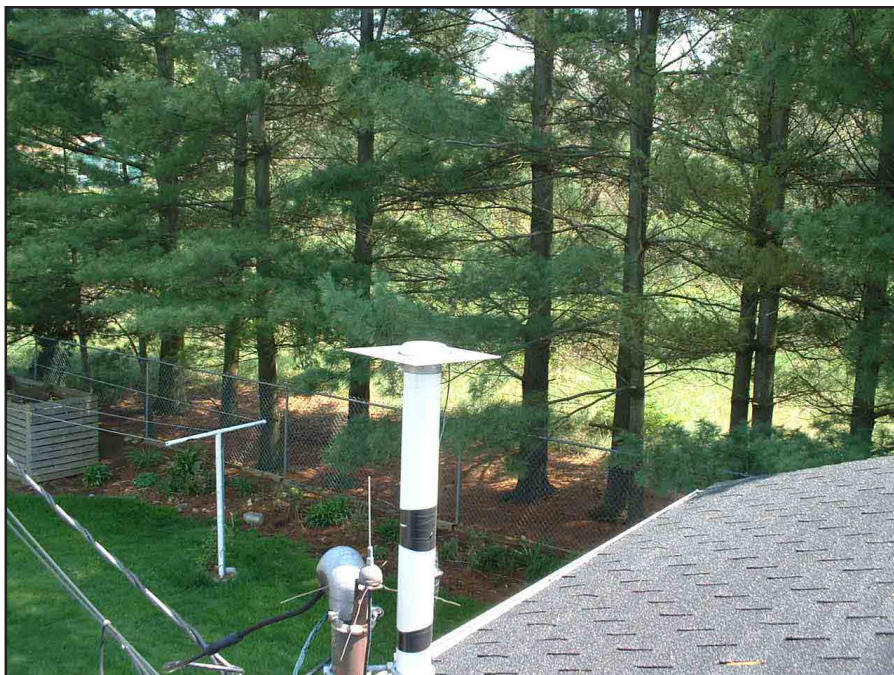
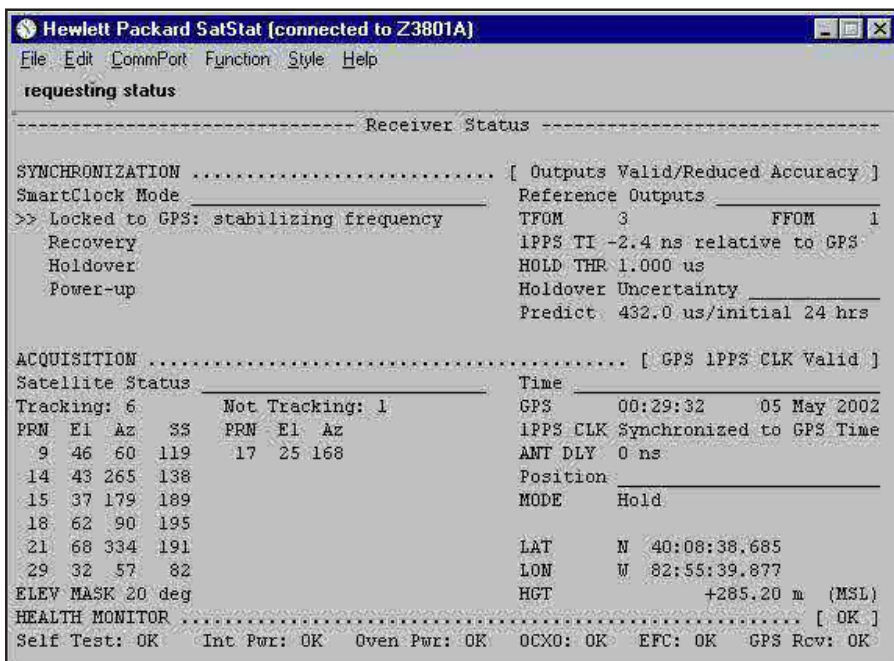
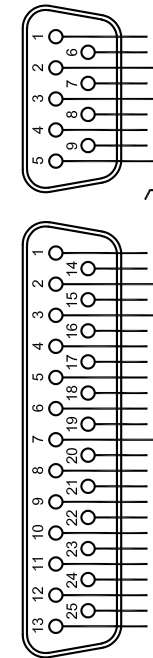


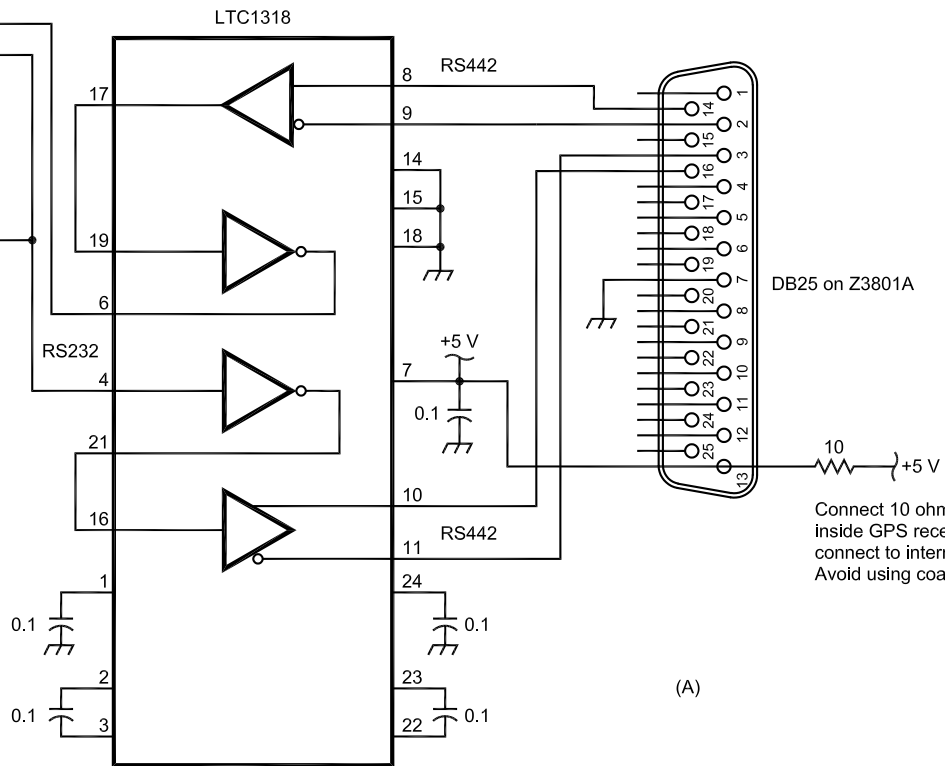
Fig 4—Photo of a mobile GPS antenna mounted on house roof.



DB9 serial cable to PC



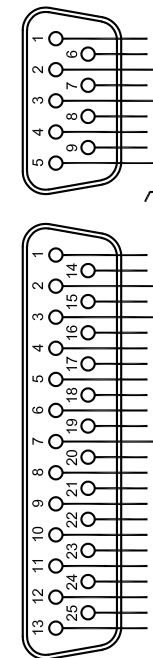
DB25 connector to PC (optional)



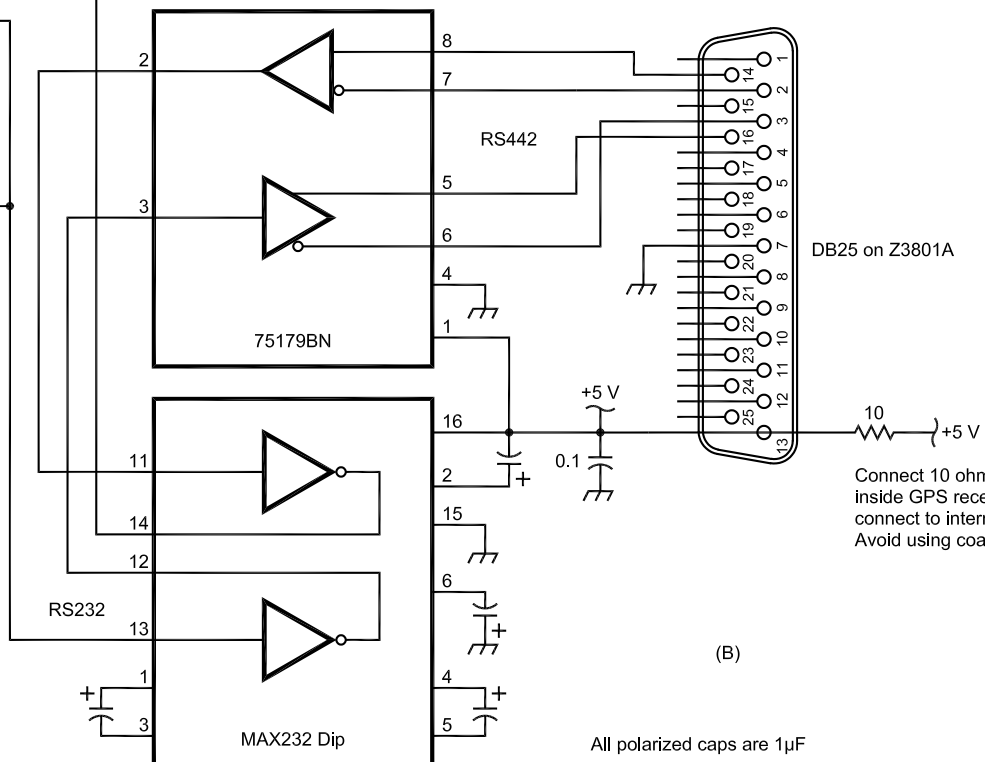
(A)

Connect 10 ohm resistor inside GPS receiver and connect to internal plus 5 V. Avoid using coax center lead.

DB9 serial cable to PC



DB25 connector to PC (optional)



(B)

All polarized caps are 1µF

Connect 10 ohm resistor inside GPS receiver and connect to internal plus 5 V. Avoid using coax center lead.

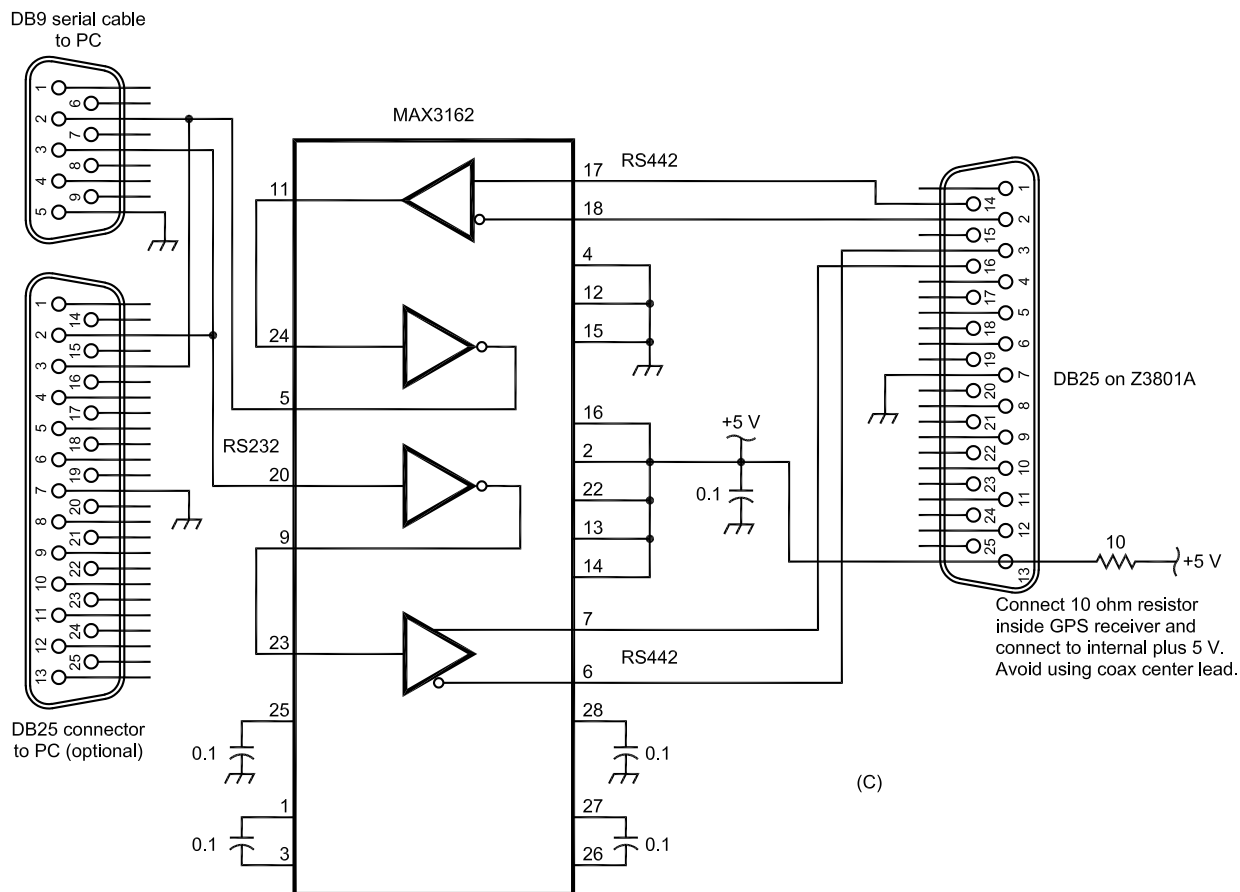


Fig 6—Schematics of several serial-interface options. (A) The LTC1318CN (24-pin DIP) or LTC1318CSW (wide surface mount) are available from Digi-Key (www.digikey.com) or www.Linear-Tech.com. (B) uses DIP components available from RadioShack (RadioShack.com). (C) uses the Maxim MAX3162 28-pin surface-mount package. Maxim offers free samples of this device; visit Maxim-ic.com for details. With care, an interface using any of these chips can be built inside the DB25 backshell as shown in Fig 2.

³The Motorola Antenna97 is available from TAPR at www.tapr.org. If you need help on another type of GPS receiver, inquire on the TAPR GPS Reflector.

⁴The ARRL Antenna Book, 18th Edition, 1997 includes, on floppy disk, a useful transmission-line-loss calculator named TL, written by Dean Straw, N6BV. Later versions are Windows-based.

⁵Thanks to Tom Van Baak at LeapSecond.com for helpful advice on this receiver.

Bill Jones, K8CU, has been an active radio amateur, CW DXer and home

project builder since first receiving his license in 1966 at age 17. Bill is an electronics professional with experience ranging from radar maintenance in Vietnam, analog and digital telephone PBX design, to imbedded-controller implementation. He spent 18 years at Optek Inc designing hardware and writing assembly-language software for embedded microcontrollers used in specialized electro-optical controls.

He has written about several of his

Amateur Radio projects in ARRL publications. His current employer is the Ohio Department of Transportation, where he works in radio communications. Some recent interests include small gas engines, 6-meter DX and maintaining his personal Web site RealHamRadio.com, on which he has placed some entries from his notebooks. A member of a nearby sports-man's and conservation club, Bill can sometimes be found fishing with his wife, Bonnie. □

Tech Notes

New Faces for Old Meters

By Tom Cefalo Jr, W1EX, 51 Oak St, Winchester, MA 01890; tdcef@110.net

Upon the completion of my RF-power-meter project, I was disappointed with the appearance of the meter face. The meter was a standard ammeter with a typical 0-100 μA scale. At the time, I had two options: I could generate a graph to speed conversion of the meter's current readings to power levels, or I could try printing the power-level readings over the meter's scale with a permanent marker. Not content with either of these methods, I decided to investigate other solutions. I soon discovered that the tools necessary to perform this task were available to me in my home. This article will describe a step-by-step procedure to fabricate professional looking custom meter faces using a computer, a scanner and a printer.

First, dismantle the meter to expose the meter's scale plate. The scale plate is usually attached to the meter with two small screws. Carefully remove the plate from the meter. With a scanner, scan a 1:1 image of the scale plate.¹ Save the scanned image as a bitmap (.BMP) file extension. High resolution is not required here since this image will only be used as a tracing template.

For the next step, I used a mechanical drawing software package called *AutoCAD 2000*. Although this article is based on *AutoCAD*, there are other mechanical drawing software programs that will produce the same results. Start *AutoCAD* and import the bitmap file of the meter's face by selecting "Insert" from the top toolbar. Next, choose "Raster Image," select the location of the bitmap file and open it. Import the file using a "Scale of 1." At this point, there will be a 1:1 image of the original meter's face on the drawing screen of *AutoCAD*.

One of the features of *AutoCAD* is drawing in *layers*. This is similar to having different parts of your drawing on transparent sheets. Since the sheets are transparent, they can all be stacked together to make a complete drawing. For example, one layer could be the original meter face, another layer the new face, another layer the new scale and so forth. This allows you

¹If your scanner is not a flat-bed model, make a photocopy of the meter face and put the paper copy through the scanner.—Ed.

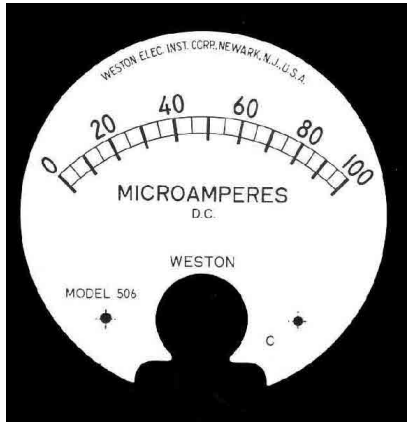


Fig 1—Original meter-scale plate.

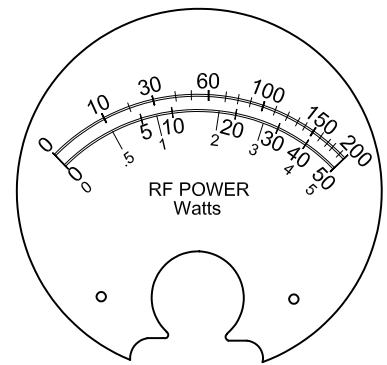


Fig 2—New meter-scale plate.

to work on each layer separately with the ability to turn layers on and off.

AutoCAD automatically sets Layer 0 to the default layer, which will be the original meter face. Now from the top toolbar, click on the "Layer" sheet icon. From this window select "New" and enter a name and color for this layer. As an example, I called this layer "New Face." I suggest using a different color for each layer because it will help to identify which layer you are working on and that is less confusing. Notice that the layer colors do not necessarily equate to the printed colors. Print colors, if selected, are assigned in the print menu. In the top toolbar where the "Layers" are shown, click on the down arrow in that box and click on the "New Face" layer. You will now be drawing on the layer for the new meter face. Using the standard drawing tools in *AutoCAD* (line, circle and three-point arc) begin tracing the outline of the original meter face. The scale bar is easily drawn with the "3-Point Arc" tool. To see a view of what you have drawn, click on the "Light Bulb" for Layer 0 in the Layer Toolbar. This turns off the original meter face and displays the new meter face on the screen. You can generate as many layers as you want—for example, one for the new face, another for the scale and graticule and another for text. Turn Layer 1 back on and using the original meter's face as a guide add in the new scale division lines with the "Line" tool and the corresponding scale numbers with the "Text" tool button. The text numbers can be angled to match the arc of the scale.

With the drawing completed, you are ready to print the new meter scale plate. The appearance of the new scale plate will be greatly enhanced if you print on high-quality paper. The first step is to turn off the default Layer 0, since you don't want to print the original meter's scale plate. From the toolbar, click on the "Print" icon and a Plot Menu dialog box will pop up. First select the "Plot Device" tab and make sure your printer is selected. Under the "Plot Style Table" click the down arrow. This is where you choose if it will be printing in color. If color is chosen, select "acad.ctb" and click on the "Edit" button. Within this menu you can select which colors will be assigned to the pens. If you have chosen color, however, I highly recommend reading the help section on assigning pen colors. This relates to the operation of *AutoCAD*, and it is beyond the scope of this article. If you want to print in black and white, select "monochrome.ctb."

Click on the "Plot Settings" tab in the main print-dialog window. Click on the "Window" tab and move the cursor to the upper left area of your drawing. Left click the mouse, move the mouse until the box encloses the whole drawing and left click the mouse again. Under the "Plot Scale" select a "Scale of 1:1". At this point you may click on "Full Preview" to examine an actual view of what will be printed. If you are satisfied with how the drawing will be printed click the "OK" button and a copy of the drawing will start printing.

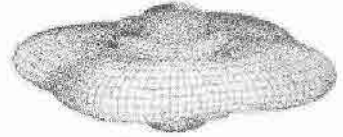
Using a pair of small sharp scissors cut the meter's scale plate from the

sheet of paper using the outline of the original scale plate as a guide. At this point you can dry fit the paper scale plate over the metal scale plate to ensure that it fits correctly. Apply a small even layer of adhesive to the metal scale plate and carefully attach the new paper scale plate to it. Apply even pressure and allow the adhesive to cure. Next, carefully reassemble the meter using the new scale plate. You're done! **Figs 1 and 2** show my original and new meter scale plates.

Conclusion

Although *AutoCAD* is a very powerful mechanical drawing package, I only used some of its fundamental functions for this project. I am by no means an expert user of *AutoCAD*; but with some basic knowledge, I was able to create a professional-looking meter. For your next or existing project that requires a custom scale plate beyond the standard voltage or current scales, consider giving your meter a computer facelift. □□

A picture is worth a thousand words...



With the all-new

ANTENNA MODEL™

wire antenna analysis program for Windows you get true 3D far field patterns that are far more informative than conventional 2D patterns or wire-frame pseudo-3D patterns.

Describe the antenna to the program in an easy-to-use spreadsheet-style format, and then with one mouse-click the program shows you the antenna pattern, front/back ratio, front/rear ratio, input impedance, efficiency, SWR, and more.

An optional Symbols window with formula evaluation capability can do your computations for you. A Match Wizard designs Gamma, T, or Hairpin matches for Yagi antennas. A Clamp Wizard calculates the equivalent diameter of Yagi element clamps. Yagi Optimization finds Yagi dimensions that satisfy performance objectives you specify. Major antenna properties can be graphed as a function of frequency.

There is no built-in segment limit. Your models can be as large and complicated as your system permits.

ANTENNA MODEL is only \$85US. This includes a Web site download and a permanent backup copy on CD-ROM. Visit our Web site for more information about ANTENNA MODEL.

Teri Software
P.O. Box 277
Lincoln, TX 78948

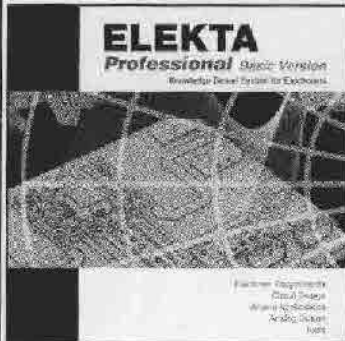
www.antennamodel.com

e-mail: sales@antennamodel.com
phone: 979-542-7862

NOW AVAILABLE!

ELEKTA Professional Basic Version

New



The best-selling *ELEKTA Professional* is now available in a basic, more economical edition for students and hobbyists. Enjoy the familiar encyclopedia of electronic terms and definitions, an introductory design course, tips & tricks, over 40 basic and mid-range tools and more than 250 circuits.

2002, CD-ROM, ISBN 1-884932-32-0
NP-51 \$49.00

Visit www.noblepub.com

for more information and on-line ordering



Noble Publishing Corporation
630 Pinnacle Court Norcross, GA 30071 USA
Call: 770-449-6774 · Fax: 770-448-2839
E-mail: orders@noblepub.com · Internet: www.noblepub.com

HP® GPS RECEIVER DISCIPLINE CLOCK



\$249
(Org. list \$4,800)

Model: Z3801A® (Refurbished)

- Disseminating precise time and frequency (time acc. <1 μS)
- NIST traceable frequency reference
- Manual and software included
- Power supply and GPS antenna available

www.buylegacy.com

info@buylegacy.com

San Marcos, CA

760-891-0810 • 800-276-1010 • Fax 760-891-0815

HP® and Z3801A® are registered trademarks of Hewlett Packard.



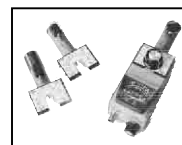
NATIONAL RF, INC.



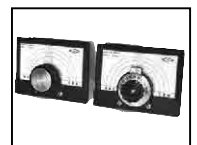
VECTOR-FINDER
Handheld VHF direction finder. Uses any FM xcvr. Audible & LED display.
VF-142Q, 130-300 MHz \$239.95
VF-142QM, 130-500 MHz \$289.95



ATTENUATOR
Switchable, T-Pad Attenuator, 100 dB max - 10 dB min BNC connectors
AT-100, \$89.95



DIP METER
Find the resonant frequency of tuned circuits or resonant networks—ie antennas.
NRM-2, with 1 coil set, \$219.95
NRM-2D, with 3 coil sets (1.5-40 MHz), and Pelican case, \$299.95
Additional coils (ranges between 400 kHz and 70 MHz avail.), \$39.95 each



DIAL SCALES
The perfect finishing touch for your homebrew projects. 1/4-inch shaft couplings.
NPD-1, 3/4" x 2 1/4" inches 7:1 drive, \$34.95
NPD-2, 5/8" x 3 1/8" inches 8:1 drive, \$44.95
NPD-3, 5 1/8" x 3 1/8" inches 6:1 drive, \$49.95

S/H Extra, CA add tax

NATIONAL RF, INC
7969 ENGINEER ROAD, #102
SAN DIEGO, CA 92111

858.565.1319 FAX 858.571.5909
www.NationalRF.com

RF

By Zack Lau, W1VT

Quarter-Wave Dipoles—Why Don't They Perform Well?

Many hams have tried quarter-wavelength ($\lambda/4$) dipoles, but have been disappointed and disillusioned by the results. After all, half-wavelength ($\lambda/2$) dipoles work great, with little fuss and bother. Shouldn't there be an easy way to make their $\lambda/4$ siblings work too? Many experts just say they are too short to be practical and leave it at that. I think it is worthwhile to see why they don't work. After all, people are more interested in learning why bridges fall down than why they stay up.

While the exact impedance of a dipole will vary, the typical impedance of

a $\lambda/4$ 80-meter inverted V dipole at 30 feet is typically around $10 -j1000 \Omega$. Not only is the resistive component relatively low, there is a lot of capacitive reactance. The low resistive component is a big problem. For equal far field strengths, a lot more current must flow in this antenna than in one with a greater radiation resistance. This results in substantially more resistive losses. This is particularly acute if the antenna wire has a lot of resistance. Thus, the use of Monel metal instead of copper may not be advisable in some situations, although Monel has been used in antennas for over 60 years.¹ The situation is even worse if you take advantage of Monel's strength and use a thinner wire.

Table 1 shows the variation in maximum gain for different wire

types. The test antenna is a $\lambda/4$ inverted V, 30 feet high at the apex and 7 feet high at the ends. Each leg of this short dipole is 34 feet long—the overall span is just 50 feet, compared to 131 feet for a full size dipole. The modeling was done using *EZNEC* with a NEC 4 engine, over real ground (medium 0.005, 13) with 100 segments.² The direction of maximum gain is straight up for all cases.

The loss can vary considerably for seemingly similar materials. I'd expect to see Monel 400 used for fishing line, rather than Monel 401, which is optimized for electrical work. Monel 401 is a much better material for making resistors. The loss for steel wire is quite high—its high permeability makes the skin effect much worse. Alloy 5356 aluminum may be too brittle for antenna wire, but it is available in wire form for TIG welding. I wasn't

225 Main St
Newington, CT 06111-1494
zlau@arrl.org

¹Notes appear on page 59.

able to determine the actual alloy of aluminum fence wire.

Cheap wire may not be such a bargain if the losses are too high. How do you find out the permeability and resistivity of an unknown piece of wire? Perhaps the quickest test is to make a test inductor and compare its Q with that of one made out of copper wire. This must be done at the frequency of interest, as the skin effect is frequency sensitive. The permeability of magnetic materials may also be frequency sensitive—adding to the confusion for anyone trying to measure inductance. To obtain a high Q coil, I suggest making the length and diameter of the coil equal, and spacing the wire so that the gap between the wires is the same as the wire diameter. Under these conditions, the Q is usually above 200—a Q of 400 isn't unusual with a good design. If you need a lossy coil for comparison, I suggest dryer-duct hose. A 320- μH coil had a Q of just 35 at 1.8 MHz. This is a very low Q .

The high reactance of the feedpoint is also a problem—it drastically increases the SWR on 50- Ω coax from 5:1 (for a resonant 10- Ω feedpoint) to well over 100:1. Perhaps the best solution is to match the dipole directly at the feed point with high quality loading coils and a matching transformer. This situation is easily modeled at a single frequency with the circuit shown in Fig 1.

A series 44.46-pF capacitor has $-j1000\ \Omega$ impedance at 3.58 MHz. The 50- Ω to 10- Ω transformer provides an easy way to determine the coil loss. The insertion loss, MS21, is a combination of the circuit loss and the mismatch loss. The output transformer, T2, is adjusted to reduce the mismatch loss to zero. If the transformers and capacitors are ideal, the only source of loss is in the inductor. You may need to substitute a 10- Ω resistor for T1 to look at the SWR with some programs. Table 2 shows loss as a function of inductor Q . An inductor Q of 400 may be an optimum solution for low-power work. A Q of 400 isn't too difficult to obtain.

A 12.5- Ω impedance can be matched quite efficiently to 50 Ω with a 1:4 balun. In practice, it is also necessary to add balanced to unbalanced transformation to the impedance transformation. This keeps unwanted currents off the coax shield. This important detail is ignored by conventional circuit-modeling programs. It is difficult to build low-loss baluns that will match the other impedances in the table to 50 Ω . A loss of 0.97 dB is a loss of 20%—at the 100-W level, 20 W will be lost in the inductor. In practice, you

should probably use a pair of identical 22.2- μH inductors, one on each side of the dipole. This is shown in Fig 2. This helps maintain antenna balance. It also spreads out the power dissipation; each inductor will need only dissipate 10 W. Forty feet of RG-58 will add 0.33 dB of loss. A good 1:4 balun

will add less than 0.1 dB of loss, for a total feed-line/balun/matching-network loss of 1.4 dB.

It is important not to use a 4:1 balun designed to match 200:50 Ω , unless reasonable performance is verified with 12.5 and 50- Ω terminations. Typically, a high-performance balun

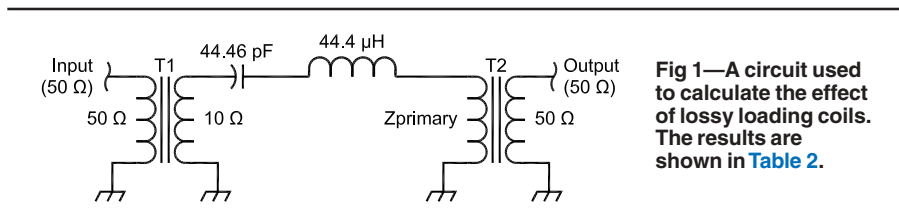


Fig 1—A circuit used to calculate the effect of lossy loading coils. The results are shown in Table 2.

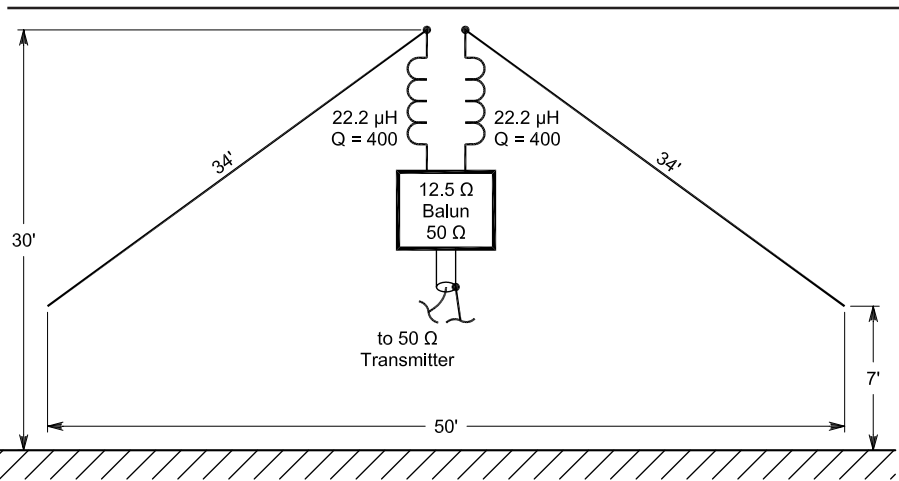


Fig 2—A relatively efficient method of feeding a $\lambda/4$ dipole—high- Q loading coils at the input and a 12.5:50 Ω balun.

Table 1—Relative Inverted-V Gains for Various Conductors

Relative maximum gain for an inverted V $\lambda/4$ 80-meter dipole with its apex 30-feet high and the ends at 7 feet. Calculated by EZNEC with NEC 4 over real ground (medium)

Material	Resistivity (ohm-m)	Permeability	Max Gain with #20 wire (dBi)	Max Gain with #14 wire (dBi)
zero loss	0	1	+1.05	+1.03
silver	1.6e-8	1	+0.36	+0.68
copper	1.74e-8	1	+0.33	+0.67
aluminum (6061-T6)	4e-8	1	-0.02	+0.48
aluminum (5356-0)	5.94e-8	1	-0.24	+0.37
zinc	6e-8	1	-0.25	+0.36
tin	1.14e-7	1	-0.70	+0.12
Monel 400	5e-7	1	-2.27	-0.78
Monel 401	2.94e-6	1	-6.81	-2.91
steel	1.2e-7	200	-7.68	-5.19
steel	1.2e-7	1000	-10.8	-8.07
steel	1.2e-7	4000	-13.66	-10.8

uses transmission-line windings with an impedance of $Z_0 = \sqrt{Z_{in} \times Z_{out}}$. This generally yields the greatest bandwidth and least insertion loss. In this case, we need 25- Ω impedance, versus the 100- Ω required for conventional baluns. Typically, 25- Ω windings are made out of coaxial cable. Windings of 100- Ω are often made out of two insulated wires placed side by side. The wires are typically wound on ferrite rods or toroids to substantially increase bandwidth—a necessity to cover 80-meters with low loss.

Perhaps the most significant disadvantage is the difficulty of adjustment. Automatic tuners typically use relays to switch inductors—this is likely to decrease inductor Q and increase losses. Mounting a tuner at the feedpoint does put a lot of weight and wind load up high in the air, but a sturdy mast or tower can usually handle it. The situation is different with a dipole hung between two trees—there's no support for the center of the dipole. In this case, you probably want the matching network at the transmitter. The situation can get quite bizarre when you have a small lossy QRP transmatch and lossy RG-58A feed line.

T-networks with shunt inductors and tunable series capacitors are popular because they can match a wide variety of impedances with reasonable component sizes. Nevertheless, they can be very lossy, so much so that reality doesn't make much sense! Amazingly, the loss for a 100-ft line is nearly the same as for a 40-ft line. This is shown in Table 3, using the transmatch shown in Fig 3.

The 10-pF capacitor represents stray capacitance—it isn't a factor on the low-impedance 50- Ω input but may be significant with high-impedance loads. The calculations were done using *TLW*, transmission-line program for Windows, companion software for the *ARRL Antenna Book*. The reduction in tuner losses can actually offset the additional line loss! If both capacitors had a maximum value of 100 pF, the T-match would not tune line

lengths of 80 and 90 feet. The SWRs would bottom out at 1.9:1 and 3.3:1. This should not be a surprise for anyone who has experience using dipoles on multiple bands with a transmatch. The efficiency for all cases is terrible—about 1/2%. Yes, 100 W at the transmitter is reduced to just 1/2 W at the antenna. Thus, just because it matches to a perfect SWR does not mean that much RF is actually getting to the antenna. Add in the loss from lossy wire and you have a signal that would be clobbered by QRP stations running 2 W to a $\lambda/2$ dipole. This is not a useful antenna/feed-line combination for many hams.

The main advantage of the T-match, its wide matching range, is also its biggest disadvantage, because it is so easily adjusted to settings that yield good SWR but poor efficiency. I suggest that you read articles by James Garland, W8ZR, and Andrew Griffith, W4ULD,

to better understand how to properly adjust a T match.^{3,4} I like W8ZR's article because it shows an easy way to estimate transmatch losses, while Andrew does a good job of explaining how to set the knobs on your transmatch. Some hams prefer L matches, which eliminate the multiple-settings problem. L networks are usually quite efficient once the SWR is finally tamed, but it is much more difficult to find the one setting that works. Sometimes, there is no setting with little QRP tuners—you must add or subtract some feed line to make it work. Alternately, you could add more capacitance or inductance. At HF, the loss in splicing cables together is negligible, unless water gets into the cable. BNC connectors can make cable-length adjustment quick and easy—perfect for field operations by hams that have difficulty determining distances.

The usual recommendation for a better signal is to use 450- Ω ladder

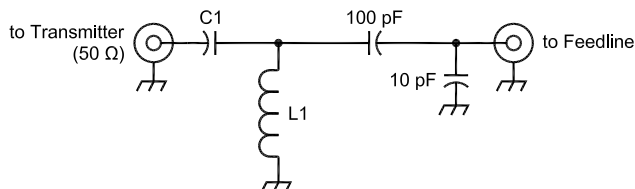


Fig 3—T-network transmatch used for Table 3. Capacitor $Q = 1000$. Inductor $Q = 200$.

Table 3—RG-58A and QRP Transmatch Losses

Feeding 10 $-j1000 \Omega$ antenna at 3.58 MHz. Inductor $Q = 200$, capacitor $Q = 1000$.

Coax Length (ft)	Coax Loss (dB)	Coax+Tuner Loss (dB)	C1 (pF)	L1 (μH)
40	18.75	23.37	32.7	15.07
50	20.57	23.97	37.1	14.17
60	21.69	23.96	44.9	12.97
70	22.29	23.49	63.7	10.99
80	22.52	22.87	147*	6.86
90	22.56	22.73	175*	9.24
100	22.61	23.41	67.6	13.52

*Value greater than 100 pF, an arbitrary maximum for this tuner.

Table 2—Matching at the Feed Point using an Inductor and Transformer

Inductor Q	Primary Impedance (Ω)	Inductor Loss (dB)
800	11.25	0.51
400	12.5	0.97
200	15	1.76
100	20	3.01
50	30	4.77

Table 4—Feeding a $\lambda/4$ Dipole with High-Impedance Transmission Line

Feed-Line Impedance (Ω)	Length (ft)	Matched Loss (dB)	Total Loss (dB)	Impedance Seen by Transmitter (Ω)
300	40	0.070	6.34	3.61-j41.0
450	40	0.018	2.30	2.47-j74.0
600	40	0.013	1.69	3.91-j21.7
300	100	0.175	9.55	10783-j3781
450	100	0.046	4.59	69.4+j1626
600	100	0.032	3.06	401+j5143

line. Generally, feed-line loss is an inverse function of impedance. Thus, 450- Ω line is less lossy than 300- Ω line, assuming they both use the same amount of copper. By raising the impedance, one lowers the current and, therefore, the I^2R losses. This is obvious from an inspection of **Table 4**. To some extent, one can compensate by using larger feed lines with more copper, but this is impractical for most hams. Hence the availability of very inexpensive but very high-quality surplus hardline. While 1/2-inch hardline is easy to sell, the very large sizes are not, dramatically reducing its price to anyone foolish enough to hazard an offer to take it away.

As **Table 4** shows, a significant improvement is possible with open-wire line—just 1.7 dB loss with 40 ft of 600- Ω line. However, this is still worse than 1.4 dB of loss for RG-58A and a matching network at the feed point. There is still the loss and difficulty of matching open wire to 50 Ω . In fact, you might even say that the 40-ft lines have made the problem worse, transforming a low 10- Ω resistive component into an even lower resistance. Ignoring the need for a balun, the little QRP transmatch used earlier would

add 3 dB of loss, for a net loss of 4.7 dB. Theoretically, the loss is even lower with 100 feet of feed line, just 4.1 dB, except that an unusually large 70- μ H inductor is needed to obtain a perfect match. Again, the extra line loss is offset by the reduced tuner loss. Transmission-line problems can be tricky because line length changes the impedance at the end of a mismatched line. Engineers like Smith charts because they provide a visual representation of what is happening—few are gifted enough to intuit from mere numbers.

One way to avoid the balun problem with open-wire line is to use link coupling. L. B. Cebik has written an excellent five-part treatise on link coupling.⁵ Choke baluns are a possible solution, but it may be difficult to get the choke impedance high enough. While 500 Ω of choke impedance may be adequate for 50- Ω dipoles, it is obviously inadequate to cover all the examples listed in **Table 4**. In fact, baluns can be yet another source of loss.

Typically, a balun's impedance is maximized by making it series resonant, so that the stray capacitance resonates with the inductance. This also means that the impedance is pure

resistance. If we set up a linear, time-invariant circuit, it is perfectly appropriate to invoke the conjugate matching theorem to estimate the maximum power that could be lost in the balun. The answer is half of the power. This is 3 dB of loss. The obvious solution is to make the balun's common mode impedance extremely high. Can anyone suggest how to make a practical balun with impedance much higher than 10,000 Ω ?

Hopefully, it is now obvious why a $\lambda/4$ dipole is such a poor antenna. Significant losses are possible in the wire, feed line, matching network and balun. Open wire, often touted as the best solution, is actually second best. The best solution seems to be to use high Q loading coils and an efficient 4:1 balun.

Notes

- ¹Circular, Monel Metal Collapsible Antennas," Premax Products, *QST*, Aug 1940, p 88.
- ²www.ez nec.com; Roy Lewallen, W7EL, tel 503-646-2885.
- ³J. Garland, W8ZR, "The EZ-Tuner," *QST*, Apr 2002, pp 40-43.
- ⁴A. Griffith, W4ULD, "Getting the Most Out of Your T-Network Antenna Tuner," *QST*, Jan 1995, pp 44-47.
- ⁵www.cebik.com/link/link0.html □□

EZNEC 3.0

All New Windows Antenna Software by W7EL

EZNEC 3.0 is an all-new antenna analysis program for Windows 95/98/NT/2000. It incorporates all the features that have made *EZNEC* the standard program for antenna modeling, plus the power and convenience of a full Windows interface.

EZNEC 3.0 can analyze most types of antennas in a realistic operating environment. You describe the antenna to the program, and with the click of a mouse, *EZNEC 3.0* shows you the antenna pattern, front/back ratio, input impedance, SWR, and much more. Use *EZNEC 3.0* to analyze antenna interactions as well as any changes you want to try. *EZNEC 3.0* also includes near field analysis for FCC RF exposure analysis.

See for yourself

The *EZNEC 3.0* demo is the complete program, with on-line manual and all features, just limited in antenna complexity. It's free, and there's no time limit. Download it from the web site below.

Prices - Web site download only: \$89. CD-ROM \$99 (+ \$3 outside U.S./Canada). VISA, MasterCard, and American Express accepted.

Roy Lewallen, W7EL phone 503-646-2885
P.O. Box 6656 fax 503-671-9046
Beaverton, OR 97007 email w7el@eznec.com

<http://eznec.com>

Down East Microwave Inc.

We are your #1 source for 50MHz to 10GHz components, kits and assemblies for all your amateur radio and Satellite projects.

Transverters & Down Converters, Linear power amplifiers, Low Noise preamps, Loop Yagi and other antennas, Power dividers, coaxial components, hybrid power modules, relays, GaAsFET, PHEMT's, & FET's, MMIC's, mixers, chip components, and other hard to find items for small signal and low noise applications.

We can interface our transverters with most radios.

Please call, write or see our web site
www.downeastmicrowave.com
for our Catalog, detailed Product descriptions and interfacing details.

Down East Microwave Inc.
954 Rt. 519
Frenchtown, NJ 08825 USA
Tel. (908) 996-3584
Fax. (908) 996-3702

We Design And Manufacture To Meet Your Requirements
*Prototype or Production Quantities

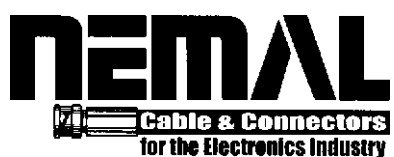
800-522-2253

This Number May Not Save Your Life...

But it could make it a lot easier! Especially when it comes to ordering non-standard connectors.

RF/MICROWAVE CONNECTORS, CABLES AND ASSEMBLIES

- Specials our specialty. Virtually any SMA, N, TNC, HN, LC, RP, BNC, SMB, or SMC delivered in 2-4 weeks.
- Cross reference library to all major manufacturers.
- Experts in supplying "hard to get" RF connectors.
- Our adapters can satisfy virtually any combination of requirements between series.
- Extensive inventory of passive RF/Microwave components including attenuators, terminations and dividers.
- No minimum order.



NEMAL
Cable & Connectors
for the Electronics Industry

NEMAL ELECTRONICS INTERNATIONAL, INC.
12240 N.E. 14TH AVENUE
NORTH MIAMI, FL 33161
TEL: 305-899-0900 • FAX: 305-895-8178
E-MAIL: INFO@NEMAL.COM
BRASIL: (011) 5535-2368

URL: WWW.NEMAL.COM

2002 Index

Issues 210 through 215

(All dates are 2002 unless otherwise indicated.)

Empirical Outlook (Smith)

Freedom of Speech: An Awesome Responsibility: [May, 2](#)
Investments in Technology: [Mar, 2](#)
It All Comes Down to Marketing: [Sep, 2](#)
New Technology and the Old Struggle for Dynamic Range: [Jul, 2](#)
New Technology Presents New Challenges: [Nov, 2](#)
You Asked for It: [Jan, 2](#)

Feedback

HF Circuits for a Homebrew Transceiver (Nov/Dec 2001) (Smith): [Jan, 62](#)
Homebrew Shaft Encoder, A (Mar/Apr) (May/Jun) (Kastigar): [Jul, 64](#)
Laser Transceiver for the ARRL 10-GHz-and-Up Contest, A (Nov/Dec 2001) (Schetgen): [Mar, 62](#)
Monopoles and Dipoles, About (Mar/Apr) (Trainotti): [May, 64](#)
RF: A Simple 10-Meter Satellite Turnstile Antenna (Nov/Dec 2001) (Lau): [Jan, 62](#)
Spreadsheet for Remote Antenna Impedance Measurement, A (Sep/Oct 2001) (Smith): [Jan, 62](#)
Two-Meter Reflective SP4T PIN-Diode Switch, A (Nov/Dec 2001) (Zanek): [Jan, 62](#)

Letters to the Editor

Amateur Image, Is the Dirodyne the Weaver Method? (Datwyler): [Nov, 62](#)
Amateur Innovation, In Search of (Lapin): [Sep, 63](#)
Amateur Radio Software: It Keeps Getting Better, (Sept/Oct) (Haddon): [Nov, 62](#)
Beyond Fractional-N, Part 2 (May/June) (Miles): [Mar, 60](#); (Dretea): [Mar, 60](#)
Dirodyne: A New Radio Architecture? The (Jul/Aug) (Schmitt): [Sep, 61](#); (Green): [Sep, 62](#); (Schmitt): [Nov, 62](#)
Filters in "A Homebrew Regenerative Superheterodyne Receiver" (May/June) (Wetherhold): [Jul, 63](#); (Young): [Jul, 63](#)
HF Receiver Dynamic Range: How Much do We Need? (May/Jun) (Allenbach): [Sep, 61](#)
High-Speed Networking for Amateur Radio, On (Toth): [Mar, 61](#)
Homebrew Regenerative Superheterodyne Receiver, A (May/Jun) (Young): [Sep, 61](#)
Homebrew Shaft Encoder, A (Mar/Apr) (Kastigar): [May, 62](#); feedback: [Jul, 64](#)

IMD Testing, On (Chadwick): [Jul, 62](#); (Smith): [Jul, 63](#)
Improved Dynamic-Range Testing (Jul/Aug) (Larkin): [Sep, 62](#); (Smith): [Sep, 63](#)
Jan/Feb 2002 Issue (Parker): [Mar, 61](#)
Jul/Aug 2002 QEX—A Banner Issue (Nold): [Nov, 62](#)
Low-Frequency Inductors, The Art of Making and Measuring (Sep/Oct 2001) (Shaw): [Jan, 61](#); (Antoniuzzi): [Jan, 62](#); (Arecco): [Jan, 62](#)
Monopoles and Dipoles, About (Mar/Apr) (Belrose): [May, 62](#); (Trainotti): [May, 63](#)
Noise/Gain Analyzer, A (Nov/Dec 1999) (Ricaud): [Mar, 60](#); (Smits): [Mar, 60](#)
PTC: Perceptual Transform Coding...Part 2 (Mar/April 2000) (Schaeffer): [Mar, 60](#); (Smith): [Mar, 60](#)
Q of Single-Layer, Air-Core Coils: A Mathematical Analysis, The (Sep/Oct 2001) (Konig): [Jan, 61](#); (Murphy): [Jan, 61](#)
Quarter-Wave Transformers, On (Klocko): [Sep, 61](#)
Tech Notes: A Compact Six-Band, Off-Center Fed Vertical Dipole (Jan-Feb) (Buus): [Mar, 61](#); (Littlefield): [Mar, 61](#)
Turnstile Antenna Properties, Some Notes on (Mar/Apr) (Blanchard): [Jul, 61](#); (Cebik): [Jul, 62](#)
Two-Meter Reflective SP4T PIN-Diode Switch, A (Nov/Dec 2001) (Zanek): [Jan, 62](#)
Wave Mechanics of Transmission Lines, Part 3: Power Delivery and Impedance Matching (Nov/Dec 2001) (Kraeuter): [Jul, 61](#)

Out of the Box

Extremely Broadband Capacitors (Mack): [Mar, 62](#)
Friendly Ionosphere, The (Mack): [May, 64](#)
L/C Meter IIB from Almost All Digital Electronics (AADE) (Dretea): [May, 60](#)
Motorola News: Sale of RF-power-semiconductor business to M/A-COM, More (Mack): [Jan, 63](#)
New Cascade RF Amplifier MMIC: MBC13916 (Mack): [Jan, 63](#)
RF Power MOSFETs, New (ARF462A/ARF462B; ARF464A/ARF464B from Advanced Power Technology) (Mack): [Jan, 32](#)

RF (Lau)

Homebrewing a Main Tuning Knob: [May, 57](#)
How to Work 10-GHz DX, Part 1: [Jan, 58](#); Part 2: [Mar, 55](#)
Quarter-Wave Dipoles—Why Don't They Perform Well?: [Nov, 56](#)

Simple 24-GHz Transceiver, A: [Jul, 55](#)
Small 2-Meter Yagi, A: [Sep, 56](#)

Technical Articles

250-MHz Network Analyzer, Build a (Hageman): [Mar, 3](#)
455-kHz IF Signal Processor for SSB/CW, A (Sabin):
[Mar, 11](#)
700-W Switch-Mode Transmitter for 137 kHz, A (Talbot):
[Nov, 16](#)
Additional Programming Resources (sidebar to Amateur
Radio Software: It Keeps Getting Better) (Mack):
[Sep, 29](#)
Advanced VHF Wattmeter, An (Kopski): [May, 3](#)
Amateur Radio Software: It Keeps Getting Better
(Gradijan): [Sep, 19](#)
APRS Satellite for Mobile/Handheld Communications, An
(Bruninga): [Jan, 47](#)
Dirodyne: A New Radio Architecture? The (Green): [Jul, 3](#)
DX Prowess of HF Receivers (Raczek): [Sep, 36](#)
Dynamic-Range Testing, Improved (Smith): [Jul, 46](#)
Fractal Loop Antenna: Understanding the Significance of
Fractal Geometry in Determining Antenna Perform-
ance, The (Best): [Mar, 25](#)
Guy-Wire Interaction Case Study (Weber): [Nov, 42](#)
HF Receiver Dynamic Range: How Much Do We Need?
(Chadwick): [May, 36](#)
High-Performance Digital-Transceiver Design, A, Part 1
(Scarlett): [Jul, 35](#)
Homebrew Regenerative Superheterodyne Receiver, A
(Young): [May, 26](#)
Homebrew Shaft Encoder, A (Smith): [Mar, 52](#); feedback:
[Jul, 64](#)
HP Z3801A GPS Frequency Standard, Using the (Jones):
[Nov, 49](#)
Intermodulation and Reciprocal Mixing: Practice, Defini-
tions and Measurements in Devices and Systems,
Theory of, Part 1 (Rohde): [Nov, 3](#)
Laboratory-Grade 10-MHz Frequency Standard, A (Evans):
[May, 13](#)
Linrad: New Possibilities for the Communications Experi-
menter, Part 1 (Åsbrink): [Nov, 37](#)
Low-Loss VHF/UHF Bias Tee, A (Cefalo Jr): [May, 52](#)
Low-Loss VHF/UHF Diplexer, A (Zanek): [Mar, 47](#)
Monopoles and Dipoles, About (Trainotti): [Mar, 17](#); feed-
back: [May, 64](#)
OWA Yagi, Notes on the (Cebik): [Jul, 22](#)


PCsat in Space Now... (sidebar to An APRS Satellite for
Mobile/Handheld Communications) (Bruninga): [Jan, 48](#)
Periscopes for Microwaves: 10-GHz without Feed-Line Loss
(Wade): [May, 42](#)
Quad Antenna Revisited, The Part 5: Quad Design Varia-
tions (Haviland): [Jan, 23](#)
Quartz Crystal Parameter Measurement (Hardcastle):
[Jan, 7](#)
Quiet Antenna Tuner, A (Lymer): [May, 9](#)
"Real" Intercept Point? What is the (sidebar to Improved
Dynamic-Range Testing) (Hare): [Jul, 50](#)
Rectangle Family of Antennas, The, Part 2: The Asymmetri-
cal Double Rectangle (ADR) (Handelsman): [Jan, 12](#)
Relationship of Dipole-Turnstile Azimuth Patterns to
Relative-Current Magnitudes, The (sidebar to Some Notes
on Turnstile Antenna Properties) (Cebik): [Mar, 44](#)
Rs, On Measuring (Bruene): [May, 22](#)
SHF Super-Regenerative Reception (Jamet): [Jan, 3](#)
Software-Defined Radio for the Masses, A, Part 1
(Youngblood): [Jul, 13](#); Part 2: [Sep, 10](#); Part 3: [Nov, 27](#)
Software-Defined Hardware for Software-Defined Radios
(Stephensen): [Sep, 41](#)
Sound-Card Antenna Measurements and Other Useful
Techniques (Sage): [Jan, 33](#)
Switching Power Supplies, Understanding, Part 1
(Mack): [Sep, 30](#)
Ten-Tec Pegasus—Without Soldering, Customize the
(Erbaugh): [Sep, 3](#)
Turnstile-Antenna Properties, Some Notes on (Cebik):
[Mar, 35](#)

Tech Notes

Compact Six-Band Off-Center Fed Vertical Dipole, A
(Littlefield): [Jan, 54](#)
New Faces for Old Meters (Cefalo): [Nov, 54](#)
Predicting the Impact of Loading Coil Q on Antenna
Performance (Littlefield): [Jul, 53](#)
Resistance of Foil Conductors For Antennas
(Severns): [May, 55](#)
SurCapAdapt (Hinz): [Sep, 51](#)
SurCapAdapt PL-259 Style, A (sidebar to Tech Notes:
SurCapAdapt) (Schetgen): [Sep, 54](#)

Upcoming Conferences

Ham Radio University 2002: [Jan, 63](#)
Long Island Mobile Amateur Radio Club Hamfair: [Jan, 62](#)



QEX Subscription Order Card

American Radio Relay League
225 Main Street
Newington, CT 06111-1494 USA

For one year (8 bi-monthly issues) of QEX.
In the US:

ARRL Member \$22.00
 Non-Member \$34.00

In Canada, Mexico and US by
First Class mail:

ARRL Member \$35.00
 Non-Member \$47.00

Elsewhere by Surface Mail
(4-6 week delivery):

ARRL Member \$27.00
 Non-Member \$39.00

Elsewhere by Airmail:

ARRL Member \$53.00
 Non-Member \$67.00

Remittance must be in US funds and checks must be drawn on a bank in the US.
Prices subject to change without notice.

11/88

QEX, the Forum for Communications Experimenters is available at the rates shown at left. Medium term is 6 issues, and because of the uncertainty of postal rates, prices are subject to change without notice.

Subscribe toll-free with your credit card 1-888-277-5289

Renewal New Subscription





Name _____ Call _____

Address _____

City _____ State or Province _____ Postal Code _____

Payment Enclosed

Change:

Account # _____ Good thru _____

Signature _____ Date _____

Letters to the Editor

Re The Dirodyne: A New Radio Architecture? (Letters, Sep/Oct 2002)

There were omissions and an error in Fig 1 of my letter to the editor in the Sept/Oct 2002 issue of *QEX*. First, the little circles on the SET terminals of the J-K flip-flops were left off. Without those circles, the +5-V supply would keep both flip-flops set. As it is, we want the SET/CLR terminals of both J-K flip-flops to remain in the off state so that they are neither set nor reset by the SET/CLR inputs. The second was an omission of a little table that got me from the counts 00, 01, 11 and 10 to actual flip-flop operations. This omission was my fault. If anyone would like to see the derivation and the table that went along with that, they can write me, and I will be glad to send it to them.

Lastly, in the letter, I said that CTL1, 2, 3 and 4 could be directly obtained from the circuit. I wrote the letter before coming up with the minimal circuit, and those outputs would not be directly derived from the circuit. Four NAND gates would be required to get those outputs.—*Alvin P. Schmitt, KE4GVG, PO Box 10336, Blacksburg, VA 24062-0336; schmitta@blacksburg.net.*

Jul/Aug 2002 *QEX*— A Banner Issue

I would like to comment on the Jul/Aug 2002 issue of *QEX*. For the first time, I found myself not only rereading, but going over *all* the articles in a single issue of *QEX* several times. In fact, I'm still not finished! Clearly, this issue is going to go down as a classic.—*Dean Nold, W9KX, 110 Eagle Fork Dr, Waynesville, NC 28786-8121; w9kx@arrl.net*

Amateur Image, Is the Dirodyne the Weaver Method?

I penned these few words in reply to the latest letters to the editor and editorial remarks in *Sep/Oct 2002 QEX*. We hams do have an image problem. It starts with public service and ends with the image of Hollywood. Do we need to rethink our image altogether?

As for public service: How much money does a radio group have to front to outfit a communications trailer with new equipment? What happened to hams being prepared with their own equipment? Did we lose sight? Part

97.1 gives us our purpose.

How about our on-the-air presence? Many conversations I hear on ham radio need to be on a cell phone. Our conduct could often be more professional.

Now to our technical competence: Hams do have a legacy, but many now innovate for corporate America, creating telemetry radios, cellular phones, software-defined radios (thanks for the articles in *QEX*) and gadgets of all varieties. Maxim even claims ham heritage in one of their memory devices (I don't remember which one). People do not see these as Amateur Radio achievements. Our claim to fame is that of being appointed EMC gurus because we are hams, or enjoying analog electronics in this digital world, or wanting to create a new device based on the technology discussed in the amateur literature. We are competent, but we cannot financially afford to innovate. We pay our mortgages, buy the food, and *only then* buy equipment—used or refurbished—so we can do public service. We do not have a lot of spare time or money to innovate and make it as amateurs.

On a further note, the Dirodyne looks very much like the Weaver method (see "A Third Method of Generation and Detection of Single-Sideband Signals," D. Weaver, *Proceedings of the IRE*, 1956). I would hope that this is mentioned in further correspondence about the article in the Jul/Aug 2002 *QEX*.—*Douglas Datwyler, WR7O, 1506 Plata Way, Sandy, UT, 84093; douglas.datwyler@ieee.org.*

Amateur Radio Software: It Keeps Getting Better, (*QEX* Sept/Oct 2002)

I take serious issue with this article, not because it was not well written (it is), but because it is incomplete regarding Apple/Mac software and software tools. The only reference is on p 23:

"Tools for Apple users are more difficult to come by..." (only if you don't bother to look) "... and beyond the scope of this article..." (Come on, that's BS—the scope of the article includes listing compilers and generally discussing software.) "A BASIC language was available for Apple users." (Right. One of the first products of the Microsoft Company was a BASIC Interpreter for the Mac—before they went on to develop *Windows*.)

I consider this oversight common among PC users, but it should have been fixed by the editor (you). So, I am *not* sending this to the writer, WB5KIA, because he is not the prob-

lem. He wrote an otherwise excellent article.

Mac ham software and the required programming tools have existed longer than *Windows* and certainly *Linux*. Only DOS Programs are older—by one year. Although not a programmer, I do play around with *RealBasic*, an excellent BASIC compiler for the Mac written by REAL Software Inc; www.realsoftware.com. I'm sure there are other compilers for *C*, *Java* and other languages out there, if you look. Better yet, ask some of the developers. Like the author, I have noted a considerable improvement in the quality of Mac ham software over the last few years. Here is a partial list:

1. Black Cat Systems: They have seven ham programs for the Mac, including *MultiMode*, which is a real gem; www.blackcatsystems.com/.

2. Dog Park Software Ltd: They developed the satellite-tracking program distributed by AMSAT: *MacDoppler-PRO*. I use this outstanding software frequently. Visit them at www.dogparksoftware.com.

3. Peachtree Solutions: Keith Bransky, KE1TH, develops the logging program *HamLog* 4.0 for the Mac. Visit www.peachtree-solutions.com.

I contacted Chris Smolinsky, N3JLY, of Black Cat Systems. He primarily uses *CodeWarrior* by Metrowerks (www.metrowerks.com) for C++ development but also *RealBasic*. Both now provide Windows builds, so you can avoid duplication of effort.

I know you are trying to bring *QEX* to the level that *ham radio* magazine once had for journalistic excellence and technical achievement, so I attribute this to a kind of blindness that exists in the ham computer community. You need to overcome this if you are to enlist and not alienate those of us in the Mac community who, although fewer in number, tend to have a brighter creative flame. I do not think yet another debate about the merits of the two systems is useful after 20 years.

One more note. Apple has now embarked on its new operating system based on a UNIX kernel: *MacOS X*. This means that much of the new and future software to be developed will have an inherently easier migration path to UNIX clones such as *LINUX* or subsequent derivatives. Think about it.—*Tom Haddon, K5VH, 1005 Hidden Hills Dr, Dripping Springs, TX 78620*

Hello Tom,

Thank you for your comments. As a forum, we are dependent on what we receive from you writers out there.



ACTIVE

ELECTRONIC
COMPONENTS
DEPOT

Your *Local* One Stop Shop for
All Your Electronic Needs!

Over 150,000 parts in stock!

- Electronic Components
- Test and Measurement Equipment
- Soldering Supplies
- Chemicals
- Wire and Cable
- Datacom
- Prototyping
- Static Control
- Hand Tools
- Books and Kits and Much More!



ActivePlus
Rewards Program

Your FREE and EASY way to earn valuable points on every in-store purchase and SAVE BIG!

*see in-store or online for more details



Active Electronics is the retail division of Future Electronics, backed by Future's worldwide reputation for available inventory and competitive pricing. With over 30 years experience, Active offers you the best products at the best price, when you need them! So whether you need an electronic component or production supplies, Active is the place to get it all, today!

Visit your local Active store today!

BALTIMORE
6714 G. Ritchie Hwy
Glen Burnie, MD 21061
Tel.: (410) 863-0070
Fax: (410) 863-0075
active.baltimore@future.ca

CAMBRIDGE
73 First Street
Cambridge, MA 02141
Tel.: (617) 864-3588
Fax: (617) 864-0855
active.cambridge@future.ca

CHERRY HILL
1871 Route 70 East
Cherry Hill, NJ 08003
Tel.: (856) 424-7070
Fax: (856) 424-7722
active.cherry.hill@future.ca

CHICAGO
1776 West Golf Road
Mt. Prospect, IL 60056
Tel.: (847) 640-7713
Fax: (847) 640-7613
active.chicago@future.ca

DETROIT
29447 Five Mile Road
Livonia, MI 48154
Tel.: (734) 525-0153
Fax: (734) 525-1015
active.detroit@future.ca

LONG ISLAND
3075 Veterans Mem. Hwy.
Ronkonkoma, NY 11779
Tel.: (631) 471-5400
Fax: (631) 471-5410
active.long.island@future.ca

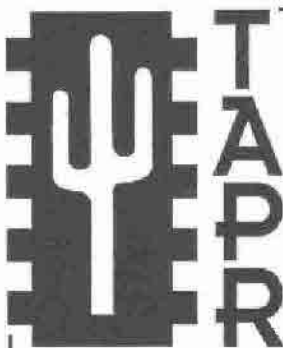
SEATTLE
13107 Northup Way
Bellevue, WA 98005
Tel.: (425) 881-8191
Fax: (425) 883-6820
active.seattle@future.ca

WOBURN
11 Cummings Park
Woburn, MA 01801
Tel.: (781) 932-0050
Fax: (781) 933-8884
active.woburn@future.ca

And 10 locations in all major Canadian cities

www.activestores.com  future-active@future.ca

- Come in and browse our vast product ranges. We have over 5,000 products on display!
- Join our ActivePlus Rewards Program. It pays to shop our stores!
- Talk to knowledgeable, helpful and friendly staff
- Sign up to our mailing list to stay informed of new product lines, promotions and discounts
- Attend in-house seminars and demonstrations from our many suppliers
- Credit terms available



Join the effort in developing Spread Spectrum Communications for the amateur radio service. Join TAPR and become part of the largest packet radio group in the world. TAPR is a non-profit amateur radio organization that develops new communications technology, provides useful/affordable kits, and promotes the advancement of the amateur art through publications, meetings, and standards. Membership includes a subscription to the *TAPR Packet Status Register* quarterly newsletter, which provides up-to-date news and user/technical information. Annual membership US/Canada/Mexico \$20, and outside North America \$25.

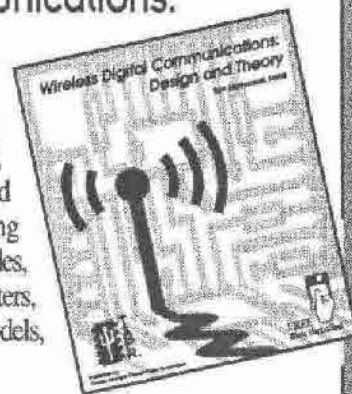


TAPR CD-ROM

Over 600 Megs of Data in ISO 9660 format. TAPR Software Library: 40 megs of software on BBSs, Satellites, Switches, TNCs, Terminals, TCP/IP, and more! 150Megs of APRS Software and Maps. RealAudio Files. Quicktime Movies. Mail Archives from TAPR's SIGs, and much, much more!

Wireless Digital Communications: Design and Theory

Finally a book covering a broad spectrum of wireless digital subjects in one place, written by Tom McDermott, N5EG. Topics include: DSP-based modem filters, forward-error-correcting codes, carrier transmission types, data codes, data slicers, clock recovery, matched filters, carrier recovery, propagation channel models, and much more! Includes a disk!



Tucson Amateur Packet Radio

8987-309 E. Tanque Verde Rd #337 • Tucson, Arizona • 85749-9399
Office: (940) 383-0000 • Fax: (940) 566-2544 • Internet: tapr@tapr.org www.tapr.org
Non-Profit Research and Development Corporation

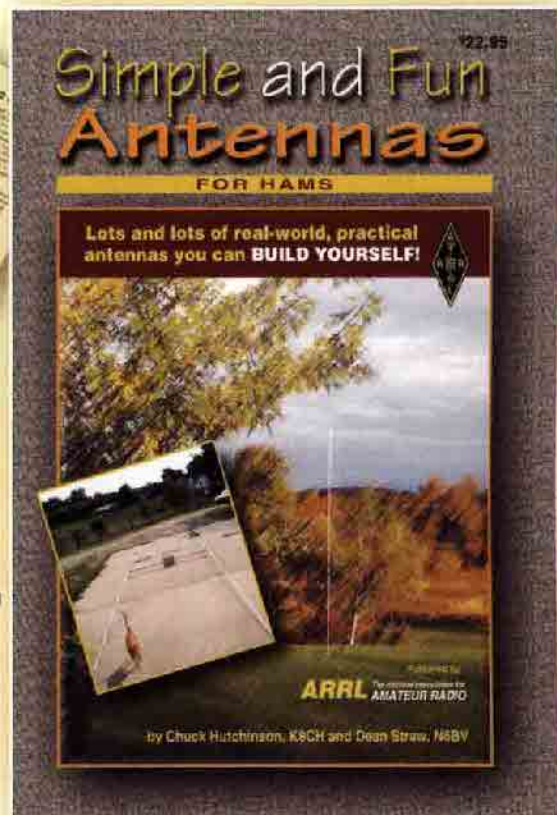
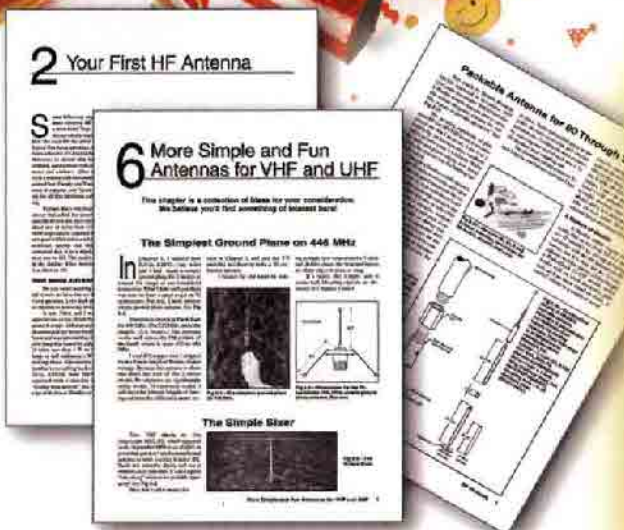
Simple Antennas? **Yes!** Fun Antennas? **You Bet!**



**NEW
BOOK!**

ORDER NOW!

**Simple and Fun
Antennas for Hams**
ARRL Order No. 8624
Only \$22.95*



Hands-on and practical: *Simple and Fun Antennas for Hams* proves that antennas do not have to be complex to work! **This new ARRL book is written for YOU:** newcomers and beginners eager to explore HF; new General-class licensees; and anyone overwhelmed with the technical details in most antenna "textbooks."
Simple and Fun Antennas For Hams brings you more than 70 well-tested, fun and entirely useful projects. Hundreds of photos and illustrations make sure you can actually build working antennas yourself. **These antennas work!**

Your First VHF Antenna
Your First HF Antenna
Facts About Transmission Lines
Antenna Masts and Supports
HF Dipoles
HF Verticals
Dual-Band VHF/UHF Antennas

An HF Vertical That Needs No Radials
—Try the HVD
More Facts About Feed Lines
HF and VHF Beam Antennas
Towers
Getting the Most
Out of Your Antenna



ARRL The national association for
AMATEUR RADIO
225 Main Street, Newington, CT 06111-1494

*Shipping & Handling charges apply: US orders add \$6 (UPS). International orders add \$8.00 (surface). Or, contact ARRL to locate a dealer. Sales Tax is required for orders shipped to CA, CT, VA, and Canada.

Order toll-free **1-888-277-5289** (US) www.arri.org/shop

New Volume!

The ARRL Antenna Compendium Volume 7

**Proven, practical antenna designs
from the world of Amateur Radio.**

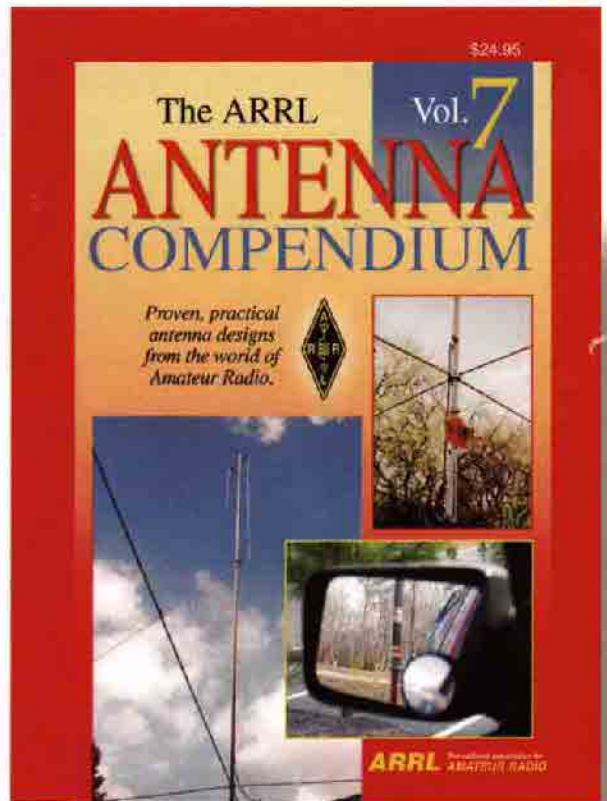
Hooray for antennas! This is the seventh in the very popular ARRL Antenna Compendium series. Inside, you'll find articles covering a very wide range of antenna-related topics:



**GREAT
GIFT
IDEAS!**

- 30, 40, 80 and 160-Meter Antennas
- Measurements and Computations
- Mobile Antennas
- Multiband Antennas
- Practical Tips
- Propagation and Ground Effects
- Quad Antennas
- Special Antennas
- Stealth Antennas
- Tuners and Transmission Lines
- Vertical Antennas
- VHF/UHF Antennas
- Wire Antennas
- Yagi Antennas

And, this volume includes even more articles on low-band antennas and operating, and great designs for operating on the road — from cars, vans or motor homes.



**The ARRL Antenna Compendium
— Volume 7**

ARRL Order No. 8608 \$24.95 plus shipping*
Available November.

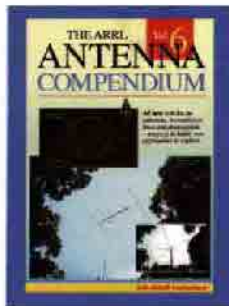
ARRL Antenna Compendiums

More antennas — ideas and practical projects

Volume 6

All new articles covering low-band antennas and operating, 10-meter designs, multiband antennas, propagation and terrain assessment. CD-ROM included with propagation prediction software!

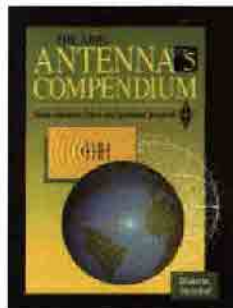
#7431 \$22.95*—Includes software



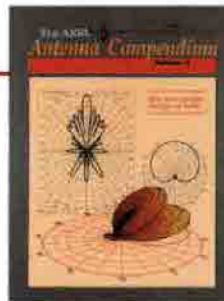
Volume 5

Enjoy excellent coverage of baluns, an HF beam from PVC, low-band Yagis, quads and verticals, curtain arrays, and more!

#5625 \$20*—Includes software



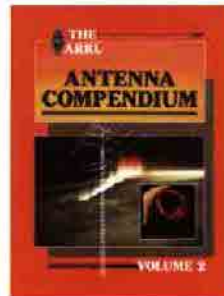
Volume 4 is out-of-print



Volume 3

Quench your thirst for new antenna designs, from Allen's Log Periodic Loop Array to Zavrel's Triband Triangle. Discover a 12-meter quad, a discone, modeling with MININEC and VHF/UHF ray tracing.

#4017 \$14*



Volume 2

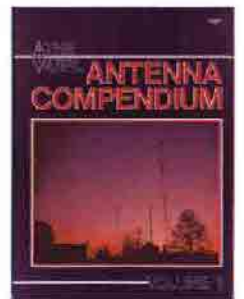
Covers a wide range of antenna types and related topics, including innovative verticals, an attic tri-bander, antenna modeling and propagation.

#2545 \$14*

Volume 1

The premiere volume includes articles on a multiband portable, quads and loops, baluns, the Smith Chart, and more.

#0194 \$10*



***Shipping:** US orders add \$5 for one item, plus \$1 for each additional item (\$10 max.). International orders add \$2.00 to US rate (\$12.00 max.). US orders shipped via UPS.

Sales Tax is required for shipments to CT, VA, CA and Canada.



ARRL The national association for
AMATEUR RADIO

225 Main Street, Newington, CT 06111-1494
tel: 860-594-0355 fax: 860-594-0303

e-mail: pubsales@arri.org

Order Toll Free
1-888-277-5289
www.arri.org/shop

8 AM-8 PM
Eastern time
Mon.-Fri.

World Wide Web: <http://www.arri.org/>